



Building Technology & Urban Systems Division
Lawrence Berkeley National
Laboratory

Measured Dataset for Validation of Building Energy Modeling Programs.

Christian Kohler, Zhaoyun Zeng¹, Ji-Hyun Kim¹, Ralph Muehleisen¹, Philip Haves

¹Argonne National Laboratory

April 2023



Disclaimer

This document was prepared as an account of work sponsored by the United States Government. While this document is believed to contain correct information, neither the United States Government nor any agency thereof, nor the Regents of the University of California, nor any of their employees, makes any warranty, express or implied, or assumes any legal responsibility for the accuracy, completeness, or usefulness of any information, apparatus, product, or process disclosed, or represents that its use would not infringe privately owned rights. Reference herein to any specific commercial product, process, or service by its trade name, trademark, manufacturer, or otherwise, does not necessarily constitute or imply its endorsement, recommendation, or favoring by the United States Government or any agency thereof, or the Regents of the University of California. The views and opinions of authors expressed herein do not necessarily state or reflect those of the United States Government or any agency thereof, or the Regents of the University of California.

Lawrence Berkeley National Laboratory is an equal opportunity employer.

Acknowledgments

This research was supported by the Assistant Secretary for Energy Efficiency and Renewable Energy, Office of Building Technologies of the United States Department of Energy, under Contract No. DE-AC02-05CH11231. The authors would like to thank the FLEXLAB staff for their assistance and dedication to this project. We also thank Cindy Regnier and Kaiyu Sun for their careful review of the document. Darryl Dickerhoff, Ronnen Levinson and Handi Chandra Putra helped early on in this project. Finally, we would like to thank Amir Roth for his long-term support for this project.

Copyright Notice

This manuscript has been authored by an author at Lawrence Berkeley National Laboratory under Contract No. DE-AC02-05CH11231 with the U.S. Department of Energy. The U.S. Government retains, and the publisher, by accepting the article for publication, acknowledges that the U.S. Government retains a non-exclusive, paid-up, irrevocable, world-wide license to publish or reproduce the published form of this manuscript, or allow others to do so, for U.S. Government purposes.

1. Table of Contents

1.	Table of Contents.....	1-3
2.	Introduction	1
3.	Methodology	2
3.1	Test Cell 3B Description	2
3.2	Sensor Details	9
3.2.1	Air and Surface Temperature	9
3.2.2	Water Temperature.....	9
3.2.3	Heat Flux	9
3.2.4	Electrical Power	10
3.2.5	Water Flow	10
3.2.6	Ventilation Rate.....	10
3.2.7	Solar Radiation.....	10
3.2.8	Weather Station.....	10
3.3	Fan coil units	11
3.4	Surface heat flux measurement techniques.....	13
3.5	Blower-door technique.....	17
4.	The Experiment.....	20
4.1	Input Variables.....	23
4.1.1	Weather	23
4.1.2	Other Input Variables	23
4.2	Direct Validation Variables	25
4.3	Indirect Validation Variables.....	26
4.4	Energy Balance of the Measured Data	28
5.	Approaches to Using the Data Set.....	30
5.1	Approaches to Using the Dataset	30
APPENDIX A.	Architectural Drawings of Cell B	A-1
APPENDIX B.	Cell 3B Surface and Construction	B-1
APPENDIX C.	Modeling of Envelope Components with Two- and Three-Dimensional Heat Flows	C-1
C.1	Two-dimensional component modeling.....	C-1
C.2	Three-dimensional component modeling	C-1

C.2.1	Conductivity of the equivalent layers.....	C-2
C.2.2	Density and specific heat of the equivalent layers.....	C-2
APPENDIX D.	Locations of Sensors	D-1
APPENDIX E.	Sun path and shading diagrams	E-1
APPENDIX F.	Data Files	F-1
F.1	Window Files.....	F-1
F.2	CSV Input files	F-1
F.3	Architectural Drawings	F-3
F.4	Pictures	F-3
F.5	Wall THERM files.....	F-3

2. Introduction

This report is part of a multi-year and multi-lab¹ project coordinated by ASHRAE SSPC 140 to quantify building energy modeling (BEM) programs' accuracy and to identify errors, inadequate assumptions and unwarranted simplifications so developers can address them. One task aspect of this effort is to make measurements of multiple physical quantities in experimental facilities over periods of weeks to create data sets that can be used to validate various BEM programs. This project addresses that need.

Berkeley Lab's measurements were performed at FLEXLAB®, which is a flexible building experimental facility (FLEXLAB.lbl.gov). It enables users to test the performance of building systems, individually or as an integrated system, under real-world conditions. These systems include heating, ventilation, and air conditioning (HVAC); lighting; windows; building envelope; control systems; and plug loads, and they can be tested in multiple combinations. Users can test components and systems, compare alternatives, and perform cost-benefit analyses. FLEXLAB's south façade is reconfigurable, and the other surfaces are highly insulated (see below). Each test cell effectively represents a single perimeter zone in a multistory, relatively deep plan building. The south façade can be covered with insulation to approximate an interior zone. Each test cell includes its own air handling unit (AHU) with an economizer, hot water and chilled water coils, and supply fan. The test cell and its adjacent cell comprise a pair that shares a chilled water and hot water plant.

This report documents two experiments performed in the FLEXLAB in 2021. One co-heating experiment and one conditioned experiment with a fan coil unit in the space to control the temperature. The co-heating experiment had no temperature control for most of the experiment to regulate the temperature in the space. Instead, a heat source in the space provides a thermal load in the zone. The heat source was at times modulating to prevent overheating of the source. During the experiment measurements were made related to the sensible heat balance in the interior space of the main zone of the test cell. These measurements included air and surface temperatures, internal heat loads, active cooling rates, airflow rates, heat fluxes through surfaces, and weather conditions.

Section 3 of this report describes the overall methodology, including a description of the FLEXLAB Test Cell, details about the sensors used, the space conditioning system and a description of surface heat transfer measurements and ventilation characterization. Section 4 describes the experiments. Section 5 describes how the measurements can be used for validating simulation tools. Appendix A provides detailed drawings of the cell construction and the windows. Appendix B contains schematics with exact dimensions of all surfaces as well as a description of all the layer-by-layer constructions. Appendix C describes how walls with non-homogeneous construction such as stud-walls and columns can be modeled. Appendix D contains diagrams that show the location of all sensors. Appendix E contains sun path diagrams for the test location. Finally, Appendix F provides a listing of all the companions data files.

¹ Oak Ridge National Laboratory (ORNL), Argonne National Laboratory (ANL), National Renewable Energy Laboratory (NREL), and Lawrence Berkeley National Laboratory (Berkeley Lab).

3. Methodology

This section introduces the experimental facility, sensors, and techniques of data measurement and quality assurance adopted in this study.

3.1 Test Cell 3B Description

The experiments were conducted in Test Cell 3B of the FLEXLAB experimental facility (also called X3B), shown in Figure 3-1. The facility is located in Berkeley, California, and the coordinates are 37.879125, -122.253856. The altitude is 232.0 m or 761 feet. As originally constructed, Test Cell 3B's interior dimensions are approximately 30 ft. deep, 20 ft. wide and 13.8-14.8 ft. high (to bottom of sloped roof) (9.14 m x 6.09 m x 4.20-4.50 m). For the experiment reported here, a highly insulated partition wall was installed 25 ft (7.59 m) from the south wall. A suspended ceiling was placed at a height of 9 ft. (2.74 m) above the floor in the main zone (i.e., between the partition and the south wall) and 8 ft (2.44 m) in the north zone (i.e., between the partition and the north wall). The floor area of the main zone is 500 ft² (46.4 m²). In the rest of this document, we will use "Cell 3B" to denote the main zone of Test Cell 3B. A general view of Test Cell 3B is shown in Figure 1. Test Cell 3B is separated from the adjacent Test Cell 3A by a highly insulated partition wall to allow their performance to be analyzed independently. The ground reflectance on the south side of the building (below the windows) is 20.8% and was measured with a Minolta handheld spectro-reflectometer.

The 3-dimensional drawings in the main body of the report are only meant to show the readers the configuration of the FLEXLAB experimental facility, some of the dimensions in these drawings are inconsistent and should be considered approximate. It is recommended that the models for the validation of BEM programs only include Test Cell 3B (and not Test Cell 3A) and readers are referred to the architectural details in Appendix A and the 2-dimensional drawings in Appendix B for the dimensions and construction of the models.

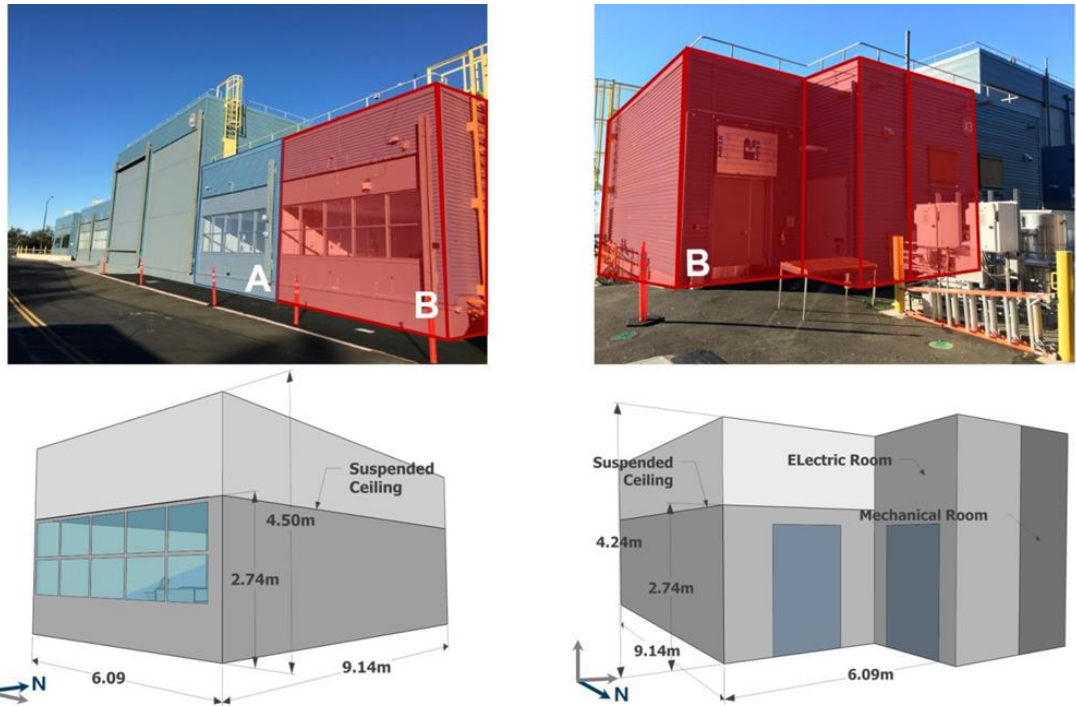


Figure 3-1 FLEXLAB Test Cell 3B (approx. dimensions)²

Table 3-1 describes the construction layers for of Cell 3B. Appendices A and B describes these construction layers in greater detail.

Figure 3-1 through Figure 3-8 illustrate the geometry of FLEXLAB Test Cell 3B. It includes three thermal zones, each consisting of a single bounded volume. As noted above, Cell 3B e and the north zone (also called the anteroom) are separated by a temporary partition wall that extends from the floor to the underside of the suspended ceiling. The suspended ceiling, which separates the ceiling plenum from the main test zone and the north zone, is insulated on its upper side. The temporary north wall was installed to create a buffer zone to separate the entry door and electrical and mechanical rooms from Cell 3B. Test Cell 3A is located on the west side of Test Cell 3B. The surface temperature on the 3A side of the partition wall separating 3B from 3A is included in the data set documented in this report. There were no measurements performed in Test Cell 3A apart from the surface temperatures of the partition wall between 3A and 3B. Test Cell 3A does not need to be included in the models. The wall separating Test Cell 3B and Test Cell 3A can be modeled by specifying the measured surface temperatures (on the 3A or 3B side) in the models. Figure 3-9 shows architectural details of various constructions that surround the control volume (Cell 3B). Figure 3-10 shows a photo of the cell interior. Figures A6-A9 in Appendix A show the cross-sections for the windows in the south wall. Table A-1 shows the overall U-factor for all 10 windows (covered with foam on the outside) is 0.350 W/m²K, and the overall SHGC is 0.004. The relevant THERM and WINDOW files are included in the data set for this project.

² Dimensions in these figures are approximate. The exact dimensions to be used for modeling can be found in Appendix B. The source for Figure 3-1 and Figure 3-3Figure 3-8 are not available anymore and cannot be modified to match the actual dimensions listed in Appendix B

Table 3-1 Construction layers for surfaces

Surface Name	Outside Layer	Layer 2	Layer 3	Layer 4	Layer 5	Layer 6	Layer 7
East Wall	Metal Panel 0.0433	Air Layer 3/4" vertical-AL11	Plywood 1/2"	Insulation (SIP) 7.25"	Plywood 1/2"	Gypsum Board 5/8"	Insulation 6" + 5/8" Gypsum Board
West Wall	Gypsum Board 5/8" R20	Ins Board 4"	Plywood 1/2"	SIP 7.25"	Plywood 1/2"	Ins Board 4" R20	Gypsum Board 5/8"
South Wall	Sealant, Wall-board	R3.8 Rigid Insulation 3/4"	Plywood 1/2"	3.5" Insul. R13, Metal Stud, 16" OC	Gypsum Board 5/8"		
South Window	6 mm single glazing with a thermally broken aluminum frame						
Temporary North Wall	Gypsum Board 1/2"	Polyiso 2.25" Temp N wall SouthFacing	Polyiso 2.25" Temp N wall NorthFacing	Gypsum Board 1/2"			
Floor	HW Concrete 5"	Slab Horizontal Insulation 5"	Topping Slab 6"	Polyiso 2"	Polyiso 2"	Plywood 1/2"	
Drop Ceiling	Cotton Batt 7"	Radiant Cooling Tiles (24"*24"): steel panels:0.15" thick, 120" of copper pipe (0.625" OD, 0.525" ID) filled with water, 1" batt insulation. Twa Panel Systems Inc. Modular Panel (6-pass). http://www.twapanels.ca/products/radiant-panels/					

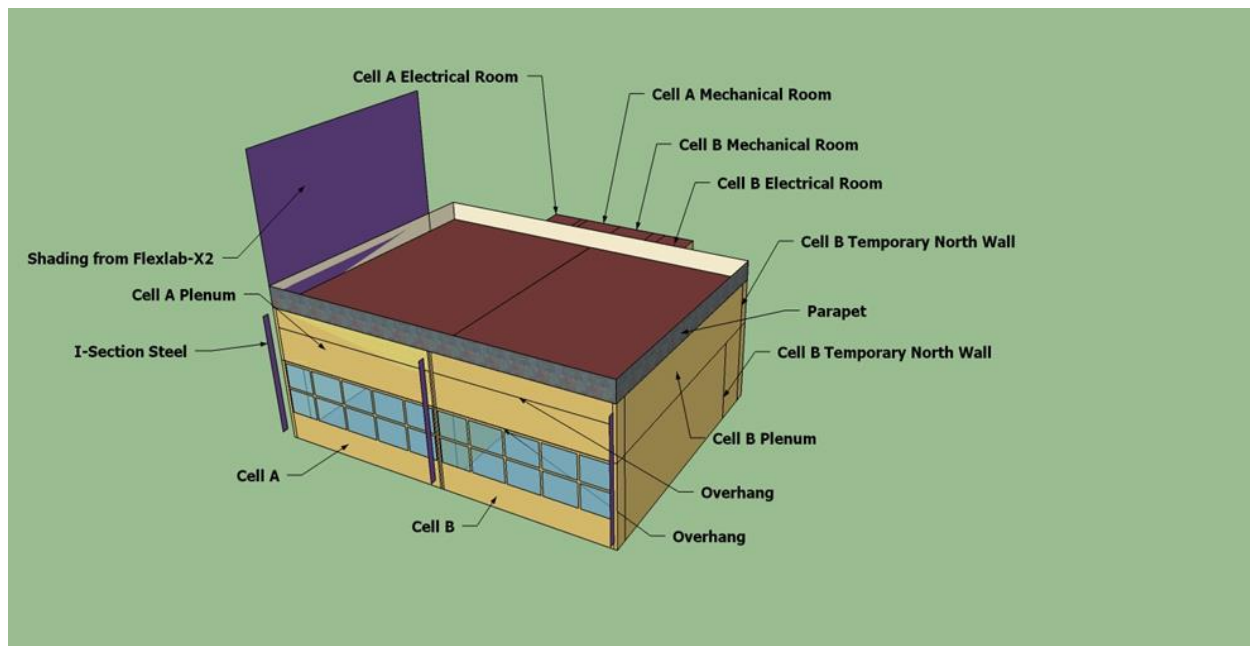


Figure 3-2 FLEXLAB Test Cells 3A and 3B overview.

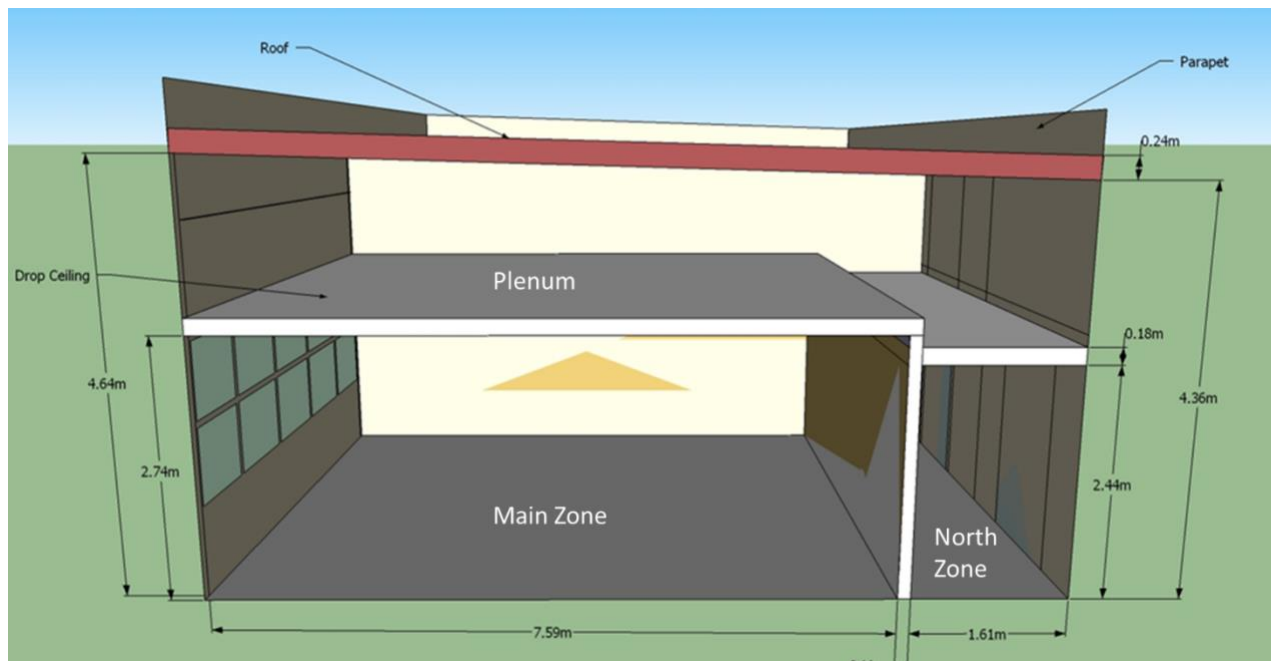


Figure 3-3 FLEXLAB Test Cell 3B north-south cross-section. South is on the left. (approx. dimensions)

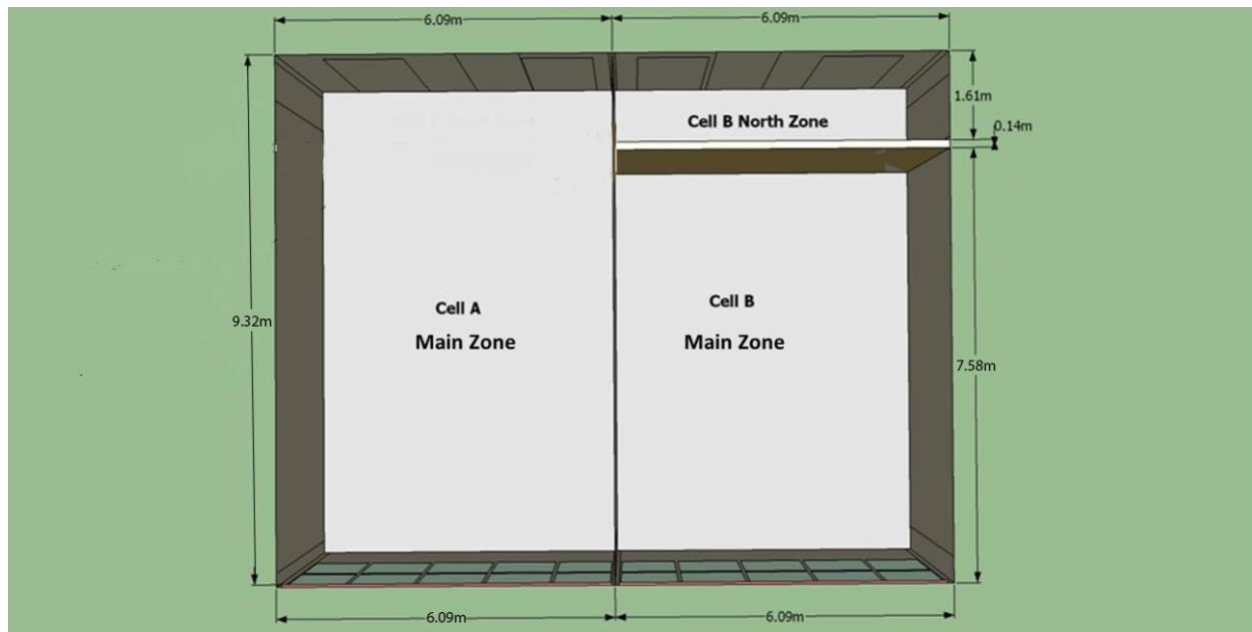


Figure 3-4 Temporary north wall location and thickness. South is at the bottom. (approx. dimensions)

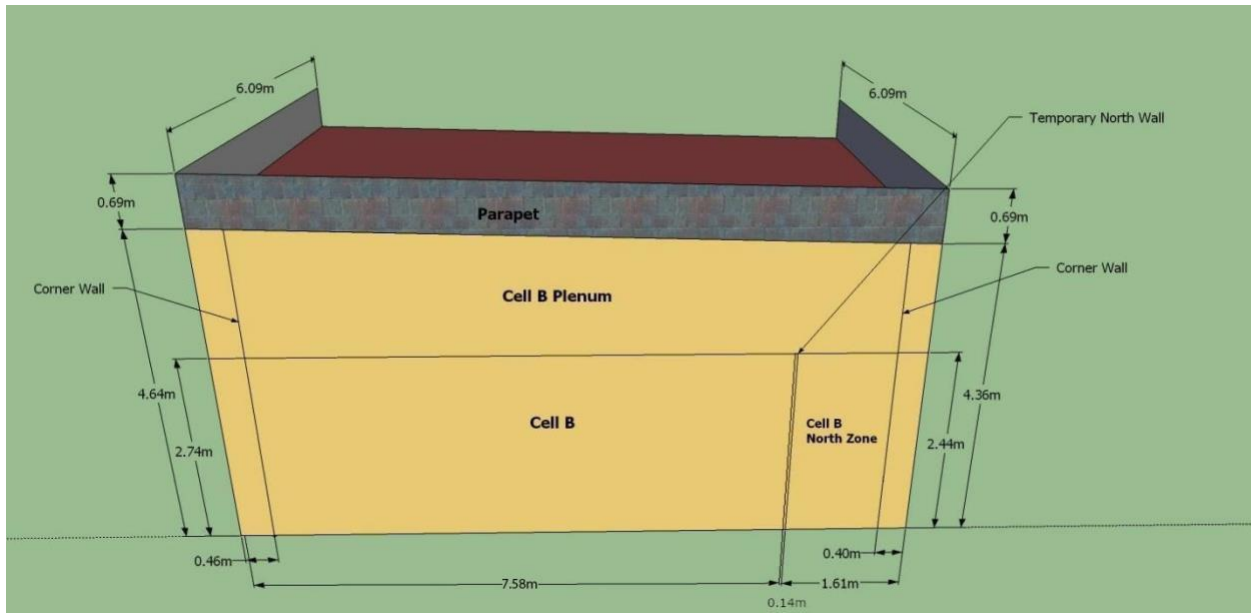


Figure 3-5 East wall. South is on the left (approx. dimensions).

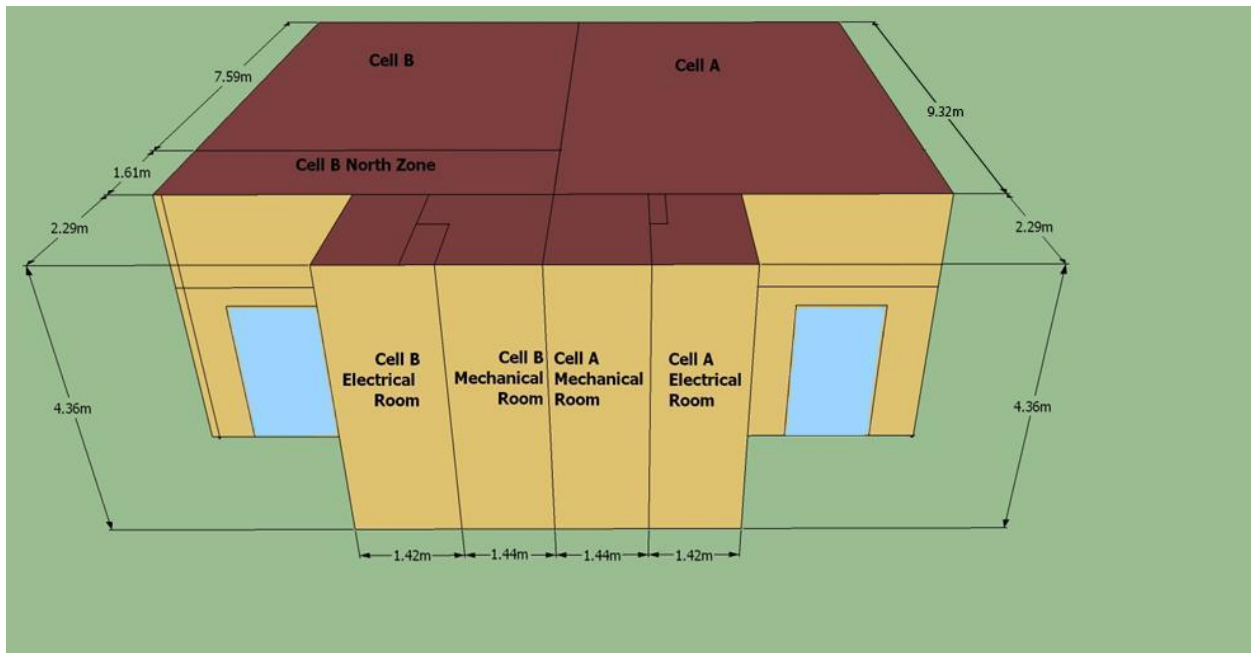


Figure 3-6 North wall (approx. dimensions).

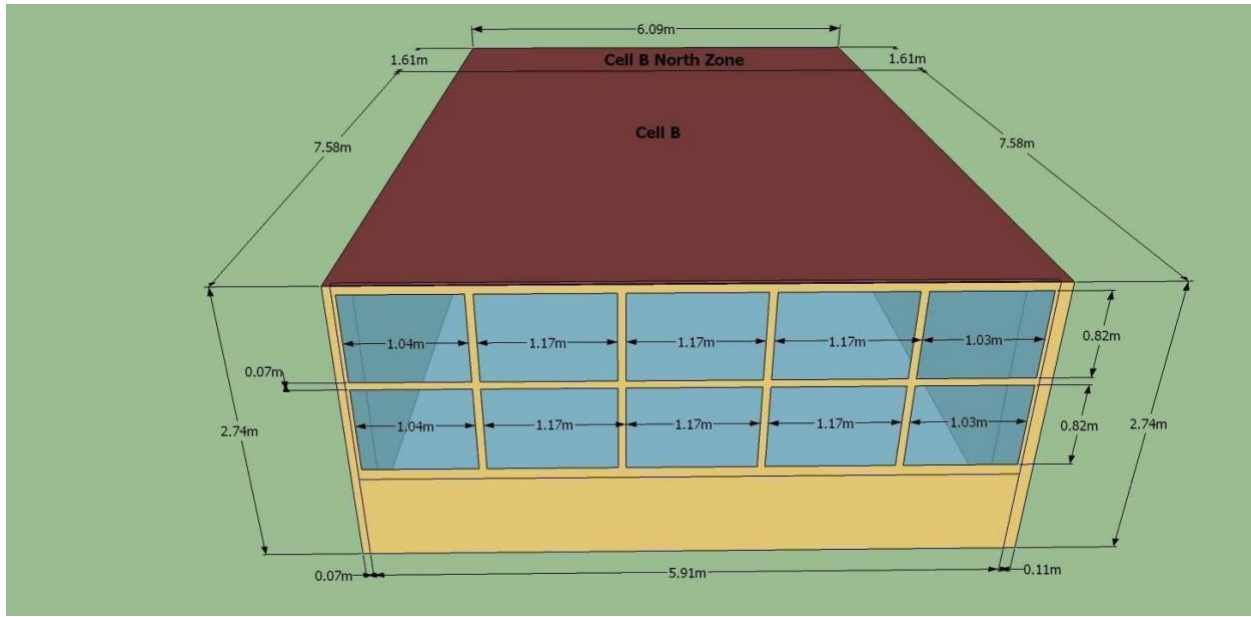


Figure 3-7 Detailed view of windows in Cell B (approx. dimensions).

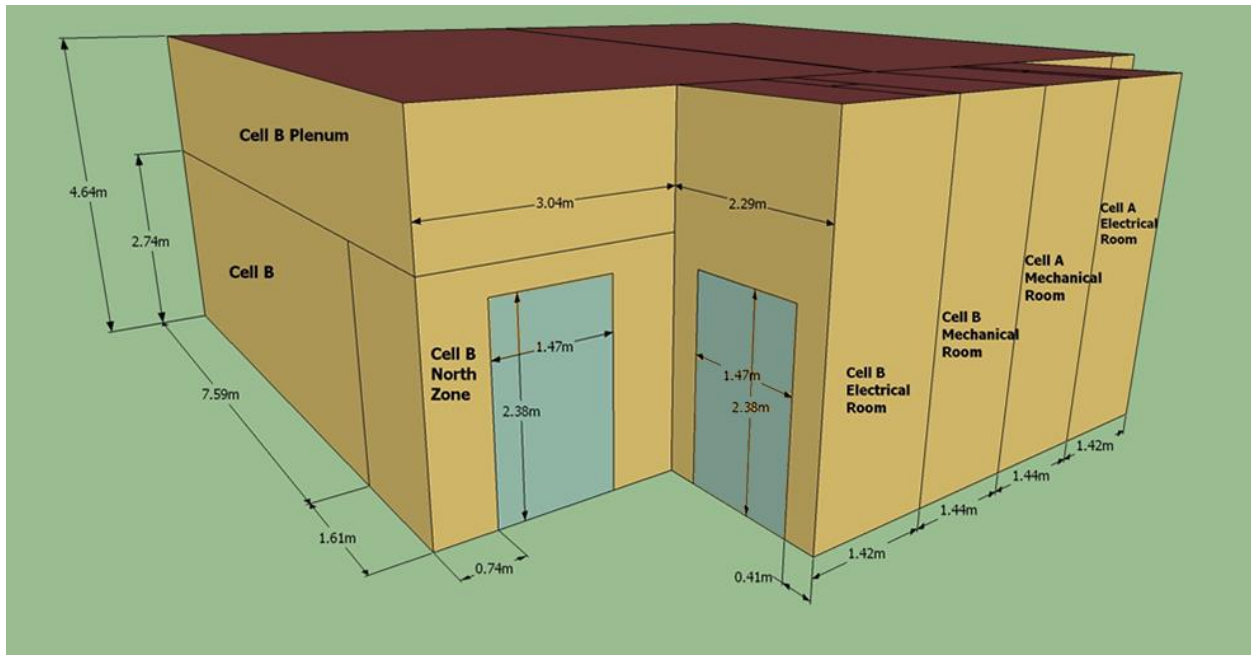


Figure 3-8 Cell B exterior doors (approx. dimensions).

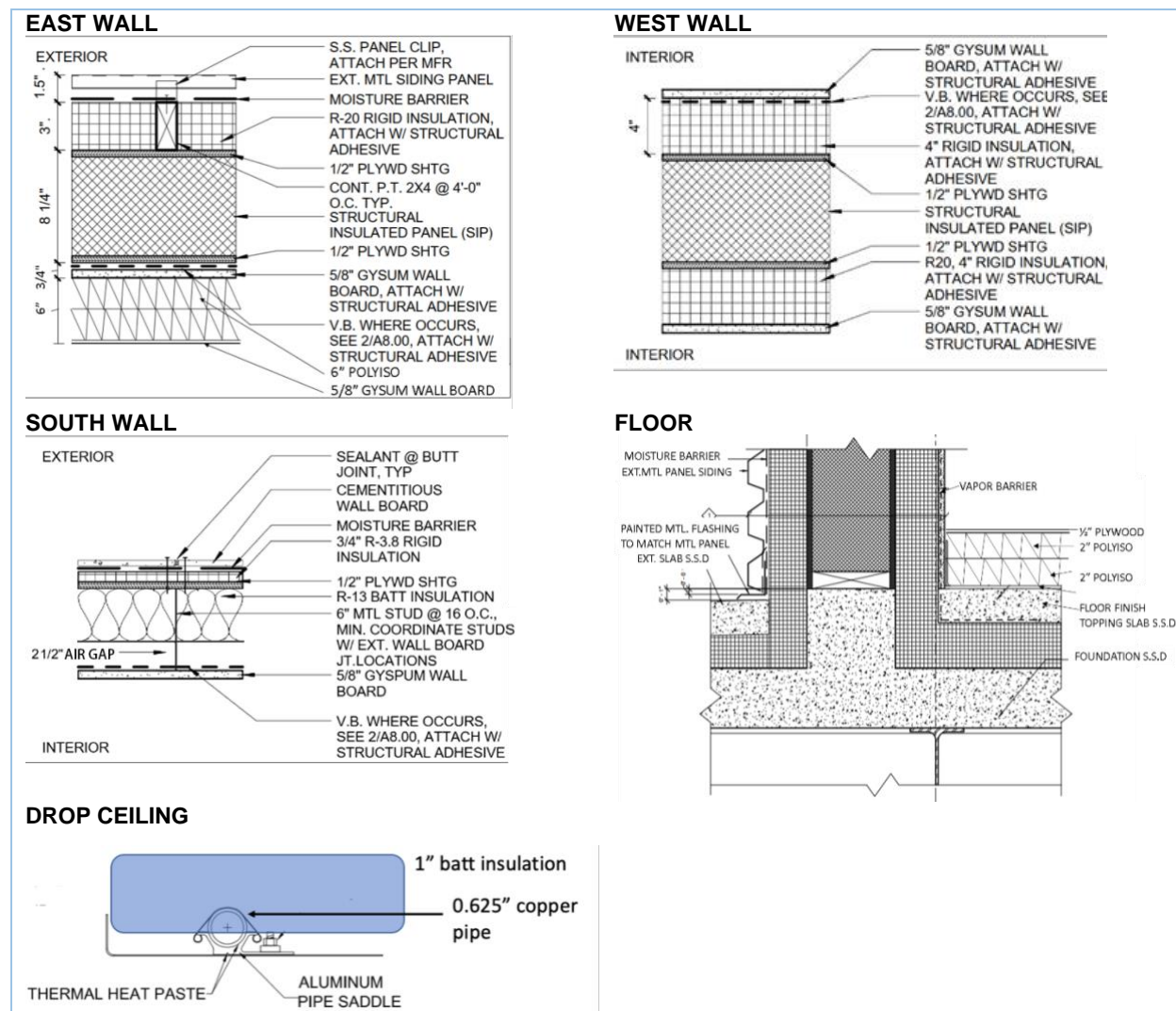


Figure 3-9 Drawings of FLEXLAB Test Cell 3B cross sections

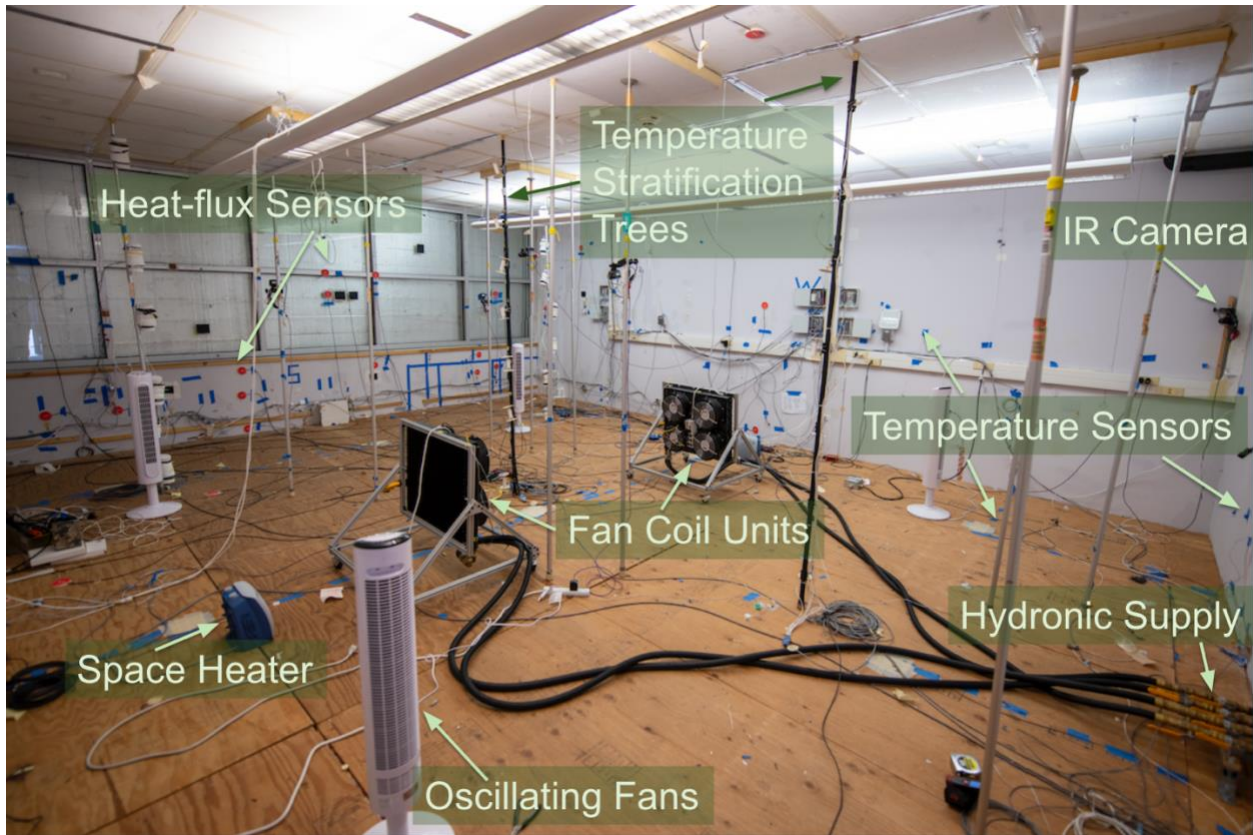


Figure 3-10 Layout of Cell 3B with equipment

3.2 Sensor Details

3.2.1 Air and Surface Temperature

All air and surface temperatures were measured using $10\text{k}\Omega$ thermistors. Two different models were used: US Sensor # PR103J210 and LittelFuse PR103J. All thermistors were calibrated in a water bath using multi-point calibration using a reference platinum resistance thermometer (PRT). The thermistor outputs were measured using a 12 bit Analog to Digital (A/D) converter, National Instruments cRIO 9205 module, in single ended mode with a 1V excitation voltage. The estimated accuracy for these measurements is $\pm 0.05 \text{ K}$.

3.2.2 Water Temperature

The supply and return water temperatures for the fan coil unit (FCU) were measured using BAPI BA/10K-2[XP]-I-4"-BBX thermistors, connected to 10K LJTick-Resistance board on a Labjack T7-Pro using a 20-bit A/D. The thermistors were calibrated using a Fluke 5626 reference thermometer in a water bath using multi-point calibration. The estimated error for these measurements is $<\pm 0.05 \text{ K}$.

3.2.3 Heat Flux

All heat flux measurements were performed using HukseFlux heat flux sensors. The sensors embedded under the topping slab were HFP03 (sensitivity: 500uV/W/m^2 , accuracy within $+\text{- } 6\%$. Range $+\text{- } 2000 \text{ W/m}^2$). The heat flux sensors on the surfaces inside Cell 3B were HFP01 (sensitivity: 60uV/W/m^2 , accuracy within $+\text{- } 3\%$. Range $+\text{- } 2000 \text{ W/m}^2$). The HFP01 heat flux sensors (see Figure 3-11 for a mounted sensor image) were connected in single-ended mode to a Labjack T7-Pro using a 20-bit A/D.

The HFP03 sensors were connected to an Acromag 801T-0500-C transmitter/amplifier. In earlier phases of this project flexible thin copper heat flux sensors from a different manufacturer were used. These sensors proved unreliable when mounted on metal surfaces such as the aluminum radiant ceiling panels and the aluminum foil surface of the Polyisocyanurate insulation. We speculate that this might be due to capacitive coupling. All heat flux sensors were replaced with the HukseFlux disc style sensors.

3.2.4 Electrical Power

Each outlet was measured individually. The real power measurement is accurate within 2% of the actual value, meeting ANSI C12.1, 4.7.2.3 over a current range of 0.15A to 20A (for 20A CTs). The measurements are typically better than 1% accuracy at 1.0 PF, and typically better than 5% accuracy at 0.5 power factor loads. Logged at a one-second interval. True RMS voltage and current, VA, VAR, and PF are also be logged at a one-second interval. The PF for the large loads in the space was >0.8, only small fans (<30 W) had PF ~0.60.

Current transducers: Verivolt Envoy-AC with 1A (individual lighting fixtures), 20A (most branch circuits), 30A and 50A (larger HVAC loads) primaries all +/- 0.2% accuracy; Voltage transducers: Triad VPT12-4170, accuracy +/- 0.1%. CTs and VTs read and processed using National Instruments 9205 C Series Voltage Input Module.

3.2.5 Water Flow

Water flow to the fan coil units was measured using Siemens Sitrans F M Mag 1100 transducers with a $\frac{1}{4}$ " bore. The accuracy for flow measurements is 1% at 0.015 GPM flow and 0.25% at 0.4 GPM flow.

3.2.6 Ventilation Rate

The ventilation rate was determined using a TEC Duct Blaster with a DG-1000 controller. The accuracy for the pressure measurement is: $\pm 0.9\%$ of pressure reading or 0.12 Pa, whichever is greater. The Duct Blaster B fan with ring 2 were used to maintain 5 Pa pressure difference between the exterior on the South side of the building and Cell 3B. The air temperature at the supply side of the fan was measured using one of the air thermistors with accuracy as described above. The CO₂ concentration was measured using SBA-5 CO₂ gas analyzers from PP Systems. The gas analyzers are calibrated to measure 0-2000 ppm and have a stated accuracy of <1% over the calibration range. The analyzers were equipped with a miniature rotary vane sampling pump and an absorber column with soda lime. The sensor auto-calibrates every 20 minutes by sampling air through the soda lime absorber column.

3.2.7 Solar Radiation

Solar radiation was measured using a MS-80 Pyranometer. An MS-57 Pyrheliometer mounted on a sun tracker was used to measure direct normal irradiation. Both devices are Class A devices per ISO 9060:2018 and have a spectral error of +/- 0.2% and a stability of <0.5% over 5 years. Since the windows in these experiments were blocked with foam, the impact of solar radiation on the indoor temperatures was limited.

3.2.8 Weather Station

Wind speed: 3-dimensional ultrasonic anemometer. Gill Instruments "Windmaster" Model 1590-PK-020. Accuracy = +/- 1.5% RMS wind speed with wind vector <30° of horizontal; wind direction +/- 2°. Outside air RH: Chilled mirror w/thermionic heat pump, GE Optisonde Model 1111144. Single-stage chilled mirror. Temp accuracy = +/- 0.15°C, dew/frost accuracy = +/- 0.2°C. An Eppley Precision Infrared

Radiometer (Pyrgeometer) with an accuracy of +/- 5 W/m² was used to measure the sky infrared (long wave) radiation.



Figure 3-11 Heat flux sensor (top) and thermistor (bottom) mounted on the south wall.

3.3 Fan coil units

Two fan coil units were custom-built at Berkeley Lab. By installing the fan coil units on movable carts, the units were able to be placed in the center of the room. The heat exchangers, hoses and fans are all inside Cell 3B, which is the control volume of the experiment. Flexible hoses for supply and return (hot and chilled) water were positioned on the floor of Cell 3B. The temperatures of the supply and return water were measured at the point where the water pipes entered Cell 3B. All heat loss or gain to the water after this point is inside Cell 3B and it does not matter if the heat is transferred to Cell 3B through the hoses or through the fan coil unit. A BAPI 4" brass thermowell with a ¼" bore was used to measure these temperatures (see Figure 3-12 below). The copper pipes and thermowells were insulated after the picture was taken.

The heat exchangers are Boyd 6340G2-M9 copper tube-fin heat exchanger with 120V fans. There were four fans per heat exchanger, but only two fans were used on each fan coil unit to maintain a large enough temperature difference between the supply and return water temperature. Figure 3-13 shows the fan coil units in the space.



Figure 3-12 Thermowells with 4" thermistor probes measuring water temperature inside the 4" polyisocyanurate wall between the north zone and Cell 3B (This picture was taken on the ante room side.)

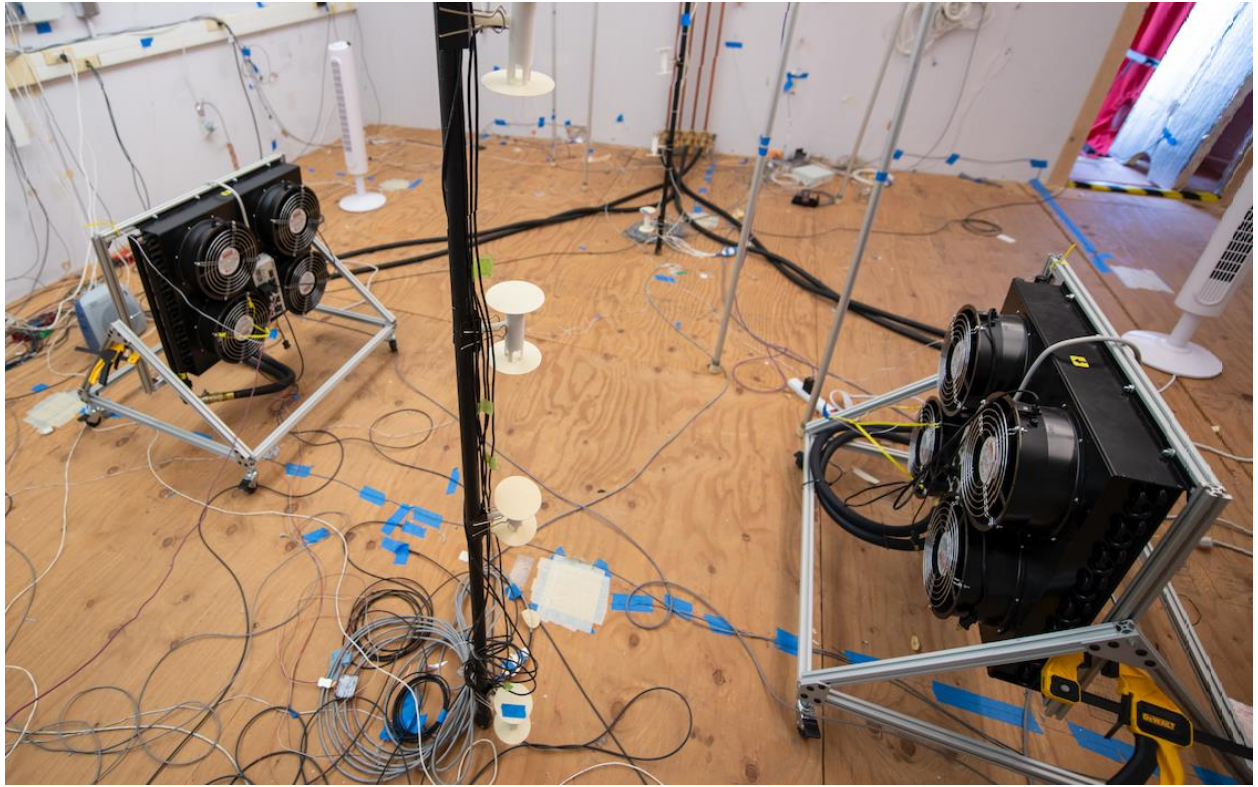


Figure 3-13 The two fan coil units inside Cell 3B.

3.4 Surface heat flux measurement techniques

The conductive heat transfer rates through the building surfaces of Cell 3B were measured by heat flux sensors. Since none of the building surfaces are uniform, due to studs, columns and beams, multiple heat flux sensors are required to accurately measure the total heat transfer rate through each surface. If each surface requires 16 sensors, a total of $16 \times 6 = 96$ sensors are required, which is a substantial and unnecessary investment. Therefore, we devised a technique to reduce the number of heat flux sensors required, as shown in Figure 3-14. This technique contains three steps. In the first step, we attach 15 to 16 heat flux sensors to all key locations on a surface, record their readings for a few weeks, and use the area-weighted average of their readings as the true average heat flux of the surface. In the second step, we first use the variation inflation factor (VIF) method to remove redundant sensors until 4 or 5 are left. VIF is a measure of the severity of multicollinearity in a set of multiple regression variables. It is calculated by the following equation:

$$\text{VIF}_j = \frac{1}{1 - R_j^2} \quad (1)$$

where R_j^2 is the coefficient of determination of the model with the j^{th} variable as the response and the remaining variables as predictors. In the context of this study, a large VIF for a sensor indicates that the readings of this sensor can be easily represented by a linear combination of the readings of the other sensors, i.e., this sensor can be removed due to redundancy. In each round, we calculate the VIF for each sensor and remove the 4 or 5 sensors with the largest VIFs. This process is repeated until there are 4 or 5 sensors left. Next, we fit a multiple linear regression (MLR) model with each combination of 3 sensors as the predictors and the true total heat transfer rate as the response. The 3 sensors whose MLR

model has the largest coefficient of determination (R^2) are adopted as the representative ones. In the third step, we create an MLR model with the three representative sensors and test its predictive power with a test dataset. An R^2 greater than 0.95 indicates that the model has strong predictive power, and it will be adopted in the subsequent measurement.

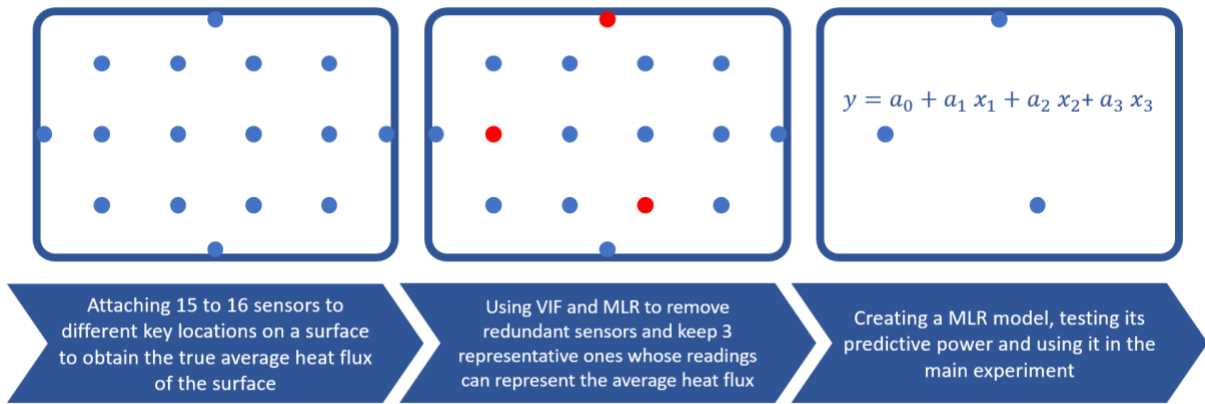


Figure 3-14 The technique to reduce the number of heat flux sensors required.

Here, we take the east wall as an example to demonstrate this technique. The east wall has a surface area of 20.56 m². A total of 16 (1 on each edge and 12 in the center) sensors were attached to the east wall and their readings were recorded from 16:00 March 19th, 2021 to 12:00 April 1st, 2021. Each sensor on the edge represents a strip area with a width of 0.15 m. The rest of the area is evenly allotted to the 12 sensors in the center. The data recorded from 16:00 March 19th to 00:00 March 30th were used as the training set and the rest were used as the test set. The area-weighted average heat flux of the east wall is calculated by

$$\bar{q}_e = \frac{1.47 \sum \text{center} + 0.411 \sum \text{vertical edge} + 1.08 \sum \text{horizontal edge}}{20.56} \quad (2)$$

where $\sum \text{center}$ is the sum of the readings of sensors in the center [W/m²]; $\sum \text{vertical edge}$ is the sum of the readings of sensors on the left and right edges [W/m²]; and $\sum \text{horizontal edge}$ is the sum of the readings of sensors on the top and bottom edges [W/m²]. The readings of all the heat flux sensors as well as the average heat flux are shown in Figure 3-15. Most of the readings have a strong correlation with each other, indicating that the average heat flux can be represented by a linear combination of the readings of only a few sensors.

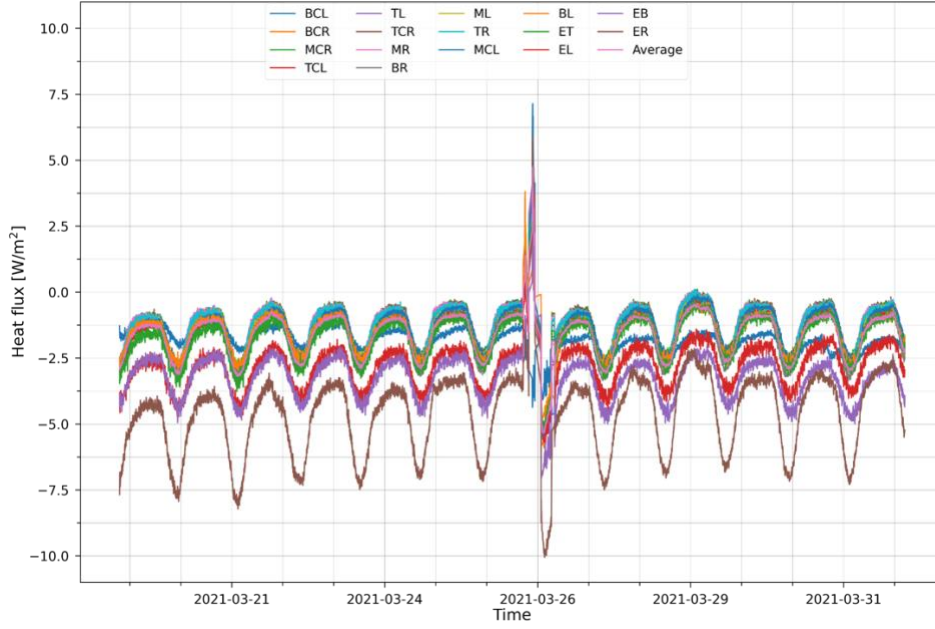


Figure 3-15 The readings of all the heat flux sensors on the east wall.

The process of removing redundant sensors is shown in Table 3-2. After 4 rounds of removing, 5 sensors were left. After testing each combination of 3 sensors out of the 5, we found that the following model has the largest R^2 of 0.9609:

$$\hat{q}_e = 0.419 + 0.342BL + 0.453ET + 0.223EB \quad (3)$$

We tested this model on the test set and obtained an R^2 of 0.9618, showing that this model has strong predictive power. The profiles of the true average heat flux (denoted as “Average”) and the average heat flux calculated by this regression model (denoted as “Regression”) on the test set are shown in Figure 3-16 Profiles of the true average heat flux and the average heat flux calculated by the regression model on the test set. We also include the profile of the mean heat flux of 3 center sensors (denoted as “Center”). It can be observed that the regression model can predict the average heat flux quite well, while the mean heat flux of 3 center sensors cannot accurately predict the average heat flux of the entire surface.

Table 3-2 Removing redundant heat flux sensors using VIF (Those crossed out are removed in each round.)

Round 1										
Sensor	BCL	BCR	MCR	TCL	TL	TCR	MR	BR	ML	TR
VIF	2.30	14.0	29.1	22.3	39.3	27.3	56.3	45.8	36.3	30.0
Sensor	MCL	BL	ET	EL	EB	ER				
VIF	25.3	8.36	11.5	6.63	6.57	18.7				
Round 2										
Sensor	BCL	BCR	MCR	TCL	TCR	TR	MCL	BL	ET	EL
VIF	2.15	13.0	28.4	21.5	26.7	19.2	49.7	7.01	11.5	6.00
Sensor	EB	ER								
VIF	6.47	15.0								
Round 3										
Sensor	BCL	BCR	TR	BL	ET	EL	EB	ER		
VIF	2.13	11.7	45.4	6.39	7.73	5.36	6.29	44.4		
Round 4										

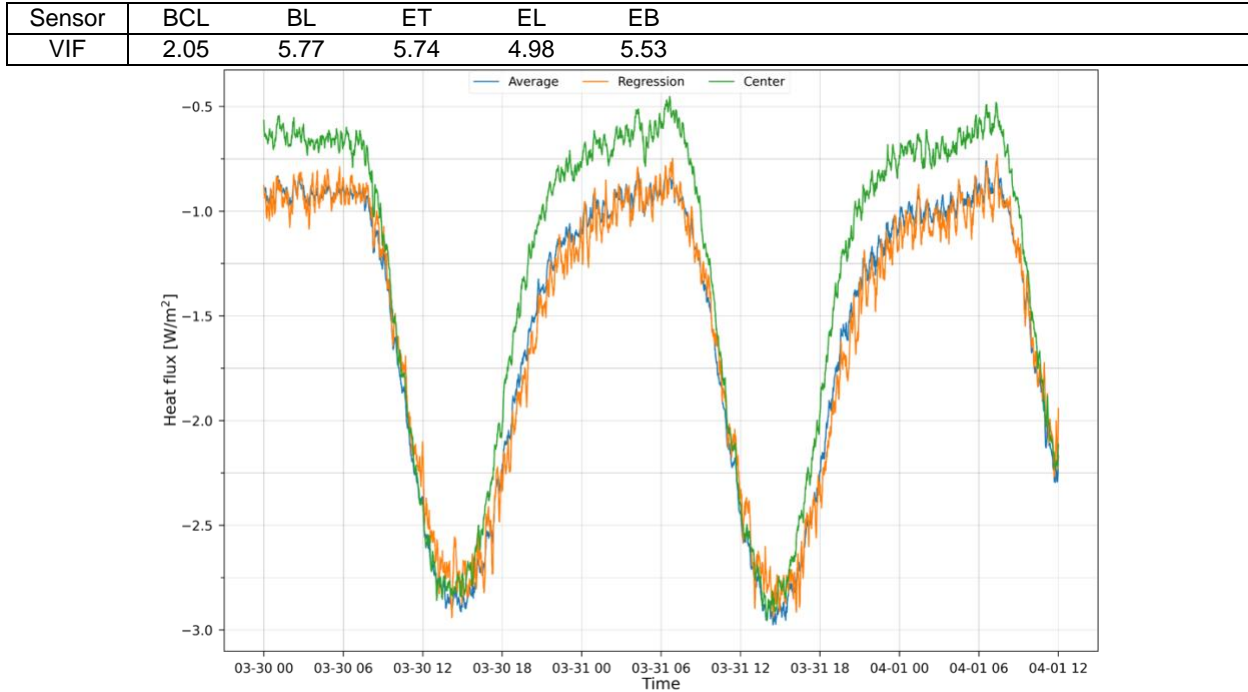


Figure 3-16 Profiles of the true average heat flux and the average heat flux calculated by the regression model on the test set.

The MLR models for the north wall, west wall, and floor were obtained similarly, as summarized in Table 3-3 . The MLR models for the north wall, west wall, and floor. Due to the limitation of time, we could not collect enough data to develop an MLR model for the ceiling. Hence, 3 sensors were attached to key locations and the mean of their readings was used as the average heat flux of the ceiling.

Table 3-3 . The MLR models for the north wall, west wall, and floor.

Surface	MLR model	R^2
North wall	$\hat{q}_n = 0.0166 + 0.400MC + 0.216D + 0.372ER$	0.9867
West wall	$\hat{q}_w = 0.0429 + 0.637TL + 0.491EB - 0.0776EL$	0.9868
Floor	$\hat{q}_f = 0.0174 + 0.260SE2 + 0.653EC1 + 0.113SW0$	0.9703

Since the south wall has the most complex configuration among all surfaces, 14 flux sensors were attached to the key locations on the south wall and the area-weighted average of their readings were used as the true average heat flux of the south wall. Specifically, 3 flux sensors were attached to the glazing, 1 was attached to the window frame, 3 were attached to the horizontal studs, 4 were attached to the vertical studs, and 3 were attached to the wall sections between the studs. The area-weighted average heat flux of the south wall is calculated by using the area of glazing (3.27 m^2), window framing etc:

$$\bar{q}_s = \left(3.27 \sum_{\text{glazing}} + 0.98 \sum_{\text{frame}} + 1.11 \sum_{\text{insulation}} + 0.483 \sum_{\text{horizontal stud}} + 0.11 \sum_{\text{vertical stud}} \right) / 16.02 \quad (4)$$

where \sum_{glazing} is the sum of the readings of sensors on the glazing [W/m^2]; \sum_{frame} is the sum of the readings of sensors on the window frame [W/m^2]; $\sum_{\text{insulation}}$ is the sum of the readings of sensors on the insulation panel [W/m^2]; $\sum_{\text{horizontal stud}}$ is the sum of the readings of sensors on the horizontal studs [W/m^2]; and $\sum_{\text{vertical stud}}$ is the sum of the readings of sensors on the vertical studs [W/m^2].

The total conductive heat transfer rate through building surfaces is calculated as

$$P_{\text{cond}} = A_s \bar{q}_s + A_n \hat{q}_n + A_e \hat{q}_e + A_w \hat{q}_w + A_f \hat{q}_f + A_c \hat{q}_c \quad (5)$$

where A_s , A_n , A_e , A_w , A_f , and A_c are the area of the south wall (including windows), north wall (including the door), east wall, west wall, floor, and ceiling [m^2], respectively; and \bar{q}_s , \hat{q}_n , \hat{q}_e , \hat{q}_w , \hat{q}_f , and \hat{q}_c are the average heat flux of the south wall, north wall, east wall, west wall, floor, and ceiling [W/m^2], respectively.

The schematic drawings of the location of the flux sensors are provided in Appendix D. The detailed coordinates of these sensors are provided in the “Sensor locations.xlsx” file contained in the dataset.

3.5 Blower-door technique

Infiltration constitutes an important part of the energy balance of buildings. There are generally two approaches to quantifying the heat exchange rate due to infiltration. The first is to measure the pressure difference on the two sides of each surface and calculate the air flow rate through each surface based on the pressure difference using empirical formulae. This approach requires the detailed air flow properties of each surface to be measured, which is a challenging task. The second approach is to maintain a positive pressure in the interior space with a fan. The positive pressure ensures that no uncontrolled or unmonitored infiltration exists and the flow rate and the temperature of the air flowing through the fan can be accurately measured. Considering the difficulty of the two approaches, we adopted the second one. This enabled us to measure the infiltration heat/gain loss separately from the other thermal tests such as the conductive losses through surfaces.



Figure 3-17 Minneapolis Blower Door™ System

We employed the Minneapolis Blower Door System with a Series B Duct Blaster Fan produced by The Energy Conservatory for the blower-door experiment, see Figure 3-17. The adjustable aluminum frame and durable nylon panel can seal the door between the north zone and Cell 3B tightly. The Series B Duct Blaster Fan has an automatic control system that can maintain the zone around a specified pressure level relative to the outside. If the specified pressure level is too high, a large airflow rate is required to maintain the pressure difference, which may dominate the heat balance of the zone (making other heat

transfer mechanisms trivial). If the specified pressure level is too low, a constant positive pressure cannot be maintained due to the interference of wind. After some trial and error, we selected 5 Pa as the target pressure level. The outside pressure of the south wall was selected as the reference point. This pressure is a good indicator of the influence of wind on the airflows between 3B and other zones since the south wall is an exterior wall of Cell 3B with lots of cracks (due to the existence of windows).

The Duct Blaster fan employs the DG-700 Digital Pressure Gauge to measure the fan flow rate, which has an accuracy of +/- 3 percent. Fan flow is determined by measuring the slight vacuum created by the air flowing over the flow sensor attached to the end of the motor. The Duct Blaster fan can accurately measure flows between 4.1 and 2549 m³/h using a series of four calibrated Flow Rings attached to the fan inlet ^[1]. Ring 2 with a flow range of 153 to 510 m³/h is selected for our experiment. The fan flow rate is calculated using the following equation

$$F_{\text{fan}} = 25.94 \text{ [m}^3/\text{h}] \times \sqrt{\frac{1.204 \text{ [kg/m}^3]}{\rho_{\text{air}}}} \times \frac{p_{\text{fan}}}{[\text{Pa}]}^{0.5064} \quad (6)$$

where ρ_{air} is the density of air flowing through the fan [kg/m³]; and p_{fan} is the fan pressure [Pa].

Figure 3-18 shows pressure measured in different locations relative to Cell 3B during a test experiment. All pressure values are constantly negative compared with that in Cell 3B, proving that a positive pressure zone can be maintained in Cell 3B.

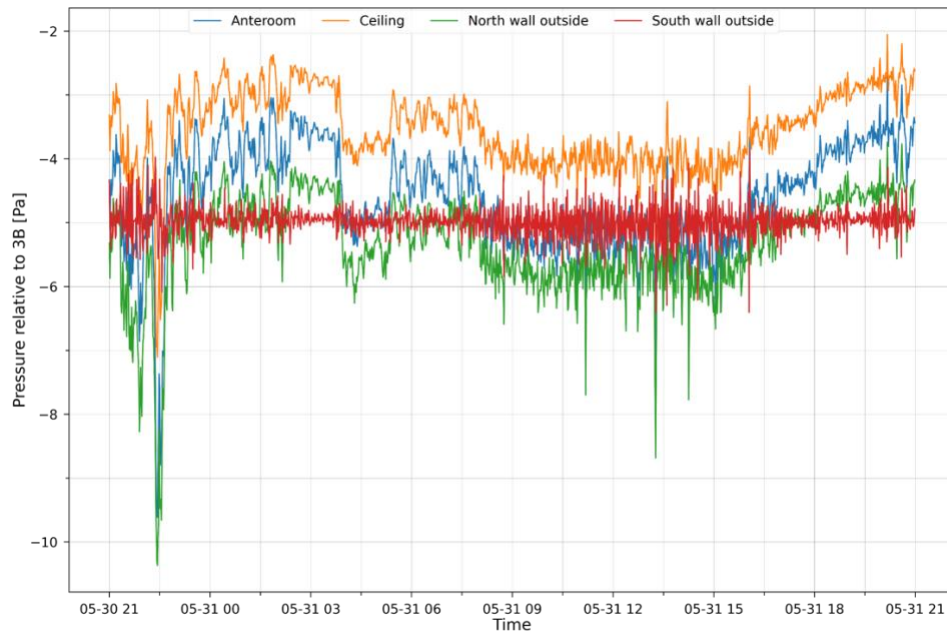


Figure 3-18 Pressure measured in different locations relative to 3B during a test experiment.

In order to verify that all the air entering Cell 3B is through the Ductblaster fan, we continuously injected CO₂ into Cell 3B at a rate of 0.072 m³/h and measured the CO₂ concentration in the 3 zones. The CO₂ concentration profiles of the 3 zones during the verification experiment is shown in Figure 3-19. Since the Duct Blaster fan blows air from the north zone into Cell 3B, the mass balance of CO₂ of the two zones can be written as the following form

$$V_3 \frac{dc_3(t)}{dt} = -F_{\text{fan}} c_3(t) + F_{\text{fan}} c_2(t) + Q_3(t) \quad (7)$$

where V_3 is the volume of Cell 3B [m^3]; c_2 and c_3 are the volumetric concentration of CO_2 in the north zone and Cell 3B, respectively; Q_3 is the injection rate of CO_2 to Cell 3B [m^3/h]; F_{fan} is the volumetric airflow rate through the fan [m^3/h]. Using Equation 7, we can calculate the fan flow rate. Then, the heat transfer rate due to ventilation can be calculated using the following equation

$$P_{\text{vent}} = F_{\text{fan}} \rho_{\text{air}} c p_{\text{air}} (T_{\text{vent}} - T_3) \quad (8)$$

where $c p_{\text{air}}$ is the specific heat capacity of air [$\text{J}/(\text{kg}\cdot^\circ\text{C})$]; T_{vent} is the temperature of the air flowing through the fan [$^\circ\text{C}$]; and T_3 is the temperature of the air in Cell 3B [$^\circ\text{C}$]. Figure 3-20 shows the ventilation heat transfer rate calculated by different methods. It can be seen that the two fan flow rate profiles coincide with each other quite well. We use the coefficient of root mean squared error (CVRMSE) to measure their coincidence, which is calculated as follows:

$$\text{CVRMSE} = \sqrt{\frac{\sum(y_i - 0)^2}{n}} / \max(|P_{\text{vent}}|) \quad (9)$$

where y_i is the energy balance value of the i^{th} time step [W]; and n is the number of timesteps. The CVRMSE between the two profiles is 9.6%. This further proves that all the air entering Cell 3B is through the fan.

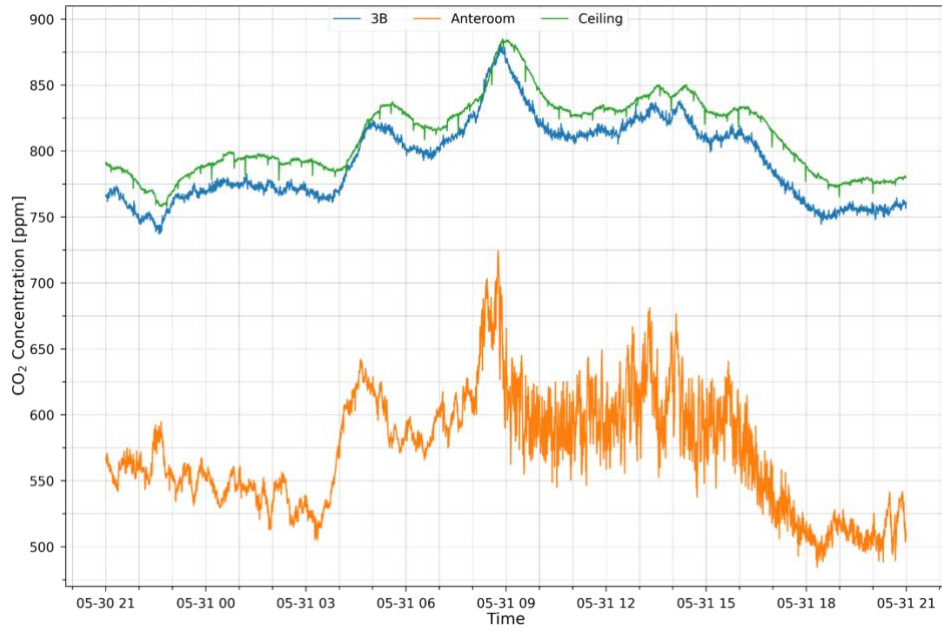


Figure 3-19 The CO_2 concentration profiles of the three zones during the verification experiment.

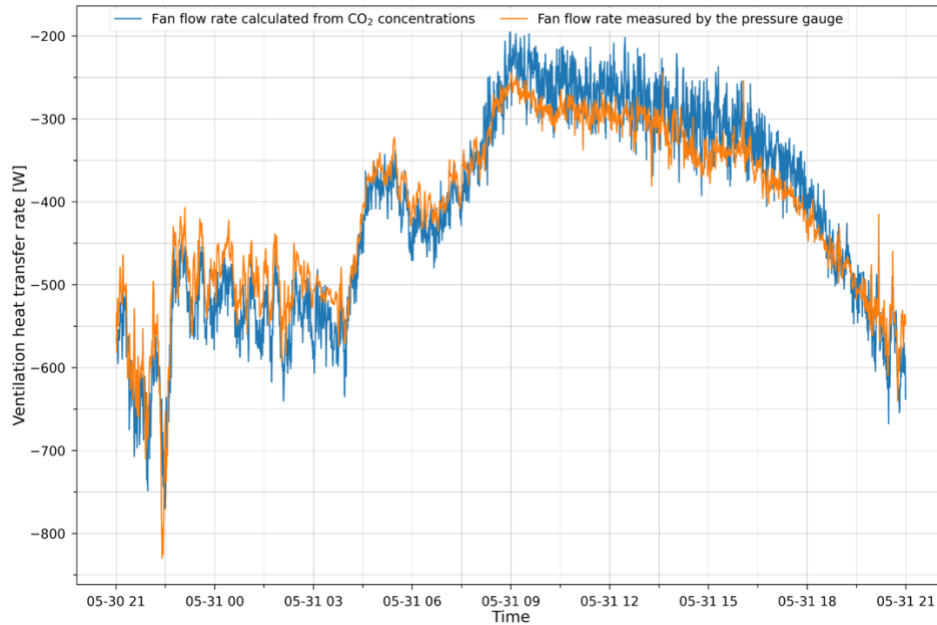


Figure 3-20 Comparison of the ventilation heat transfer rates calculated from fan flows obtained through different methods.

4. The Experiment

We conducted two experiments in different operating conditions to measure the validation data. The first experiment was a co-heating experiment where the indoor air temperature floated freely most of the time, while the second experiment was a conditioned experiment where the indoor air temperature was controlled to a specific setpoint. The co-heating experiment reported here was conducted in FLEXLAB between 14:00 on June 8th, 2021, and 8:00 on June 14th, 2021. During the experiment, there was a variable internal gain alternating between 246 W and 925 W, as shown in Figure 4-1. Before June 11th, 2021, there were periods when the internal gain heat load was switched on and off to attempt temperature control to a specific zone temperature set point. The Air Handling Unit (AHU) was not active during the experiment, and there was no temperature control in Cell 3B. The interior air and surface temperatures fluctuated as a result of the changes in weather conditions as shown in Figure 4-2.

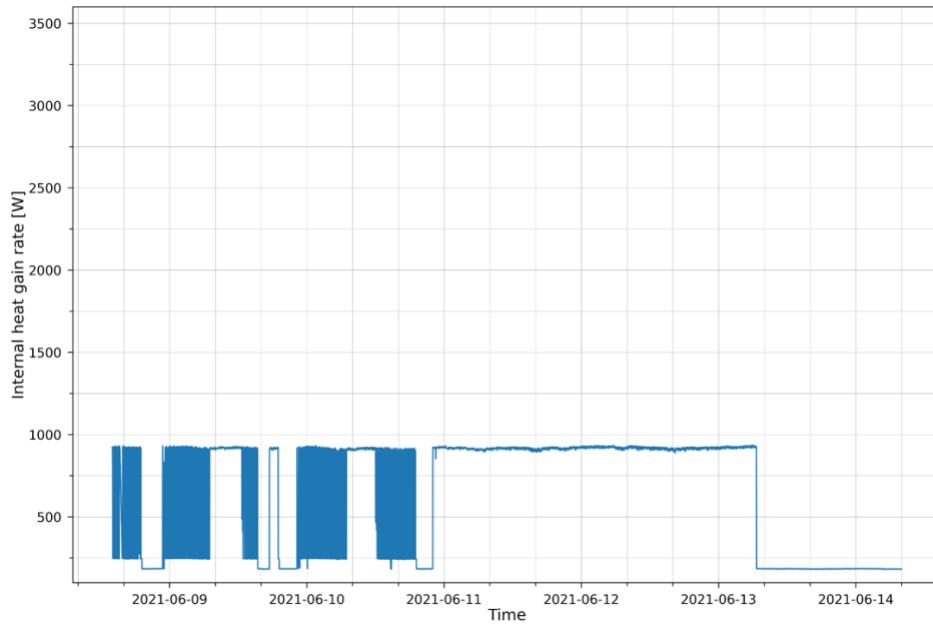


Figure 4-1 Internal heat gain profile during the co-heating experiment.

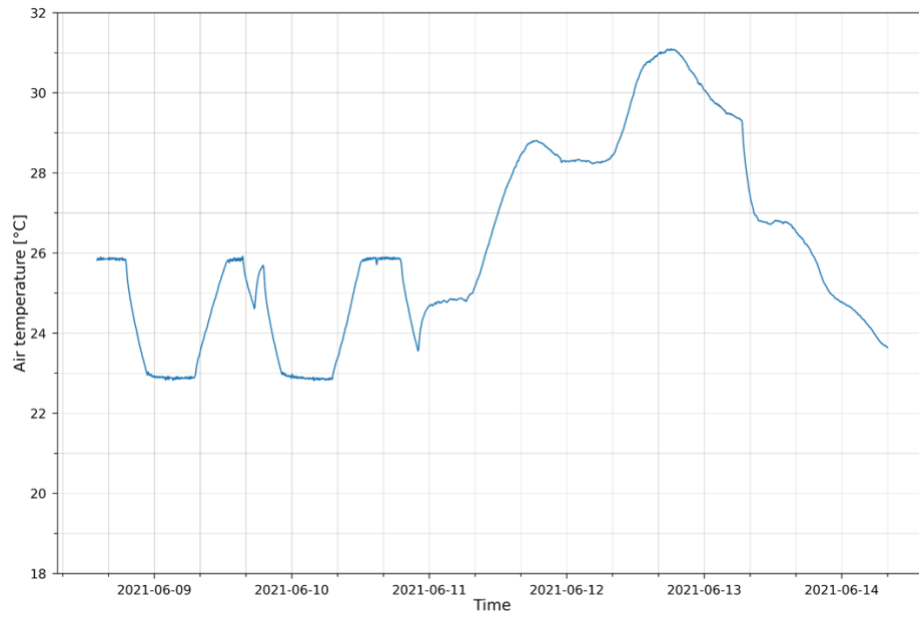


Figure 4-2 Air temperature profile during the co-heating experiment

The conditioned experiment was conducted in FLEXLAB between 00:00 on June 22nd and 00:00 on June 27th 2021. During the experiment, two fan coil units (FCUs) were active trying to maintain the air temperature in Cell 3B at 20° C. At the beginning, there was a small internal gain at 345 W. At 15:00 on June 25th, two additional space heaters were turned on resulting in an internal heat gain around 3,400 W to test the robustness of the energy balance of Cell 3B (Figure 4-3). There were 4 glitches in the control system during that period which resulted in short term temperature fluctuations (Figure 4-4).

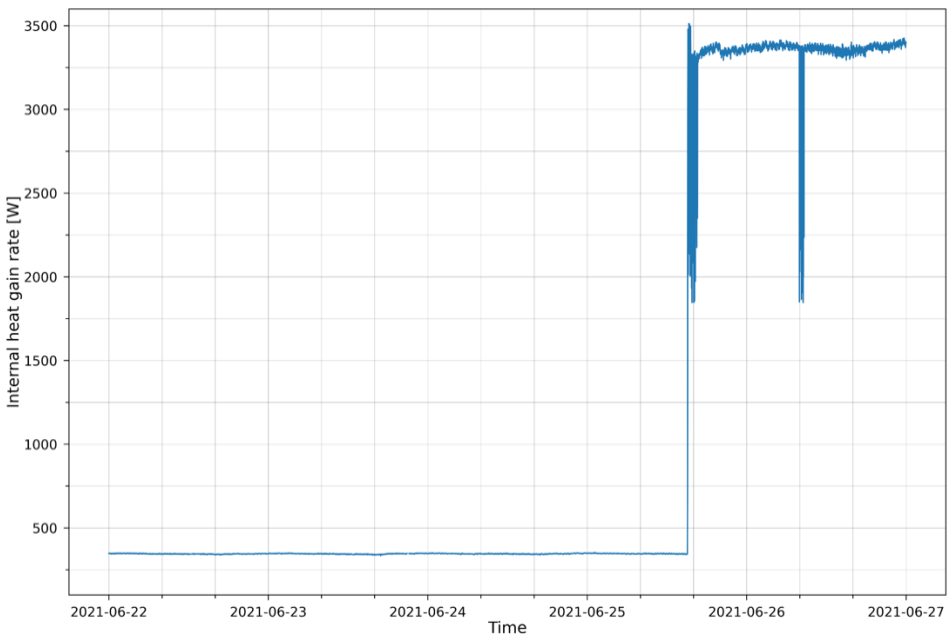


Figure 4-3 Internal heat gain profile during the conditioned experiment.

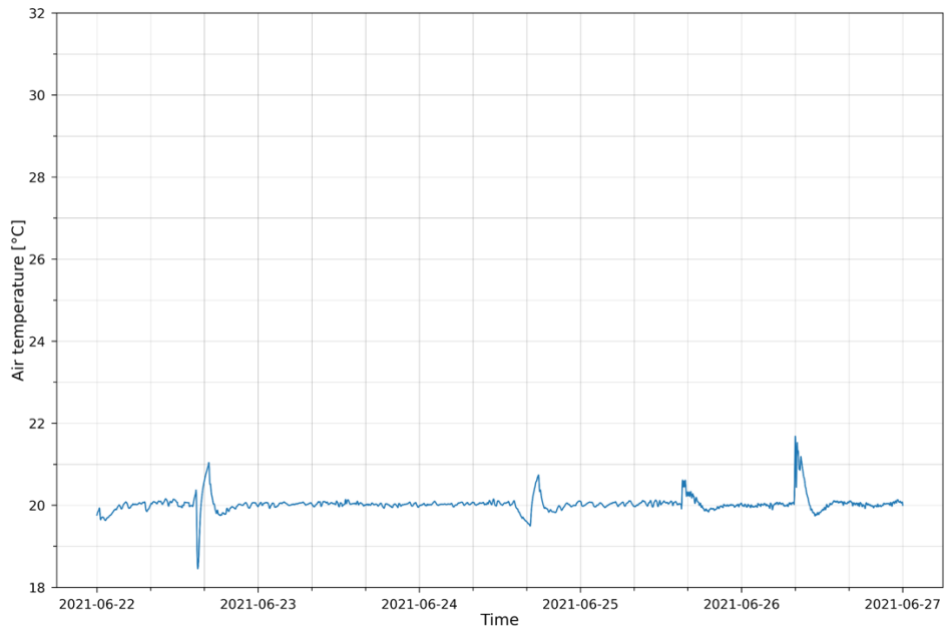


Figure 4-4 Air temperature profile during the conditioned experiment.

The variables measured in these two experiments can be divided into three groups, i.e., input variables, direct validation variables, and indirect validation variables. They will be introduced in detail in the following sections. The characteristics and location of each sensor used to measure these variables are presented in two files named “Meta data.xlsx” and “Sensor locations.xlsx”, respectively, that are contained in the dataset.

4.1 Input Variables

The input variables serve as the inputs to the building energy models regardless of the validation method selected by the users.

4.1.1 Weather

The measurements listed in Table 4-1 were made on site at FLEXLAB, using a weather station installed on the roof of Test Bed 2.

Table 4-1 Meteorological measurements made on site at FLEXLAB.

VARIABLE	UNIT
Dry bulb temperature	°C
Dew point temperature	°C
Wind direction	degrees
Wind speed	m/s
Global and diffuse hemispheric solar radiation rate per area	W/m ²
Direct normal solar radiation per area	W/m ²
Atmospheric pressure	mbar
Horizontal sky infrared radiation rate per area	W/m ²

4.1.2 Other Input Variables

Table 4-2 shows the input variable format and descriptions of the input variables calculated by the 10-minute average from sensor measurements inside Cell 3B. All references to time in this specification and the associated files are to Pacific Standard Time (PST). No corrections were applied for Daylight Savings Time. The AHU was not active during the experiment described in this document. The diffusers of the AHU were blocked in Cell 3B and all dampers were closed.

Table 4-2 Input variables.

No	VARIABLE	DESCRIPTION
1	Drop Ceiling Exterior Surface Temperature [°C]	Surface temperature measurements on top of the drop ceiling insulation
2	Floor Exterior Surface Temperature [°C]	Surface temperature measurements between the topping slab and the insulation, above the topping slab.
3	Temporary North Wall Exterior Surface Temperature [°C]	Surface temperature measurements on the far side of the temporary north wall
4	West Wall Exterior Surface Temperature [°C]	Surface temperature measurements on the far side of the west wall
5	East Wall Exterior Surface Temperature [°C]	Surface temperature measurements on the outside of the east wall
6	South Wall Exterior Surface Temperature [°C]	Surface temperature measurements on the outside of the south wall

7	Ground temperature [°C]	Temperature measurements at different depths and locations of the slab
8	Internal heat gain [W]	The sum of all plug load heat sources in Cell-3B
9	Ventilation heat transfer rate [W]	The calculated heat transfer rate due to the forced ventilation of the duct blaster

Figures Figure 4-5, Figure 4-6, Figure 4-7 show the profiles of the input variables in Table 4-2 in the conditioned experiment.

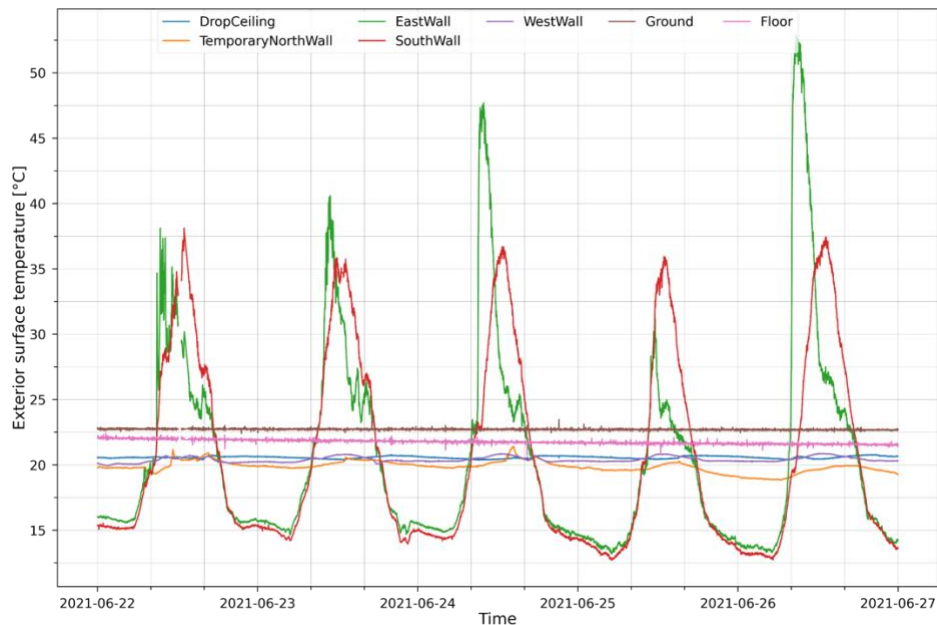


Figure 4-5 Exterior surface temperature profiles during the conditioned experiment.

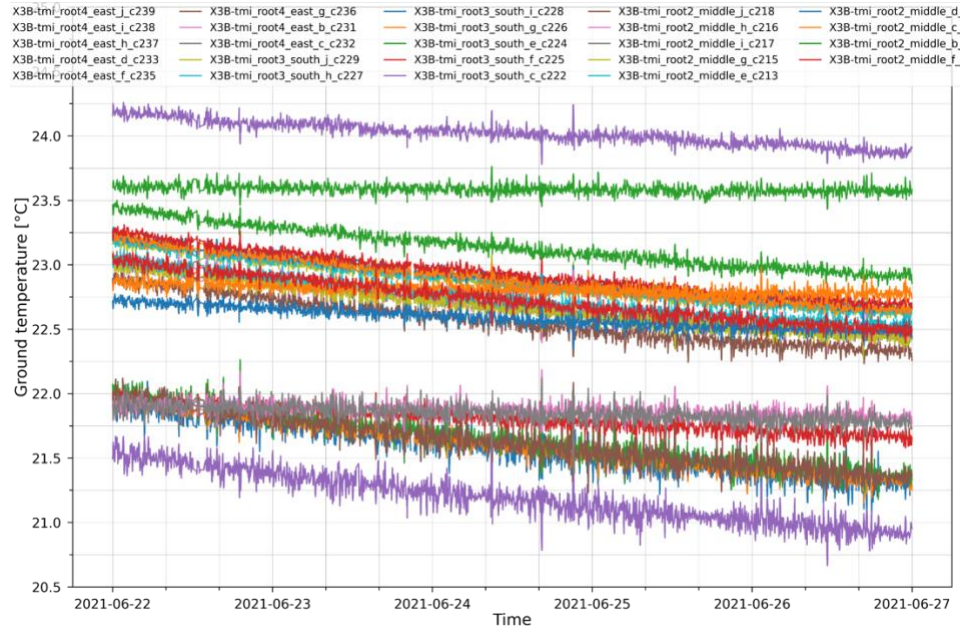


Figure 4-6 Ground temperature profiles during the conditioned experiment. Temperatures are taken up to 380 mm below the top of the slab.

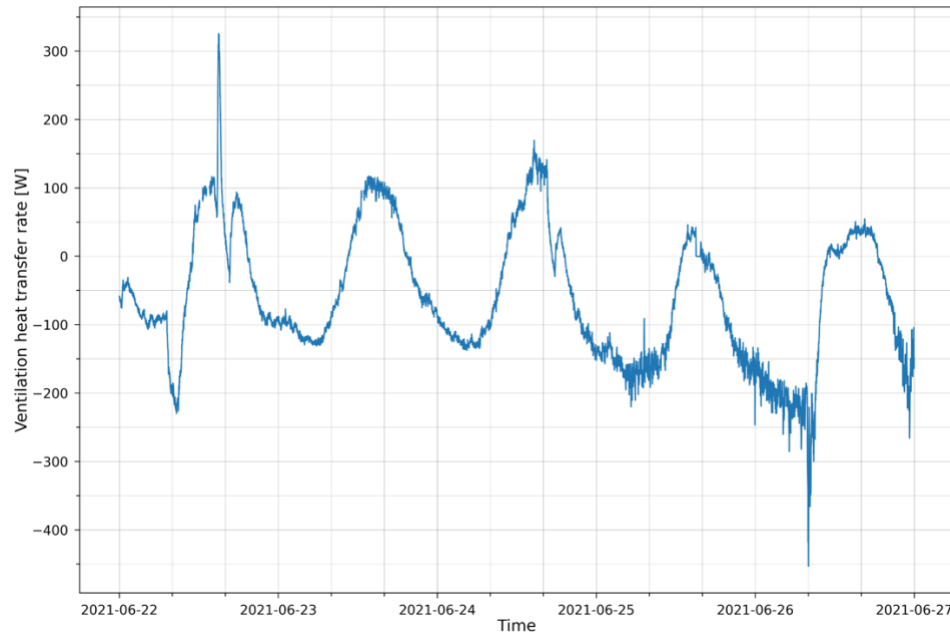


Figure 4-7 Ventilation heat transfer rate profile during the conditioned experiment.

4.2 Direct Validation Variables

The direct validation variables may serve as the inputs to or the outputs of the building energy models depending on which validation method is selected by the user. The validation methods will be introduced in Section 5. The direct validation variables are summarized in Table 4-3. The mean indoor air temperature profile is shown in Figure 4-2 and Figure 4-4. The profiles of all the temperature measurements on the stratification trees during the conditioned experiment are shown in Figure 4-8.

Figure 4-9 shows the total cooling rate profile provided by the two fan coil units during the conditioned experiment.

Table 4-3 Direct validation variables.

No	VARIABLE	DESCRIPTION
1	Indoor Air Temperature [°C]	The mean of the air temperature measured at different heights on four stratification trees
2	Total Cooling Rate [W]	The calculated total cooling rate provided by two fan coil units

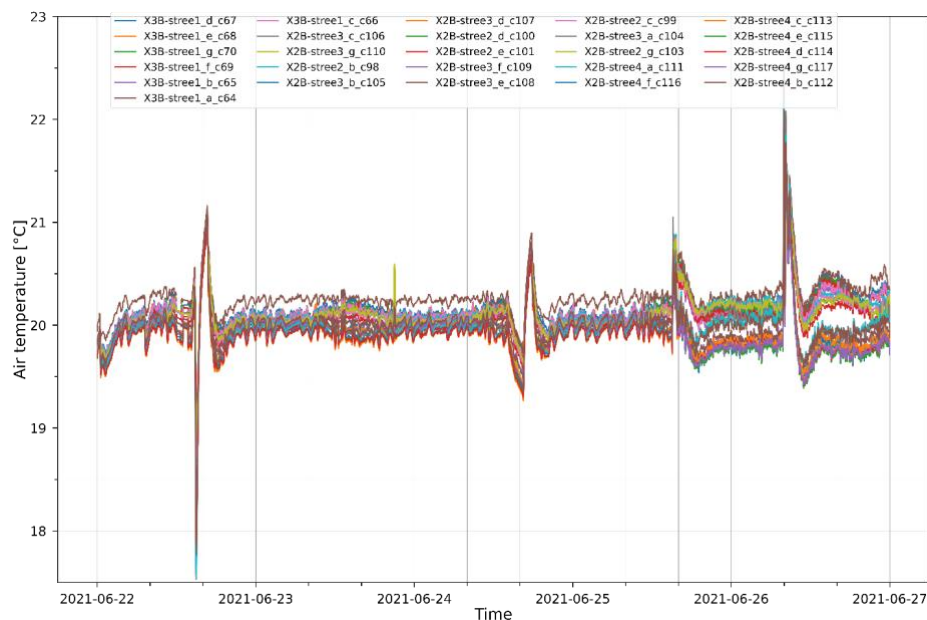


Figure 4-8 Air temperature profiles measured on the stratification trees during the conditioned experiment.

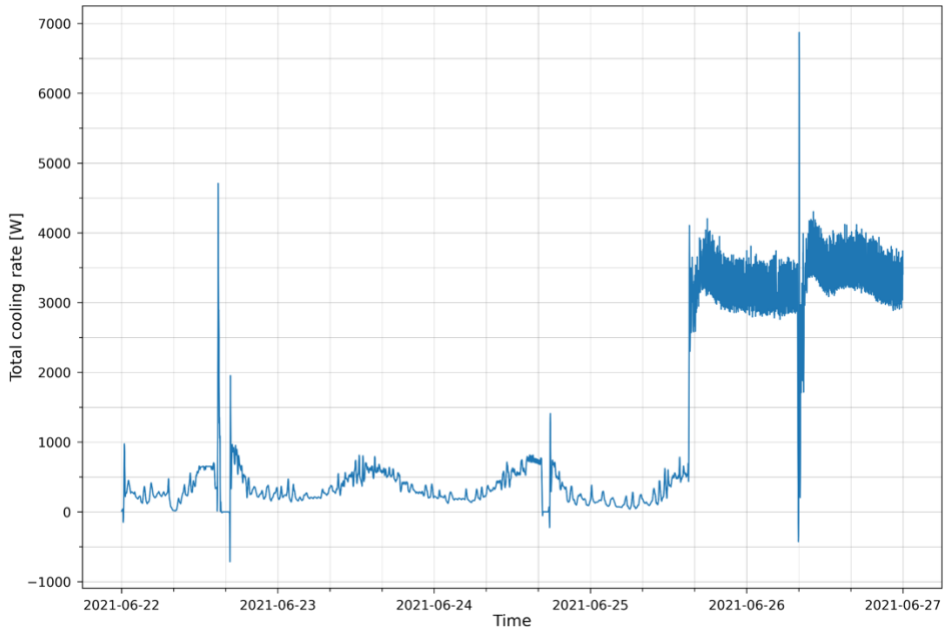


Figure 4-9 Total cooling rate profile during the conditioned experiment.

4.3 Indirect Validation Variables

The indirect validation variables are the state variables of the building energy models. In most cases, they are not the primary outputs of the building energy models but can be output by most BEM programs on the market. The indirect validation variables are summarized in Table 4-4. The south wall interior surface temperature profiles during the conditioned experiment are shown in Figure 4-10 as an example. Surface heat transfer rate profiles during the conditioned experiment are shown in Figure 4-11.

Table 4-4 Indirect validation variables.

No	VARIABLE	DESCRIPTION
1	DropCeiling Interior Surface Temperature [°C]	Surface temperature measurements at the bottom of the drop ceiling panels
2	Floor Interior Surface Temperature [°C]	Surface temperature measurements on top of the topping slab
3	Temporary North Wall Interior Surface Temperature [°C]	Surface temperature measurements on the inside of the temporary north wall
4	West Wall Interior Surface Temperature [°C]	Surface temperature measurements on the inside of the west wall
5	East Wall Interior Surface Temperature [°C]	Surface temperature measurements on the inside of the east wall
6	South Wall Interior Surface Temperature [°C]	Surface temperature measurements on the inside of the south wall
7	Drop Ceiling Surface Heat Transfer Rate [W]	Total heat transfer rate through the drop ceiling

8	Floor Surface Heat Transfer Rate [W]	Total heat transfer rate through the floor
9	Temporary North Wall Surface Heat Transfer Rate [W]	Total heat transfer rate through the temporary north wall
10	West Wall Surface Heat Transfer Rate [W]	Total heat transfer rate through the west wall
11	East Wall Surface Heat Transfer Rate [W]	Total heat transfer rate through the east wall
12	South Wall Surface Heat Transfer Rate [W]	Total heat transfer rate through the south wall

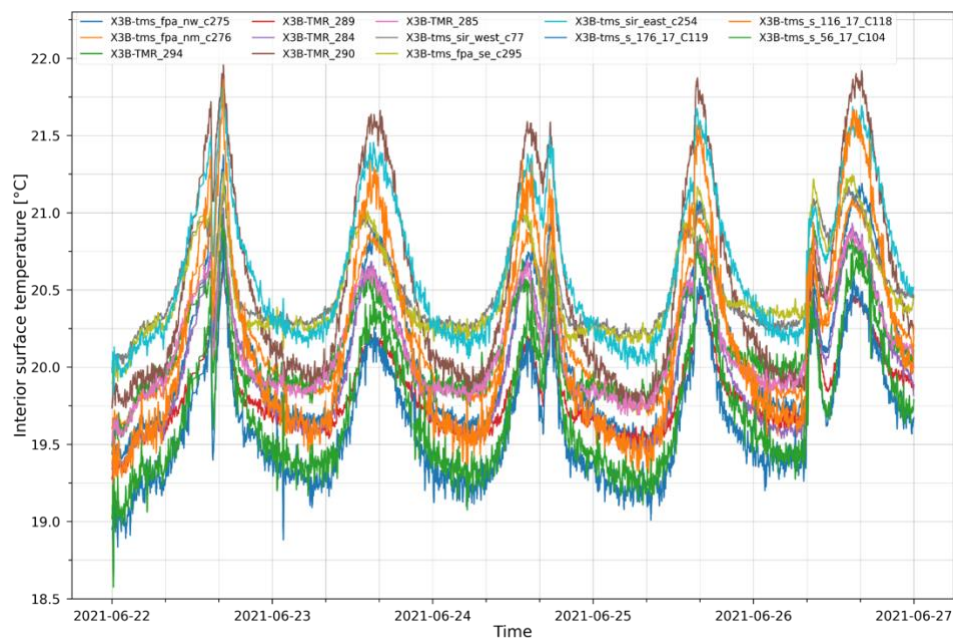


Figure 4-10 South wall interior surface temperature profiles during the conditioned experiment.

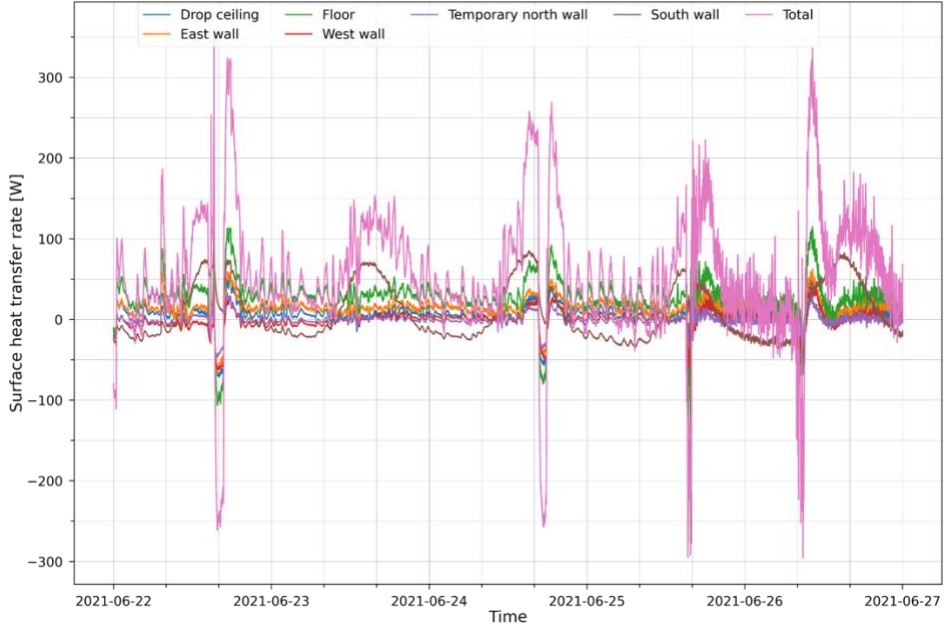


Figure 4-11 Surface heat transfer rate profiles during the conditioned experiment.

4.4 Energy Balance of the Measured Data

One way to verify the measured data is by using the law of energy conservation. If there is no appreciable error in the measured data, the energy balance of Cell 3B, as represented by the following equation, should hold:

$$V_3 \rho_{\text{air}} c p_{\text{air}} \frac{dT_3}{dt} - P_{\text{vent}} - P_{\text{cond}} - P_{\text{internal}} - P_{\text{cooling}} = 0 \quad (10)$$

where $V_3 \rho_{\text{air}} c p_{\text{air}} \frac{dT_3}{dt}$ is the energy storage rate of the air in Cell 3B [W]; P_{vent} is the ventilation heat transfer rate [W]; P_{cond} is the conductive heat transfer rate [W]; P_{internal} is the internal heat gain rate [W]; and P_{cooling} is the cooling rate [W].

Figure 4-12 shows all heat transfer rate profiles and the energy balance profile during the conditioned experiment. In order to test the robustness of the energy balance model, we conducted the experiment at two different states. From 00:00 June 22nd to 15:00 June 25th, the internal heat gain was entirely from the electric equipment and was at a level around 345 W. At 15:00 June 25th, two electric heaters were turned on, increasing the internal heat gain rate to around 3370 W. Since the internal heat gain rate and cooling rate were dramatically higher than other heat transfer rates in the second state, their profiles are hidden in Figure 4-13 to show other profiles more closely. We can see that the air energy storage rate is close to 0 the whole time. The energy balance, despite some peaks due to the control glitches of the fan coil units, fluctuated around 0. We use two indices to measure how well the energy balance is achieved, which are the CVRMSE and the normalized mean bias error (NMBE), as recommended by ASHRAE Guideline 14 [2]. The NMBE is calculated using the following equation:

$$\text{NMBE} = \left(\frac{\sum (y_i - 0)}{n} \right) / \max(|P_{\text{vent}}|) \quad (11)$$

where y_i is the energy balance value of the i^{th} time step [W]; and n is the number of timesteps. When normalizing root mean squared error and mean bias error, we selected the maximum absolute value of

ventilation heat transfer as the denominator. The maximum absolute value of other natural heat transfer rates (e.g., conductive heat transfer rate) can also be selected as the denominator. For a data interval of 30 minutes, the CVRMSE is 32.8% and the NMBE is 3.79%. This proves that energy balance is achieved for Cell 3B during the conditioned experiment. The co-heating experiment did not achieve a satisfactory energy balance and is not further analyzed in this document. The data is however available in the Github repository.

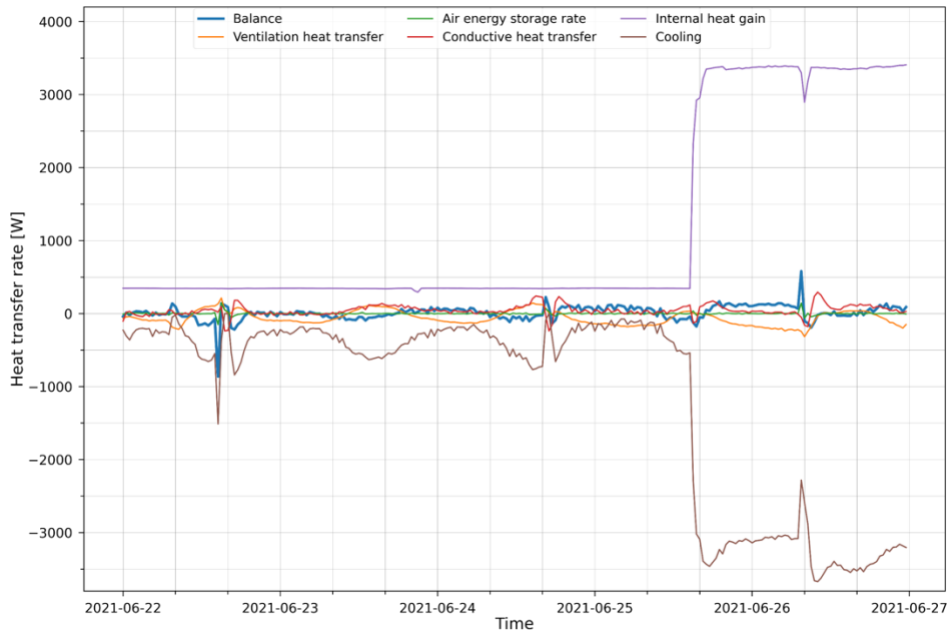


Figure 4-12 Heat transfer rate profiles and the energy balance profile during the experiment.

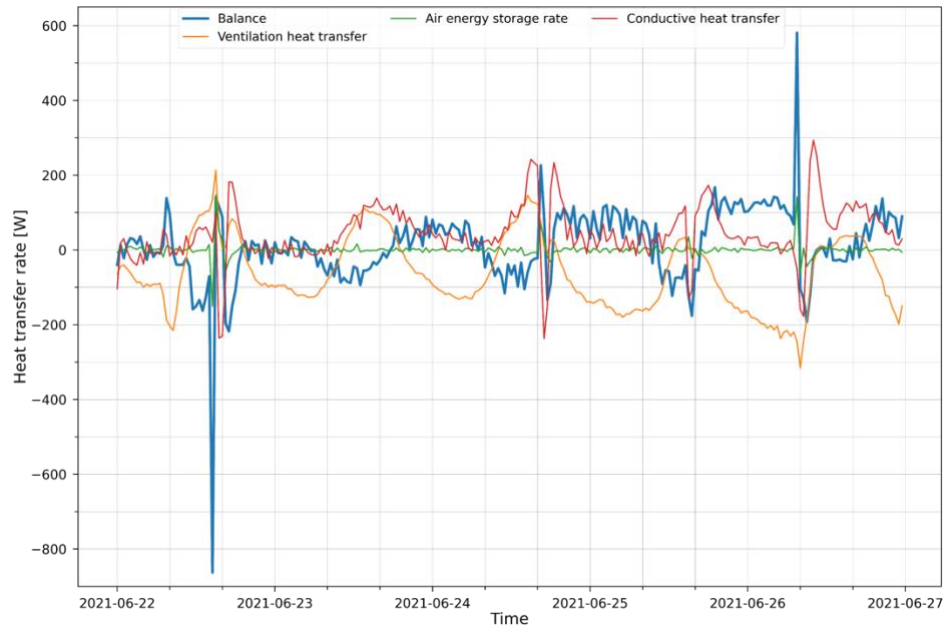


Figure 4-13 Heat transfer rate profiles except those of internal heat gain rate and cooling rate and the energy balance profile during the experiment.

5. Approaches to Using the Data Set

This section of this report describes how to validate BEM programs using the dataset provided by this project. Since the conditioned experiment results (with the fancoils operating) passed the energy balance test, while the co-heating experiment results did not, we recommend the users to use the data from 00:00 June 22nd to 00:00 June 27th for BEM programs validation. The co-heating experiment data can be used to validate components such as individual walls.

5.1 Approaches to Using the Dataset

The users should be aware of the following before using the dataset:

- The model's dimensions described in this document are internal dimensions of all the three zones (Cell 3B, north zone and ceiling/plenum).
- If BEM program allows for preconditioning, such as iterative simulation of an initial time period until temperatures and/or fluxes stabilize at initial values, then that capability should be used.
- The timestamps in the data are in PST. Daylight savings time plays no role in the tests.

Figure 5-1 shows the three validation approaches using the dataset provided by this project. In all three approaches, the building geometry and construction information is used to construct the building energy model and input variables (including weather data, ventilation rate, and internal heat gain rate) are used as the inputs to the building energy model. Afterwards, the three approaches adopt different additional inputs and compare different outputs.

The first approach is called the forward validation approach. In this approach, the measured indoor air temperature sequence should be input into the building energy model as the cooling/heating setpoint schedule. Then, a simple cooling/heating system sometimes called “purchased air” or “ideal loads” should be selected as the output and compared with the measured total cooling rate of the fan coil units.

The second approach is the opposite of the first one and hence called the backward validation approach. In this approach, the measured cooling/heating rate should be used as additional inputs and the indoor air temperature output by the building energy model should be compared with the measured indoor air temperature.

The third approach is called the indirect validation approach, in which the measured cooling/heating rate should be used as additional inputs and the state variables such as the interior surface temperature and the conductive heat fluxes through the building surfaces should be selected as the output. Then, the values output by the building energy model should be compared with the corresponding measured ones. Since these state variables are seldom the primary output of building energy models, this approach is called the indirect validation approach.

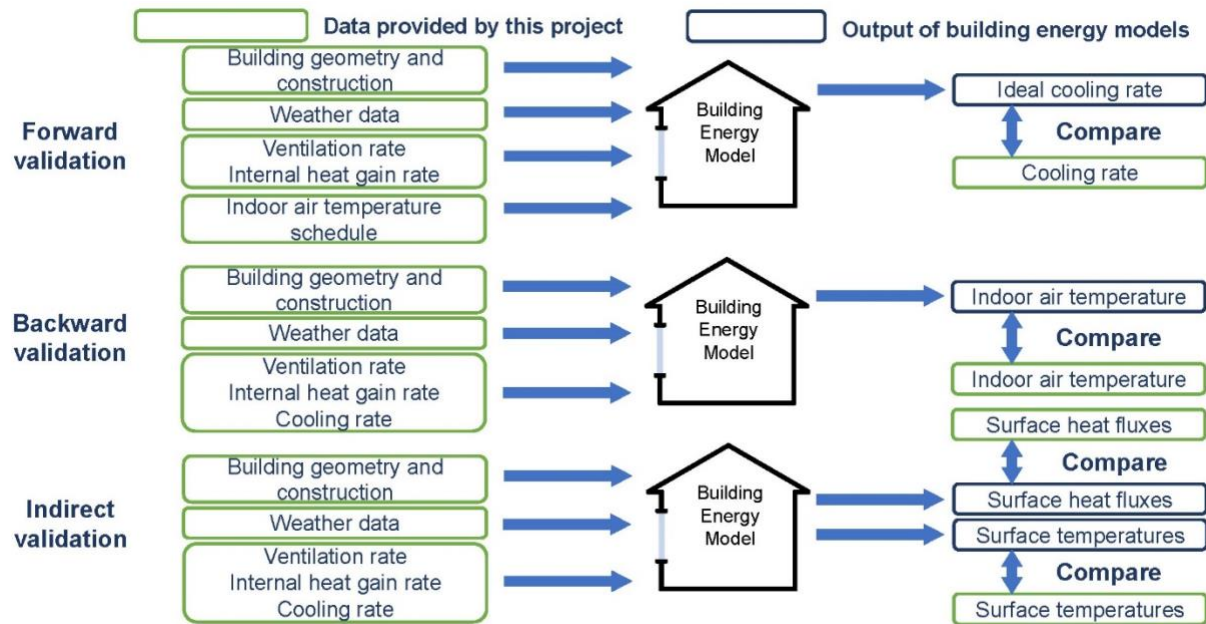


Figure 5-1 Validation approaches using the dataset provided by this project.

APPENDIX A. Architectural Drawings of Cell B

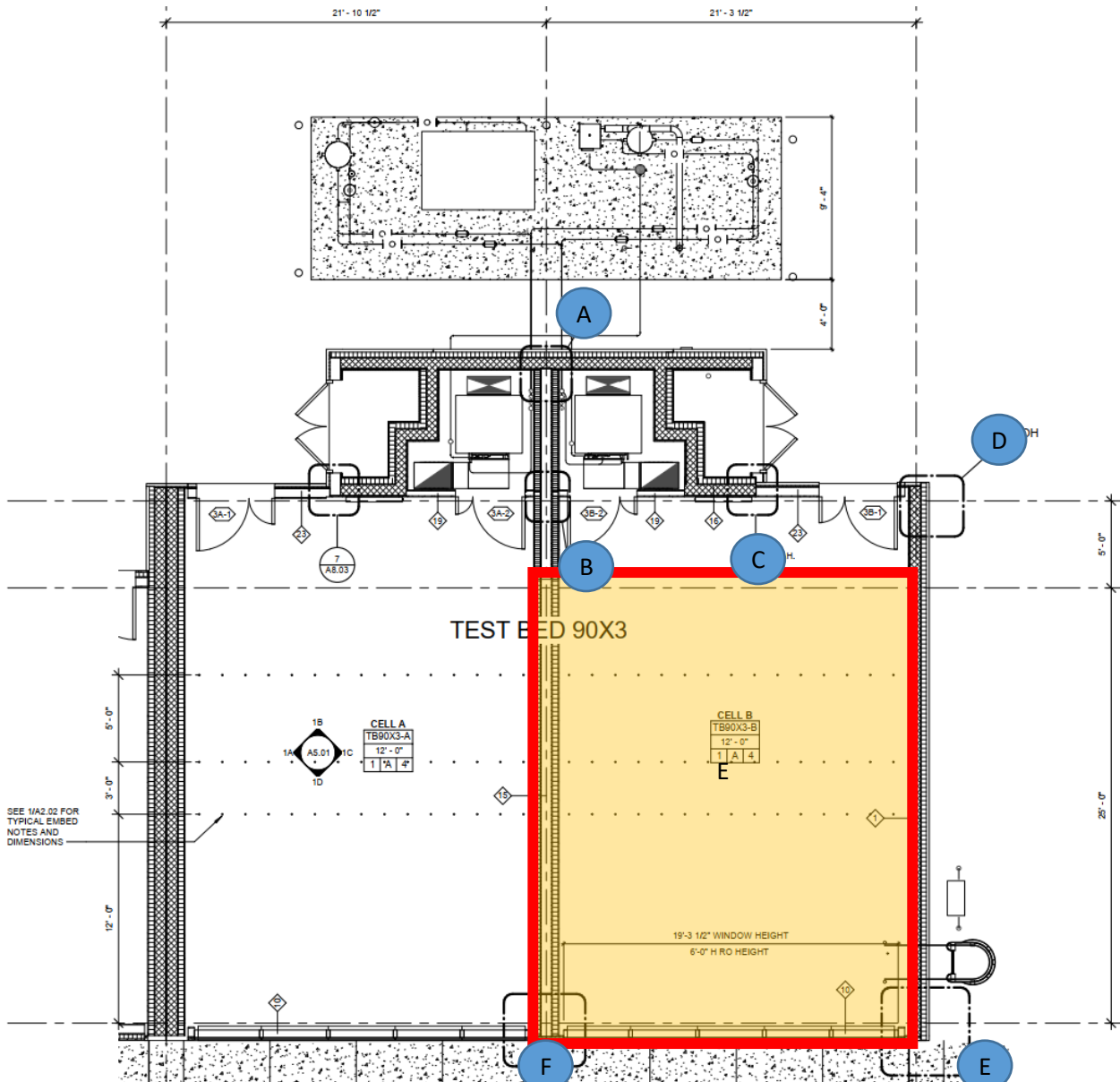


Figure A-1 Detailed architectural drawings of Cell A and Cell B. Cell B is shaded on the right. Taken from the FLEXLAB construction drawings by Stantec.

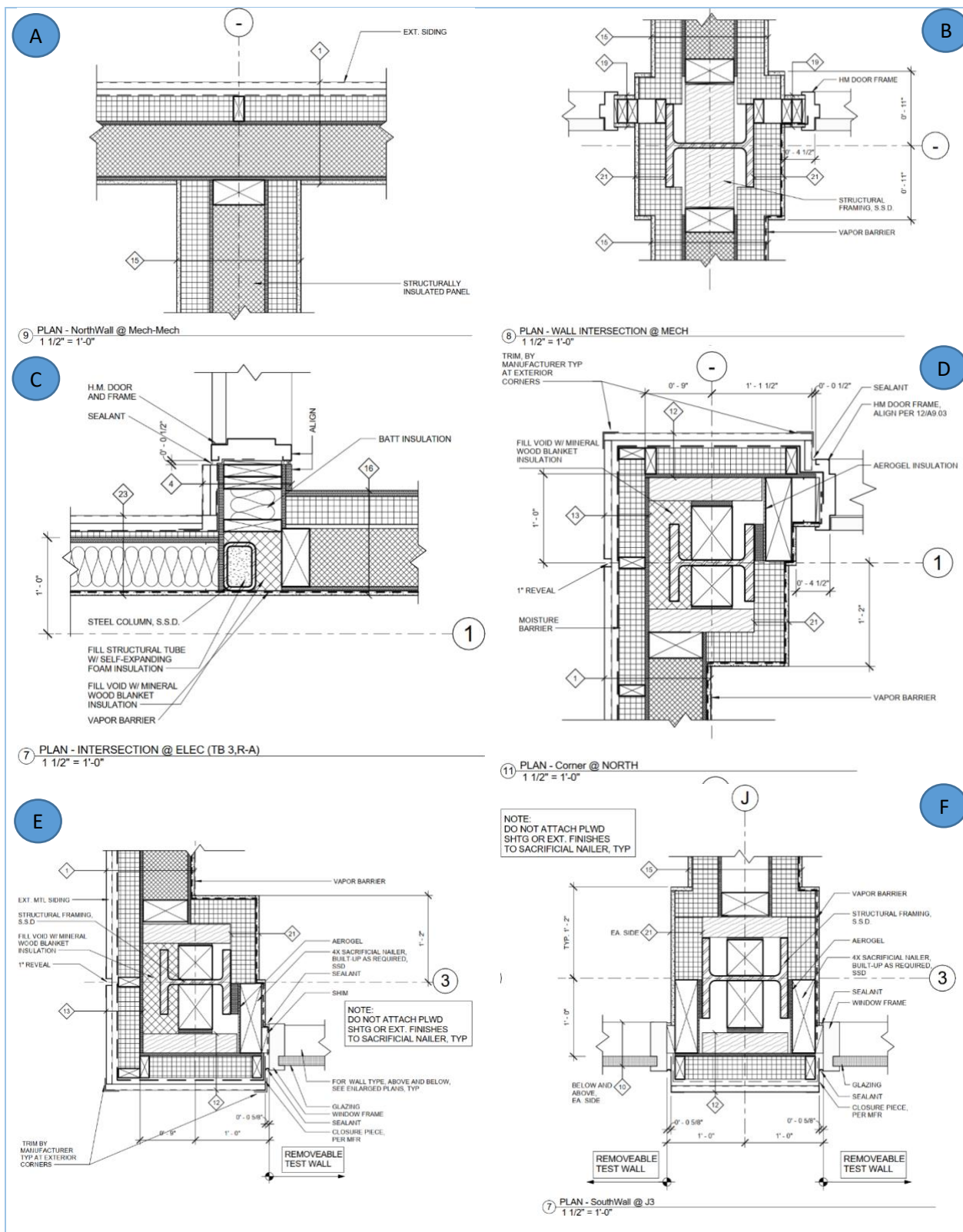


Figure A-2 Detailed architectural drawings of Cell B wall intersections and corners.

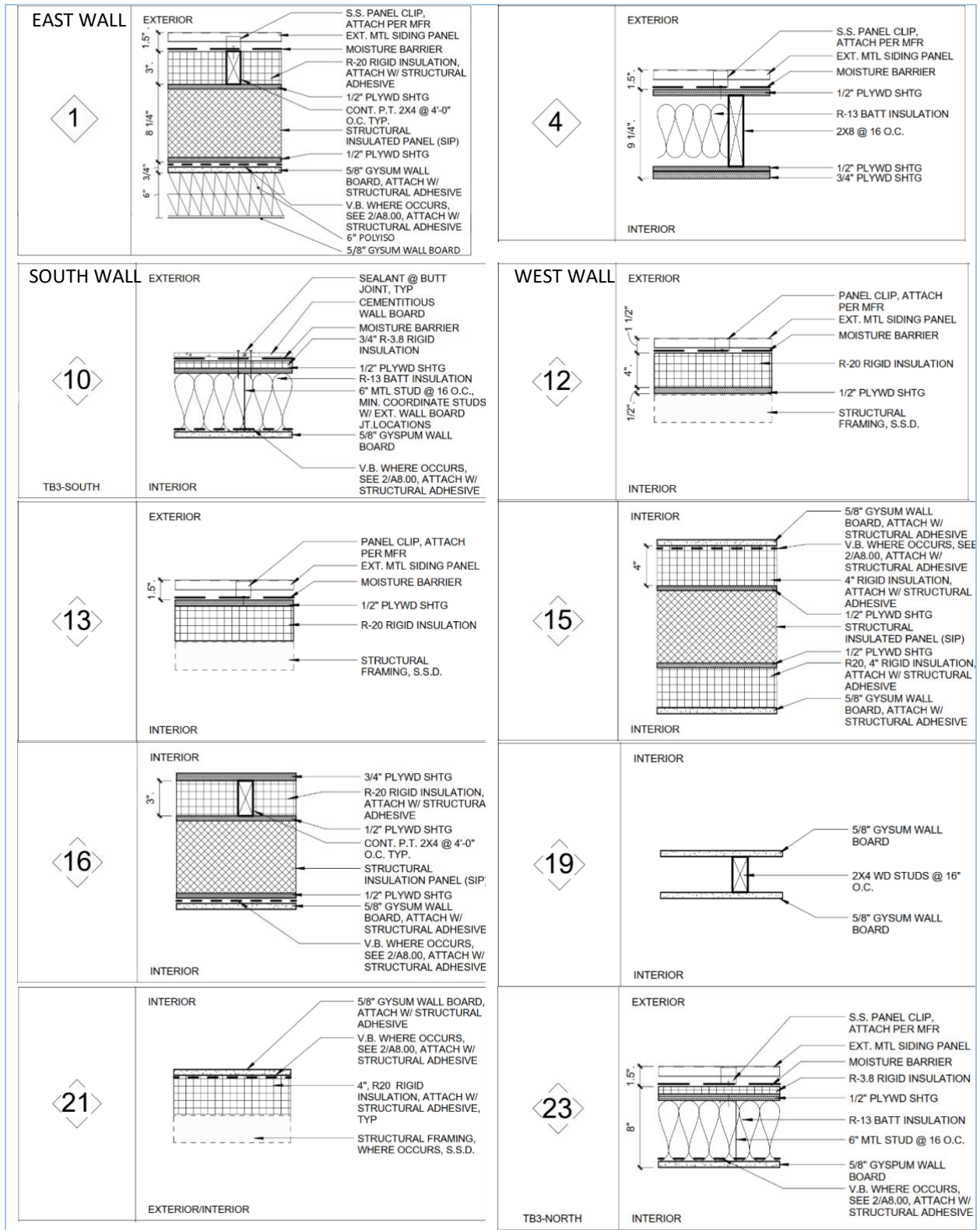


Figure A-3 Detailed architectural drawing of the wall sections.

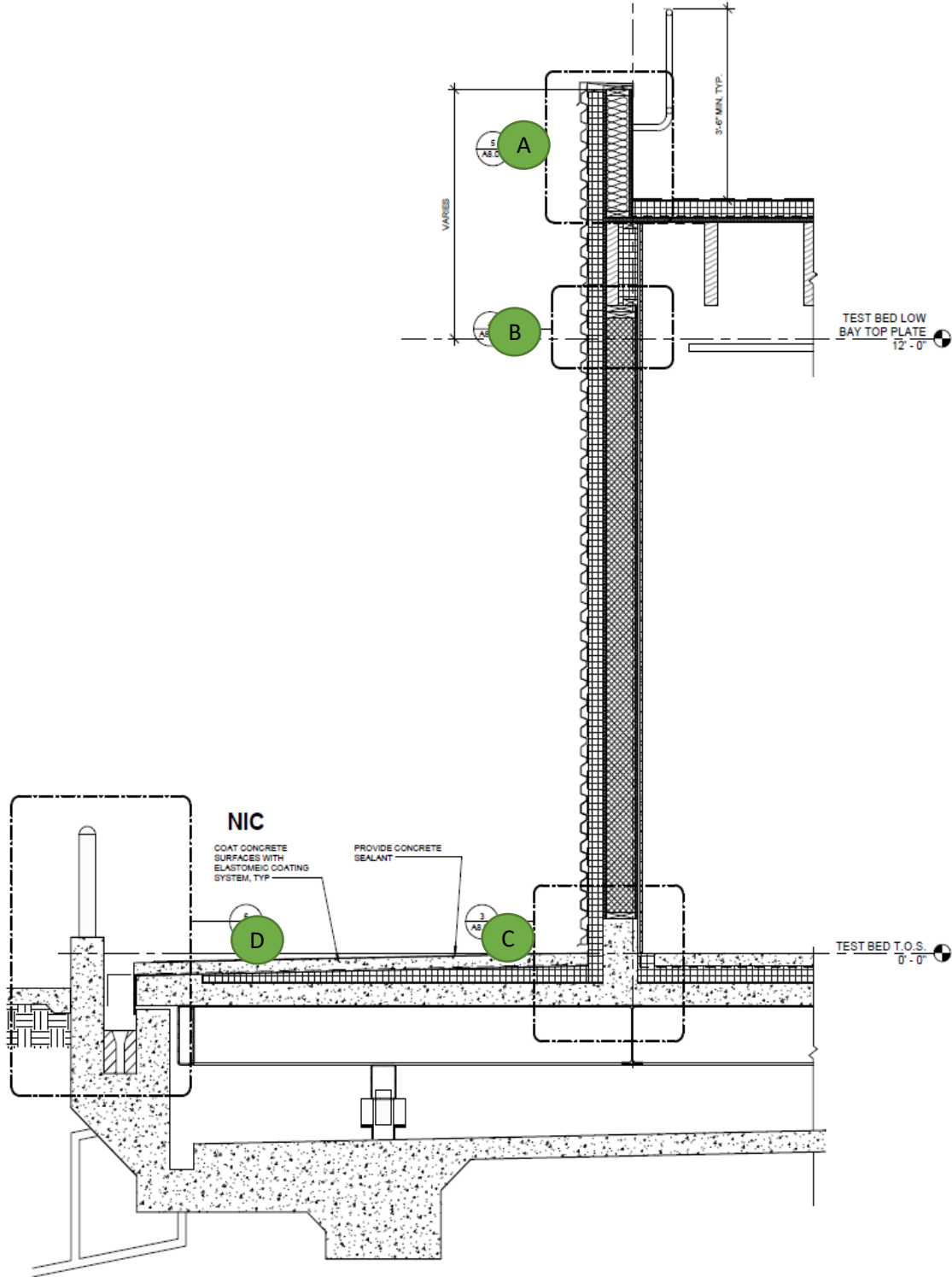


Figure A-4 Detailed architectural drawing of vertical cross-sections

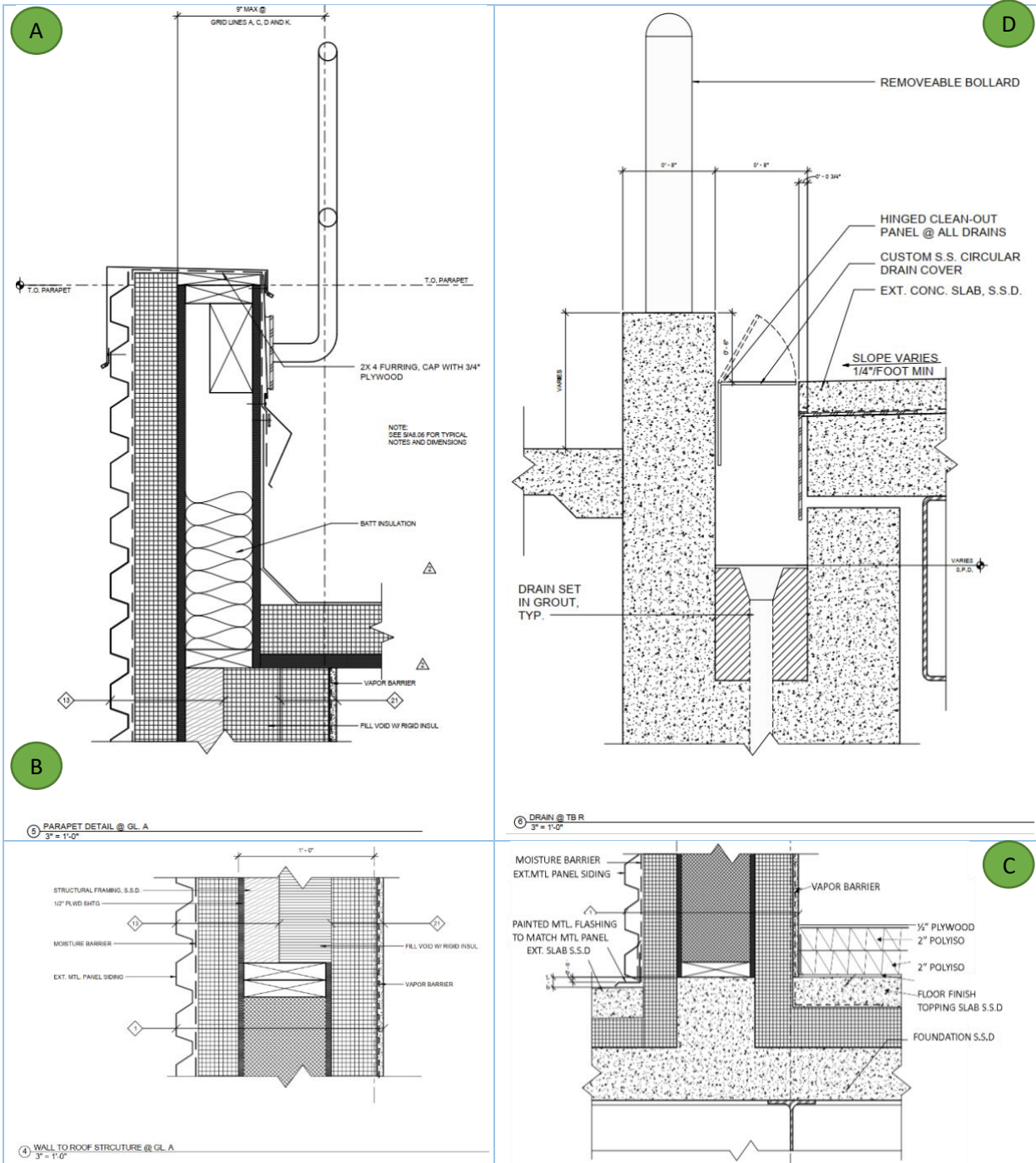
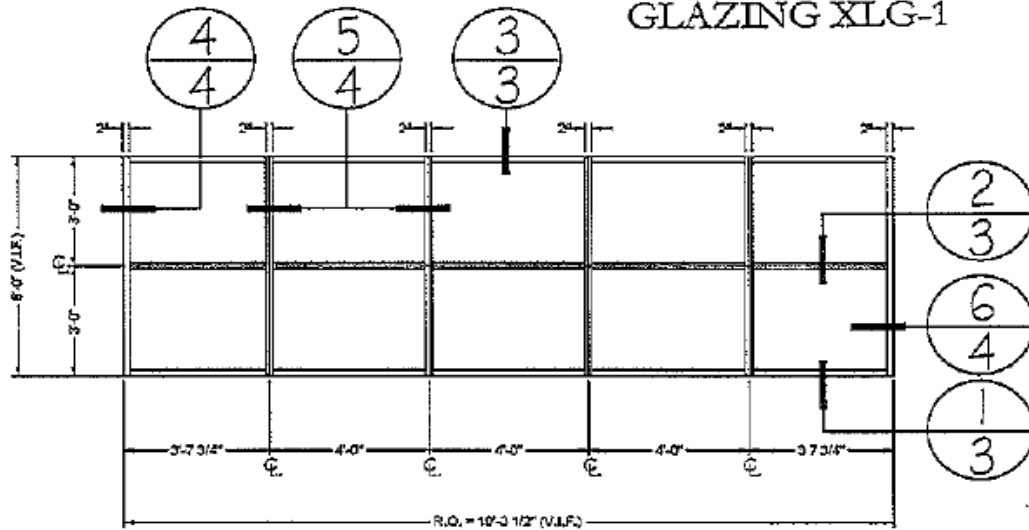


Figure A-5 Detailed architectural drawings of vertical corner cross sections.

EFCO SERIES 403
GLAZING XLG-1



STOREFRONT SF-1/XGL-1 FRONT ELEV.

TB-90 X3B -SOUTH

Figure A-6 South wall glazing elevation.

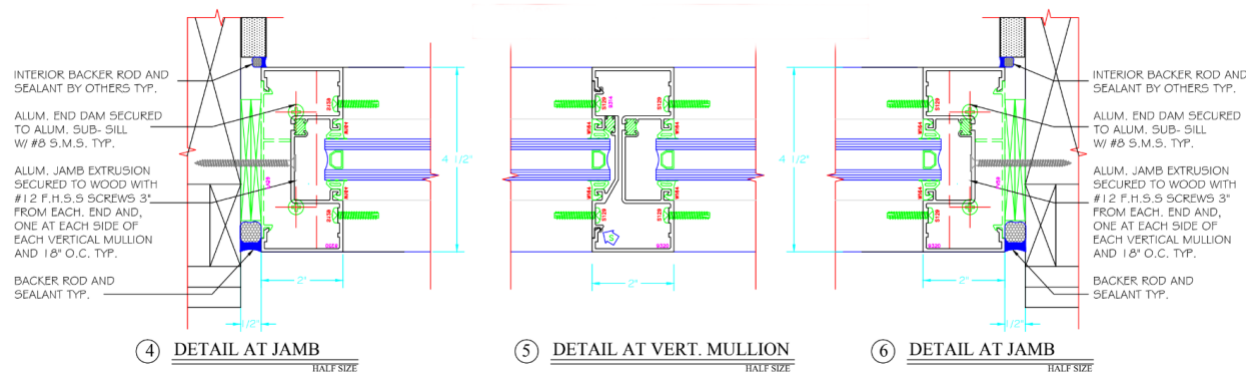


Figure A-7 Horizontal cross-section of window framing on the south walls/windows (These drawings show double glazed windows, during the experiment single glazed windows covered with 2" of polyisocyanurate were used as shown in figures A-10,11).

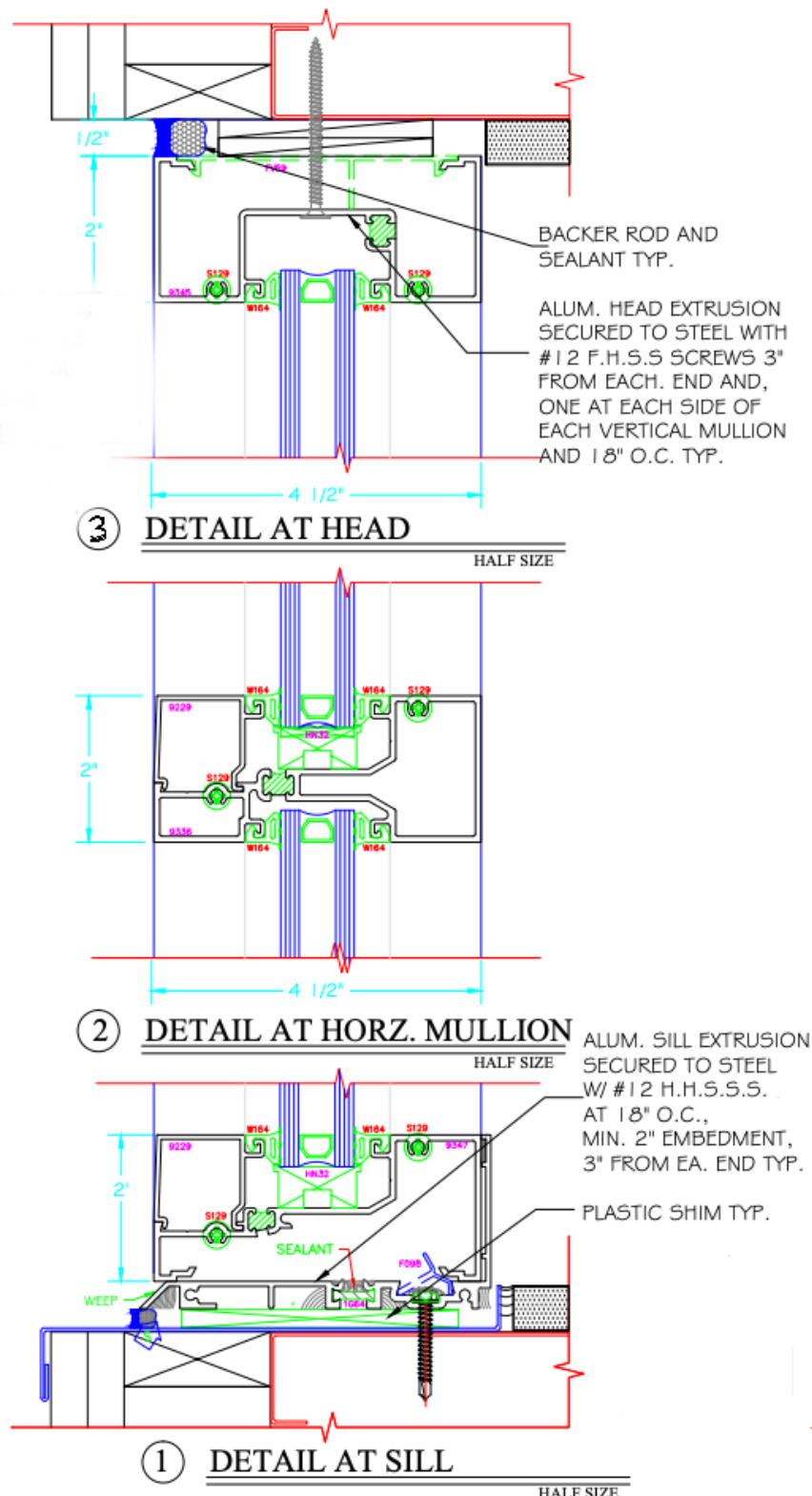


Figure A-8 Vertical cross-section of window framing on the south walls/windows (These drawings show double glazed windows, during the experiment single glazed windows covered with 2" of polyisocyanurate were used as shown in figure A-9,10,11).

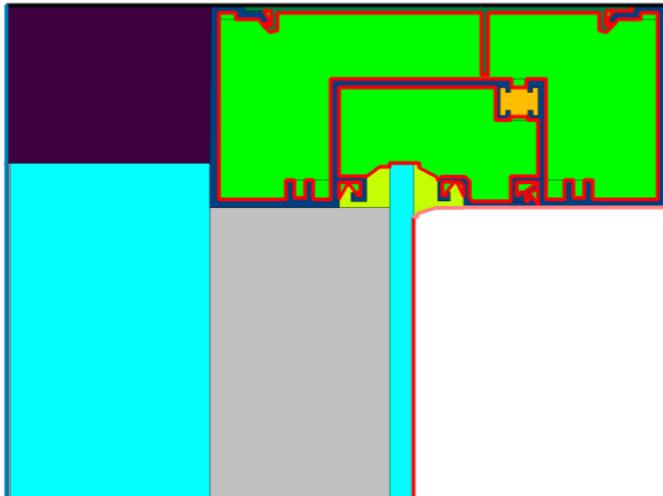


Figure A-9 Head cross-section with single glazing and 2" polyisocyanurate on the outside covering glass and frame.

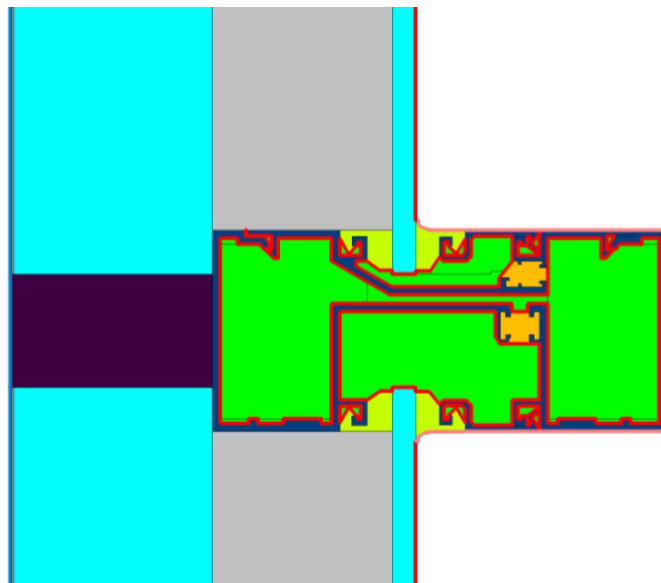


Figure A-10 Intermediate horizontal/vertical mullion cross-section with single glazing and 2" polyisocyanurate on the outside covering glass and frame.

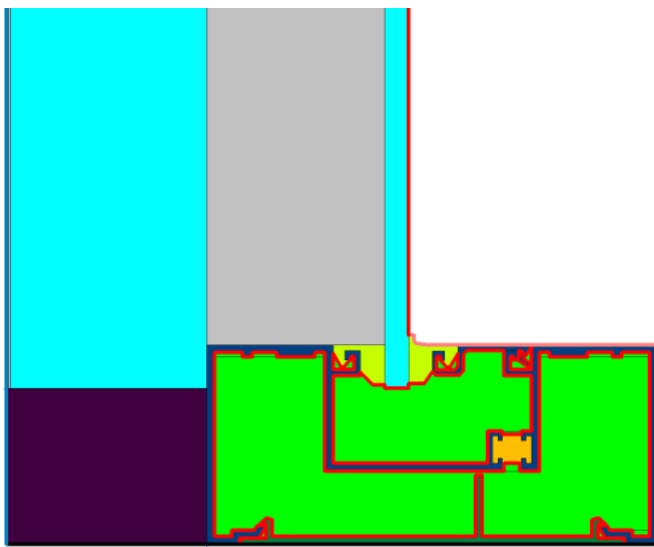


Figure A-11 Sill cross-section with single glazing and 2" polyisocyanurate on the outside covering glass and frame.

The windows were modeled in THERM 7.8.57 and WINDOW 7.8.57. The window wall was separated into 10 different windows. For intermediate horizontal or vertical mullions, the full mullion was modeled in THERM (see Figure A-8), but the heat flow through half of the width of the mullion was attributed to each of the adjacent windows.

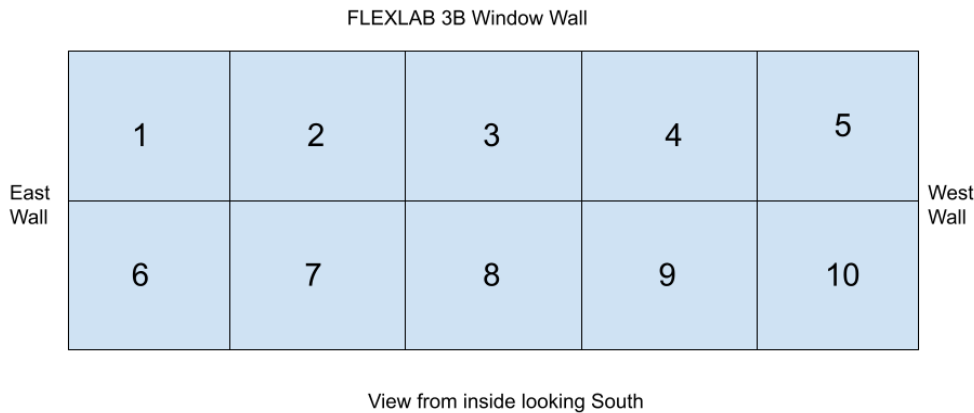


Figure A-12 Window numbering of South Wall windows.

Table A-1 Window sizes and properties, as well as the overall weighted U-value and SHGC.

Window #	width [m]	height [m]	Area [m ²]	U [W/m ² K]	UA[W/K]	SHGC
1	1.12	0.93	1.042	0.351	0.366	0.004
2	1.22	0.93	1.130	0.350	0.396	0.004
3	1.22	0.93	1.130	0.350	0.396	0.004
4	1.22	0.93	1.130	0.350	0.396	0.004

5	1.12	0.93	1.042	0.351	0.366	0.004
6	1.12	0.93	1.042	0.351	0.366	0.004
7	1.22	0.93	1.130	0.350	0.396	0.004
8	1.22	0.93	1.130	0.350	0.396	0.004
9	1.22	0.93	1.130	0.350	0.396	0.004
10	1.12	0.93	1.042	0.351	0.366	0.004
Total			10.949		3.836	
Weighted				U=0.350		SHGC=0.004

Window wall size: width=5.88 m, height=1.86 m

APPENDIX B. Cell 3B Surface and Construction

The figures in this appendix show the detailed geometry and construction of each surface of the building model. The tables record the configurations of the constructions and the properties of the materials. Some surfaces are divided into multiple sections to represent the inhomogeneities in constructions such as structural columns. The users may either follow this detailed modeling method or model the walls with simplified homogeneous equivalent layers. It should be noted that in each figure the shaded area represents the control volume of our energy and mass balance model, i.e., Cell 3B itself. We recommend that only this part be modeled. The rest can be represented by boundary conditions.

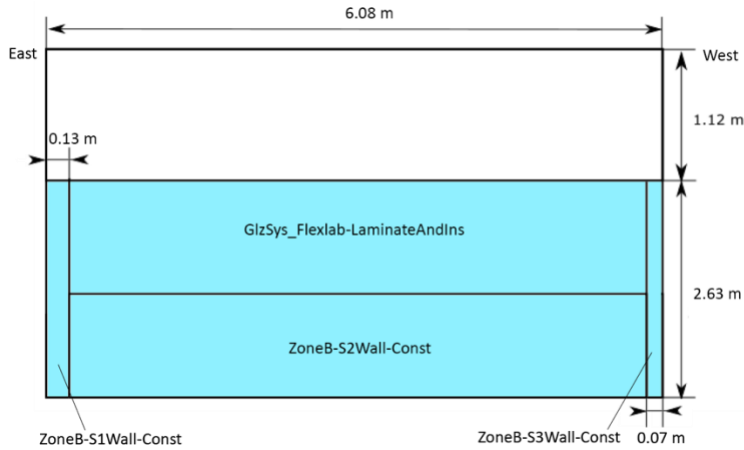


Figure B-1 South wall of Cell 3B, showing both opaque and glazed sections.

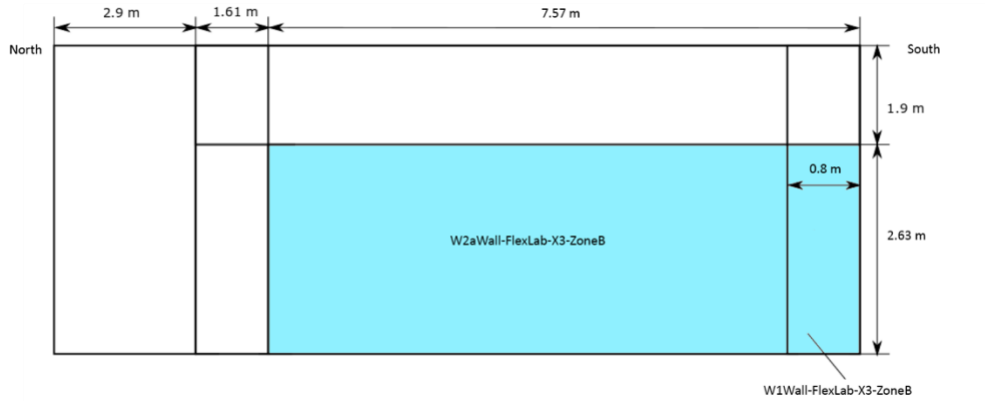


Figure B-2 15 West wall of Cell 3B.

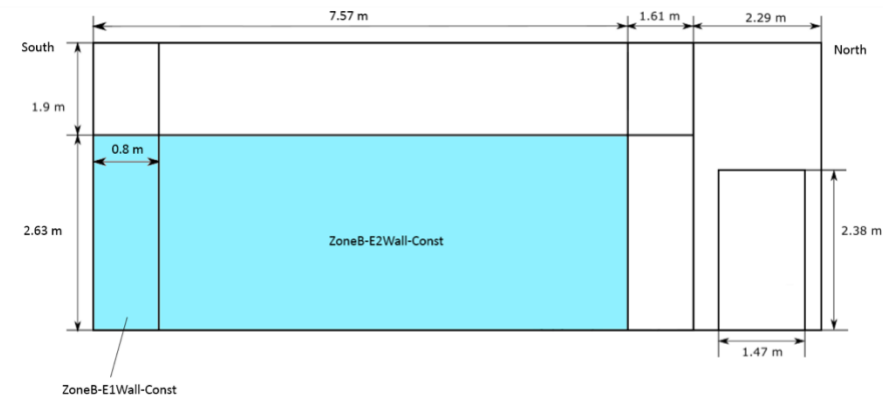


Figure B-3 East wall of Cell 3B.

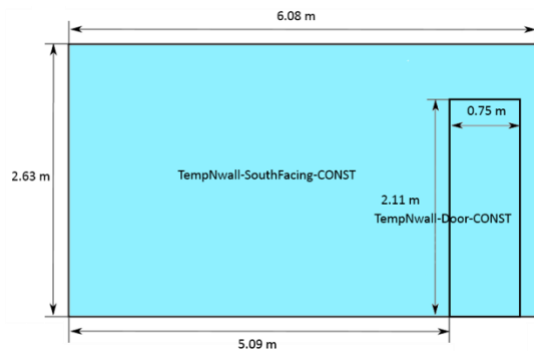


Figure B-4 The "temporary north wall", a foam wall that separates the cell from the ante room.

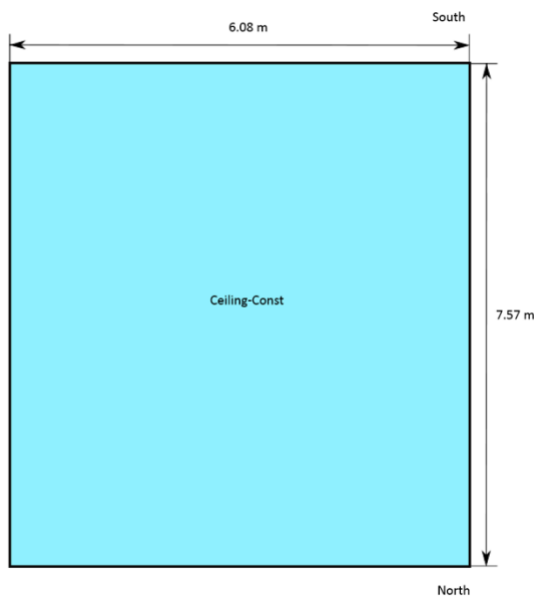


Figure B-5 Drop ceiling of Cell 3B.

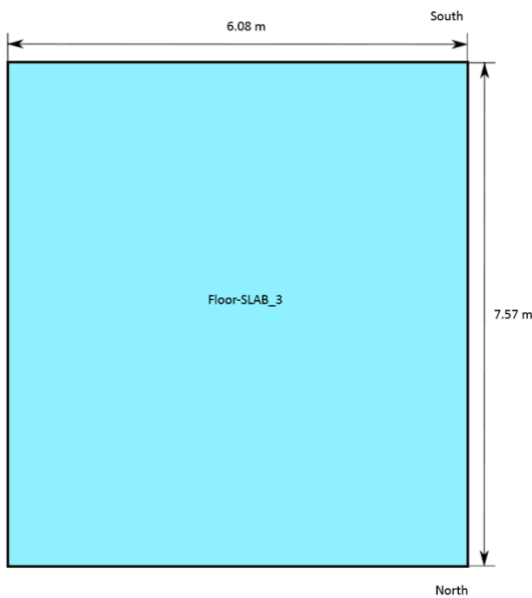


Figure B-6 Floor of Cell 3B.

Table B-1 Construction layers for surfaces.

Surface Name	Outside Layer	Layer 2	Layer 3	Layer 4	Layer 5	Layer 6	Layer 7	Layer 8	Layer 9	Layer 10
Floor-SLAB_1	HW CONCRETE 5"	Slab Horizontal Insulation 5"	Topping Slab 6"							
Floor-SLAB_2	HW CONCRETE 5"	Slab Horizontal Insulation 5"	Topping Slab 6"	Carpet 1/4"	Polyiso 2"	Polyiso 2"	Plywood 1/2"			
Floor-SLAB_3	HW CONCRETE 5"	Slab Horizontal Insulation 5"	Topping Slab 6"	Polyiso 2"	Polyiso 2"	Plywood 1/2"				
Ceiling-Const	Cotton Batt 7"	Acous Tile 3/4"								
FloorPln m-Const	Acous Tile 3/4"	Cotton Batt 7"								
TempNw all-SouthFacing-CONST	Gypsum Board 1/2"	Polyiso 2.25" TempNw all SouthFacing	Polyiso 2.25" TempNw all SouthFacing	Gypsum Board 1/2"						
TempNw all-NorthFacing-CONST	Gypsum Board 1/2"	Polyiso 2.25" TempNw all SouthFacing	Polyiso 2.25" TempNw all NorthFacing	Gypsum Board 1/2"						
Roof-Const	Roof Decking 1/2"	Ins Board 4" R20	Plywood 1.125"	Spray-on Insul and Wood						
ZoneB-S1Wall-Const	Metal Panel 0.0433	Air Layer 3/4" vertical-AL11	Equiv Layer K2-Kwall South Corner	Plywood 1/2"	Equiv Layer K3-Kwall South Corner	Gypsum Board 5/8"				

ZoneB-S2Wall-Const	Cement Board 0.65"	Air Layer 3/4" vertical-AL11	Ins Board 3/4" R3.8	Plywood 1/2"	Equiv Layer K1-SouthWall	Gypsum Board 5/8"				
ZoneB-S3Wall-Const	Metal Panel 0.0433	Air Layer 3/4" vertical-AL11	Equiv Layer K1-Jwall South	Plywood 1/2"	Equiv Layer K2-Jwall South	Gypsum Board 5/8"				
ZoneB-E1Wall-Const	Metal Panel 0.0433	Air Layer 3/4" vertical-AL11	Equiv Layer K1-Kwall South Corner	Plywood 1/2"	Equiv Layer K3-Kwall South Corner	Additional Insulation 6"	Gypsum Board 5/8"			
ZoneB-E2Wall-Const	Metal Panel 0.0433	Air Layer 3/4" vertical-AL11	Equiv Layer K1-Kwall Middle	Plywood 1/2"	SIP 7.25"	Plywood 1/2"	Additional Insulation 6"	Gypsum Board 5/8"		
ZoneB-E3Wall-Const	Metal Panel 0.0433	Air Layer 3/4" vertical-AL11	Equiv Layer K1-Kwall North Corner	Plywood 1/2"	Equiv Layer K3-Kwall North Corner	Additional Insulation 6"	Gypsum Board 5/8"			
ZoneB-N1Wall-Const	Metal Panel 0.0433	Air Layer 3/4" vertical-AL11	Equiv Layer K2-Kwall North Corner	Plywood 1/2"	Equiv Layer K3-Kwall North Corner	Gypsum Board 5/8"				
ZoneB-N2Wall-Const	Metal Panel 0.0433	Air Layer 3/4" vertical-AL11	Ins Board 3/4" R3.8	Plywood 1/2"	Equiv Layer K4-NorthWall	Gypsum Board 5/8"				
ZoneB-N3Wall-Const	Plywood 3/4"	Equiv Layer K2-NorthWall	Plywood 1/2"	Equiv Layer K1-NorthWall	Plywood 1/2"	Gypsum Board 5/8"				
ZoneB-N4Wall-Const	Gypsum Board 5/8"	Equiv Layer K5-NorthWall	Gypsum Board 5/8"							
ZoneB-N5Wall-Const	Gypsum Board 5/8"	Equiv Layer K1-Jwall North	Gypsum Board 5/8"							
ZoneB-W1Wall-Const	Gypsum Board 5/8"	Equiv Layer K2-Jwall South	Plywood 1/2"	Equiv Layer K3-Jwall South	Plywood 1/2"	Equiv Layer K2-Jwall South	Gypsum Board 5/8"			
ZoneB-W2Wall-Const	Gypsum Board 5/8"	Ins Board 4" R20	Plywood 1/2"	SIP 7.25"	Plywood 1/2"	Ins Board 4" R20	Gypsum Board 5/8"			
ZoneB-W3Wall-Const	Gypsum Board 5/8"	Equiv Layer K1-Jwall North	Plywood 1/2"	Equiv Layer K2-Jwall North	Plywood 1/2"	Equiv Layer K1-Jwall North	Gypsum Board 5/8"			
ZoneA-S1Wall-Const	Metal Panel 0.0433	Air Layer 3/4" vertical-AL11	Equiv Layer K1-Jwall South	Plywood 1/2"	Equiv Layer K2-Jwall South	Gypsum Board 5/8"				
ZoneA-S2Wall-Const	Cement Board 0.65"	Air Layer 3/4" vertical-AL11	Ins Board 3/4" R3.8	Plywood 1/2"	Equiv Layer K1-SouthWall	Gypsum Board 5/8"				
ZoneA-S3Wall-Const	Metal Panel 0.0433	Air Layer 3/4" vertical-AL11	Equiv Layer K1-Hwall South	Plywood 1/2"	Equiv Layer K2-Hwall South	Gypsum Board 5/8"				
ZoneA-E1Wall-Const	Gypsum Board 5/8"	Equiv Layer K2-Jwall South	Plywood 1/2"	Equiv Layer K3-Jwall South	Plywood 1/2"	Equiv Layer K2-Jwall South	Gypsum Board 5/8"			

ZoneA-E2Wall-Const	Gypsum Board 5/8"	Ins Board 4" R20	Plywood 1/2"	SIP 7.25"	Plywood 1/2"	Ins Board 4" R20	Gypsum Board 5/8"			
ZoneA-E3Wall-Const	Gypsum Board 5/8"	Equiv Layer K1-Jwall North	Plywood 1/2"	Equiv Layer K2-Jwall North	Plywood 1/2"	Equiv Layer K1-Jwall North	Gypsum Board 5/8"			
ZoneA-N1Wall-Const	Metal Panel 0.0433	Air Layer 3/4" vertical-AL11	Equiv Layer K1-Hwall North	Plywood 3/4"	Equiv Layer K3-Kwall North Corner	Gypsum Board 5/8"				
ZoneA-N2Wall-Const	Metal Panel 0.0433	Air Layer 3/4" vertical-AL11	Ins Board 3/4" R3.8	Plywood 1/2"	Equiv Layer K4-NorthWall	Gypsum Board 5/8"				
ZoneA-N3Wall-Const	Plywood 3/4"	Equiv Layer K2-NorthWall	Plywood 1/2"	Equiv Layer K1-NorthWall	Plywood 1/2"	Gypsum Board 5/8"				
ZoneA-N4Wall-Const	Gypsum Board 5/8"	Equiv Layer K5-NorthWall	Gypsum Board 5/8"							
ZoneA-N5Wall-Const	Gypsum Board 5/8"	Equiv Layer K1-Jwall North	Gypsum Board 5/8"							
ZoneA-W1Wall-Const	Gypsum Board 5/8"	Equiv Layer K2-Hwall South	Plywood 1/2"	Equiv Layer K3-Hwall South	Plywood 1/2"	Equiv Layer K2-Hwall South	Gypsum Board 5/8"			
ZoneA-W2Wall-Const	Gypsum Board 5/8"	Ins Board 4" R20	Plywood 1/2"	SIP 7.25"	Plywood 1/2"	Plywood 1/2"	SIP 7.25"	Plywood 1/2"	Ins Board 4" R20	Gypsum Board 5/8"
ZoneA-W3Wall-Const	Metal Panel 0.0433	Air Layer 3/4" vertical-AL11	Equiv Layer K2-Hwall North	Plywood 1/2"	Equiv Layer K3-Hwall North	Gypsum Board 5/8"				
ZONEB-S1WALL-ElecRoo m-Const	Gypsum Board 5/8"	Plywood 1/2"	Equiv Layer K1-NorthWall	Plywood 1/2"	Equiv Layer K2-NorthWall	Plywood 3/4"				
ZoneB-S2Wall-ElecRoo m-Const	Gypsum Board 5/8"	Plywood 1/2"	SIP 7.25"	Plywood 1/2"	Ins Board 4" R20	Plywood 3/4"				
ZoneB-NorthWall - ElecRoo m-Const	Metal Panel 0.0433	Air Layer 3/4" vertical-AL11	Ins Board 4" R20	Plywood 1/2"	SIP 7.25"	Plywood 1/2"	Plywood 3/4"			
ZoneB-W1Wall-ElecRoo m-Const	Gypsum Board 5/8"	Plywood 1/2"	SIP 7.25"	Plywood 1/2"	Ins Board 4" R20	Plywood 3/4"				
ZoneB-W2Wall-ElecRoo m-Const	Gypsum Board 5/8"	Plywood 1/2"	SIP 7.25"	Plywood 1/2"	Ins Board 4" R20	Plywood 3/4"				
ZoneB-EastWall-ElecRoo m-Const	Metal Panel 0.0433	Air Layer 3/4" vertical-AL11	Plywood 1/2"	Ins Board 7.5" R13	Plywood 1/2"	Plywood 3/4"				
ZoneB-S1WALL-MECHRO OM-Const	Gypsum Board 5/8"	Equiv Layer K1-Jwall North	Gypsum Board 5/8"							

ZoneB-S2WALL-MECHRO OM-Const	Gypsum Board 5/8"	Equiv Layer K5-NorthWall	Gypsum Board 5/8"							
ZoneB-WestWall - MechRoo m-Const	Gypsum Board 5/8"	Ins Board 4" R20	Plywood 1/2"	SIP 7.25"	Plywood 1/2"	Ins Board 4" R20	Gypsum Board 5/8"			
ZoneB-N1Wall-MechRoo m-Const	Metal Panel 0.0433	Air Layer 3/4" vertical-AL11	Ins Board 4" R20	Plywood 1/2"	SIP 7.25"	Plywood 1/2"	Gypsum Board 5/8"			
ZoneB-N2Wall-MechRoo m-Const	Plywood 3/4"	Ins Board 4" R20	Plywood 1/2"	SIP 7.25"	Plywood 1/2"	Gypsum Board 5/8"				
ZoneB-E1Wall-MechRoo m-Const	Plywood 3/4"	Ins Board 4" R20	Plywood 1/2"	SIP 7.25"	Plywood 1/2"	Gypsum Board 5/8"				
ZoneB-E2Wall-MechRoo m-Const	Plywood 3/4"	Ins Board 4" R20	Plywood 1/2"	SIP 7.25"	Plywood 1/2"	Gypsum Board 5/8"				
ZoneA-S1WALL-ElecRoo m-Const	Gypsum Board 5/8"	Plywood 1/2"	Equiv Layer K1-NorthWall	Plywood 1/2"	Equiv Layer K2-NorthWall	Plywood 3/4"				
ZoneA-NorthWall - ElecRoo m-Const	Metal Panel 0.0433	Air Layer 3/4" vertical-AL11	Ins Board 4" R20	Plywood 1/2"	SIP 7.25"	Plywood 1/2"	Plywood 3/4"			
ZoneA-E1Wall-ElecRoo m-Const	Gypsum Board 5/8"	Plywood 1/2"	SIP 7.25"	Plywood 1/2"	Ins Board 4" R20	Plywood 3/4"				
ZoneA-E2Wall-ElecRoo m-Const	Gypsum Board 5/8"	Plywood 1/2"	SIP 7.25"	Plywood 1/2"	Ins Board 4" R20	Plywood 3/4"				
ZoneA-S2Wall-ElecRoo m-Const	Gypsum Board 5/8"	Plywood 1/2"	SIP 7.25"	Plywood 1/2"	Ins Board 4" R20	Plywood 3/4"				
ZoneA-WestWall - ElecRoo m-Const	Metal Panel 0.0433	Air Layer 3/4" vertical-AL11	Plywood 1/2"	Ins Board 7.5" R13	Plywood 1/2"	Plywood 3/4"				
ZoneA-S1WALL-MECHRO OM-Const	Gypsum Board 5/8"	Equiv Layer K1-Jwall North	Gypsum Board 5/8"							
ZoneA-S2WALL-MECHRO OM-Const	Gypsum Board 5/8"	Equiv Layer K5-NorthWall	Gypsum Board 5/8"							
ZoneA-EastWall-MechRoo m-Const	Gypsum Board 5/8"	Ins Board 4" R20	Plywood 1/2"	SIP 7.25"	Plywood 1/2"	Ins Board 4" R20	Gypsum Board 5/8"			
ZoneA-N1Wall-	Metal Panel 0.0433	Air Layer 3/4"	Ins Board 4" R20	Plywood 1/2"	SIP 7.25"	Plywood 1/2"	Gypsum Board 5/8"			

MechRoo m-Const		vertical- AL11								
ZoneA- W1Wall- MechRoo m-Const	Plywood 3/4"	Ins Board 4" R20	Plywood 1/2"	SIP 7.25"	Plywood 1/2"	Gypsum Board 5/8"				
ZoneA- W2Wall- MechRoo m-Const	Plywood 3/4"	Ins Board 4" R20	Plywood 1/2"	SIP 7.25"	Plywood 1/2"	Gypsum Board 5/8"				
ZoneA- N2Wall- MechRoo m-Const	Plywood 3/4"	Ins Board 4" R20	Plywood 1/2"	SIP 7.25"	Plywood 1/2"	Gypsum Board 5/8"				
TempNw all-Door- CONST	Polyiso 2" Aluminum Coil	EPS 7/8"	Polyiso 2" Aluminum Coil							

Table B-2 Properties of materials used in FLEXLAB.

Material	Roughnes s	Thicknes s (m)	Conductivi ty (W/m-K)	Densit y (kg/m ³)	Specifi c Heat (J/kg- K)	Thermal Absorptanc e	Solar Absorptanc e	Visible Absorptanc e
Topping Slab 6"	Rough	0.1524	1.95	2087	900	0.9	0.65	0.65
Slab Horizontal Insulation 5"	Smooth	0.127	0.035	265	1300	0.9	0.65	0.65
HW Concrete 5"	Rough	0.127	1.311	2240	836.8	0.9	0.7	0.7
Metal Panel 0.0433	Medium Smooth	0.0011	62	7580	485	0.9	0.5	0.5
Cement Board 0.65"	Medium Smooth	0.0165	0.597	1922	837	0.9	0.5	0.5
SIP 7.25"	Medium Smooth	0.1842	0.038	29	1210	0.9	0.5	0.5
R20 Ins Board 4"	Medium Smooth	0.1016	0.037	29	1213	0.9	0.5	0.5
R3.8 Ins Board 3/4"	Medium Smooth	0.0191	0.035	29	1213	0.9	0.5	0.5
R13 Insulation Board 7.5"	Medium Smooth	0.1905	0.039	48	1318	0.9	0.5	0.5
Acous Tile 3/4"	Medium Smooth	0.0191	0.057	288	1331	0.9	0.2	0.2
Spray-on Insul and Wood	Rough	0.2413	0.0324	68.71	1558	0.9	0.12	0.7
Roof Decking 1/2"	Medium Smooth	0.0127	0.13	850	1300	0.9	0.12	0.7
Polyiso 2"	Medium Smooth	0.0508	0.022	31.65	1500	0.9	0.5	0.5
Polyiso 2.25"	Medium Smooth	0.0572	0.0186	31.65	1500	0.1	0.3	0.3
Additional Insulation 6" Polyiso	Medium Rough	0.1524	0.023	40	1500	0.9	0.7	0.7
Cotton Batt 7"	Medium Smooth	0.178	0.059	1480	1307	0.2	0.5	0.5
HW CONCRETE 5"	Rough	0.127	1.311	2240	836.8	0.9	0.7	0.7
Plywood 1/2"	Medium Smooth	0.0127	0.115	545	1213	0.9	0.5	0.5
Plywood 3/4"	Medium Smooth	0.0191	0.115	545	1213	0.9	0.5	0.5
Plywood 1.125"	Medium Smooth	0.0286	0.115	545	1213	0.9	0.5	0.5
Gypsum Board 5/8"	Medium Smooth	0.0159	0.16	801	837	0.9	0.69	0.63
Gypsum Board 1/2"	Medium Smooth	0.0127	0.16	801	837	0.9	0.69	0.63

Ins Board 4" R20	Medium Smooth	0.1016	0.037	29	1213	0.9	0.5	0.5
Ins Board 3/4" R3.8	Medium Smooth	0.0191	0.035	29	1213	0.9	0.5	0.5
Ins Board 7.5" R13	Medium Smooth	0.1905	0.039	48	1318	0.9	0.5	0.5
Carpet 1/4"	Medium Smooth	0.0064	0.06	288	1380	0.9	0.7	0.7
Polyiso 4.5"	Medium Smooth	0.1143	0.0186	31.65	1500	0.2	0.5	0.5
Polyiso 2.25" Temp Nwall SouthFacing	Medium Smooth	0.0572	0.0186	31.65	1500	0.9	0.3	0.3
Polyiso 2.25" Temp Nwall NorthFacing	Medium Smooth	0.0572	0.0186	31.65	1500	0.1	0.3	0.3
AdditionalInsulation 6"	Medium Rough	0.1524	0.023	40	1500	0.9	0.7	0.7
Equiv Layer K1-Kwall South Corner	Medium Smooth	0.0762	0.035	109.2	1276	0.9	0.5	0.5
Equiv Layer K2-Kwall South Corner	Medium Smooth	0.0762	0.046	111.3	1278	0.9	0.5	0.5
Equiv Layer K3-Kwall South Corner	Medium Smooth	0.197	0.042	853.6	1300	0.9	0.5	0.5
Equiv Layer K1-Kwall North Corner	Medium Smooth	0.0762	0.055	109.2	1276	0.9	0.5	0.5
Equiv Layer K2-Kwall North Corner	Medium Smooth	0.0762	0.065	111.3	1278	0.9	0.5	0.5
Equiv Layer K3-Kwall North Corner	Medium Smooth	0.197	0.052	874.9	1312	0.9	0.5	0.5
Equiv Layer K1-Kwall Middle	Medium Smooth	0.0762	0.0504	48.3	1228	0.9	0.5	0.5
Equiv Layer K1-Jwall South	Medium Smooth	0.0889	0.0465	105.1	1273	0.9	0.5	0.5
Equiv Layer K2-Jwall South	Medium Smooth	0.1053	0.096	873	1109	0.9	0.5	0.5
Equiv Layer K3-Jwall South	Medium Smooth	0.1827	0.292	694	1287	0.9	0.5	0.5
Equiv Layer K1-Jwall North	Medium Smooth	0.1016	0.0565	619.6	1010	0.9	0.5	0.5
Equiv Layer K2-Jwall North	Medium Smooth	0.1848	0.184	747.9	1599	0.9	0.5	0.5
Equiv Layer K1-Hwall South	Medium Smooth	0.1016	0.046	75.3	1250	0.9	0.5	0.5
Equiv Layer K2-Hwall South	Medium Smooth	0.1016	0.0488	297.9	1411	0.9	0.5	0.5
Equiv Layer K3-Hwall South	Medium Smooth	0.3927	0.066	1428	1044	0.9	0.5	0.5
Equiv Layer K1-Hwall North	Medium Smooth	0.0889	0.0503	107.1	1274	0.9	0.5	0.5
Equiv Layer K2-Hwall North	Medium Smooth	0.1803	0.0635	89.6	1261	0.9	0.5	0.5
Equiv Layer K3-Hwall North	Medium Smooth	0.508	0.116	563.7	968	0.9	0.5	0.5
Equiv Layer K1-SouthWall	Medium Smooth	0.1524	0.174	105.9	1312	0.9	0.5	0.5
Equiv Layer K1-NorthWall	Medium Smooth	0.1842	0.205	270	1300	0.9	0.5	0.5
Equiv Layer K2-NorthWall	Medium Smooth	0.0762	0.0418	72.9	1249	0.9	0.5	0.5
Equiv Layer K4-NorthWall	Medium Smooth	0.1524	0.136	80.1	1314	0.9	0.5	0.5
Equiv Layer K5-NorthWall	Medium Smooth	0.0889	0.3706	79.4	230	0.9	0.5	0.5
Polyiso 2" Aluminum Coil	Medium Smooth	0.0508	0.022	31.65	1500	0.04	0.1	0.1
EPS 7/8"	Medium Rough	0.0222	0.035	20	1500	0.9	0.5	0.5

Table B-3 Properties of air gaps used in FLEXLAB.

Name	Thermal Resistance (m ² -K/W)
Air Layer 3/4" vertical-AL11	0.158
Air Layer 1.24" vertical-AL21	0.156

APPENDIX C. Modeling of Envelope Components with Two- and Three-Dimensional Heat Flows

The following information is provided in case a simulator wants to create a more detailed simulation model that incorporates various inhomogeneities such as corners with structural columns. This level of detail will usually be outside the scope of regular building simulations.

C.1 Two-dimensional component modeling

Converting a two-dimensional heat flow to a one-dimensional heat flow is done using the following steps:

1. Use THERM software to create a detailed model of each wall section from detailed architectural drawings.
2. Have THERM calculate the heat flow through the modeled section.
3. Step-by-step, replace sections of the model with uniform layers and set the conductivity of the newly created equivalent layers such that the heat flow through the model stays the same as in the original model (Step 2 above). The conductivity of the equivalent layer is therefore calculated in this step.
4. Calculate the density and specific heat of each equivalent layer by calculating the area weighted average of the original section that the layer is replacing.

C.2 Three-dimensional component modeling

Converting a three-dimensional, thermal bridging component to one-dimension is more complicated. Thermal bridging is usually caused by structural components, combined with discontinuities in thermal insulation. It can be easily identified in places where highly conducting components are passing through the exterior thermal insulation in multi-layer wall assemblies. Thermal bridges provide a path of higher conduction through the insulation, allowing for more heat to bypass the building thermal barrier. These thermal pathways often have strong multi-dimensional characteristics.

Using the THERM software, which is part of the WINDOW software suite developed by Berkeley Lab, the heat flow is calculated in both vertical and horizontal paths and then combined to calculate the one-dimensional equivalent heat flow. The multi-layer thermal bridging layers are then replaced by a single equivalent layer that produces the same heat flow. The following methodology is used to create an equivalent layer using THERM and to calculate the effective U-value:

1. Calculate the horizontal heat flow for the left, right and middle section of the wall (three values).
2. Calculate the vertical heat flow for the top and bottom of the wall section (two values).
3. Combine the five U-values to produce the overall equivalent U-value.
4. Using THERM, define a new material with the U-value calculated in Step 3.

The calculation of the equivalent U-value from the horizontal and vertical U-values is described in the following paper:

Curcija, D.C.; Goudey, H.; Bhandari, M.; Green, V.; Parrish, D.; Fisler, D.; and Kohler, C. 2022. "Improving the Energy Performance of the Building Envelope Through Factory Produced Wall Panels, Better Windows, and Improved Window-Wall Interface"

The THERM files can be found in the "Appendix C - Walls - THERM Files" folder in the <https://github.com/LBNL-ETA/FLEXLAB-ASHRAE140> Github repository.

C.2.1 Conductivity of the equivalent layers

The conductivity of the equivalent layer is calculated by the THERM software when multiple layers are replaced by a single layer.

C.2.2 Density and specific heat of the equivalent layers

The density and the specific heat of the equivalent layer are the area weighted averages for all the layers the equivalent layer is replacing. The following is an example of a calculation for an equivalent layer, replacing layers of wood, R20, R4.2, and Aerogel insulation, Plywood, Air, and Steel, with different thicknesses:

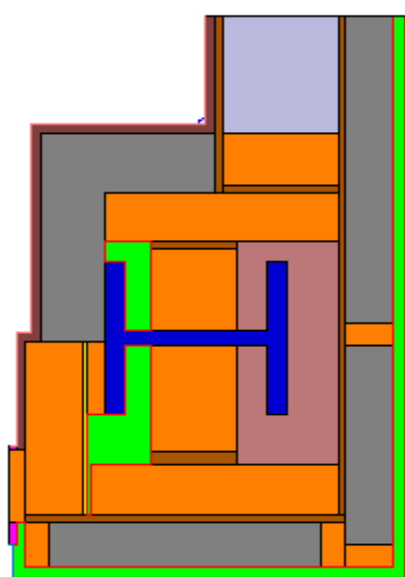
Table C-1 Example of calculation table for an equivalent layer.

Layer	Density kg/m ³	Specific Heat J/kg-K	Area inch ²
Wood	559	1,630	259.12
R20 insulation	29	1,213	80.8
R4.2 insulation	48	1,318	69.77
Aerogel	150	840	2.9
Plywood	545	1,213	8.67
Air	1	1	31.69
Steel	7,580	485	

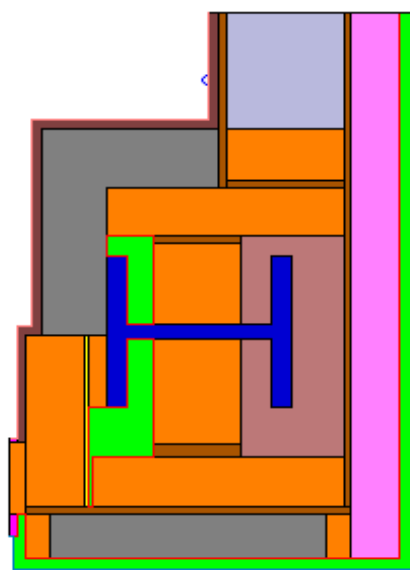
$$\begin{aligned} \text{Density of Equivalent Layer K3} &= [(259.12 * 559) + (80.8 * 29) + (69.77 * 48) + (2.9 * 150) + (8.67 * 545) + \\ &\quad (31.69 * 1) + (35.5 * 7580)] / (259.12 + 80.8 + 69.77 + 2.9 + 8.67 + 31.69 + 35.5) \\ &= 869.9 \text{ [Kg/m}^3\text{]} \end{aligned}$$

$$\begin{aligned} \text{Specific Heat of Equivalent Layer K3} &= [(259.12 * 1630) + (80.8 * 1213) + (69.77 * 1318) + (2.9 * 840) + \\ &\quad (8.67 * 1213) + (31.69 * 1) + (35.5 * 485)] / \\ &\quad (259.12 + 80.8 + 69.77 + 2.9 + 8.67 + 31.69 + 35.5) \\ &= 1315.4 \text{ [J/kg-K]} \end{aligned}$$

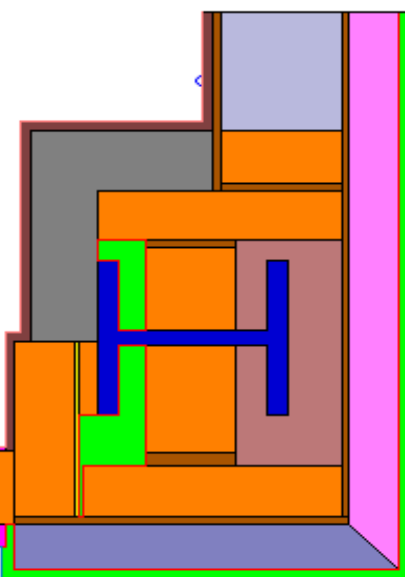
THERM Full Model



Step 1: First Equivalent Layer (K1)



Step 2: Second Equivalent Layer (K2)



Step 3: Third Equivalent Layer (K3)

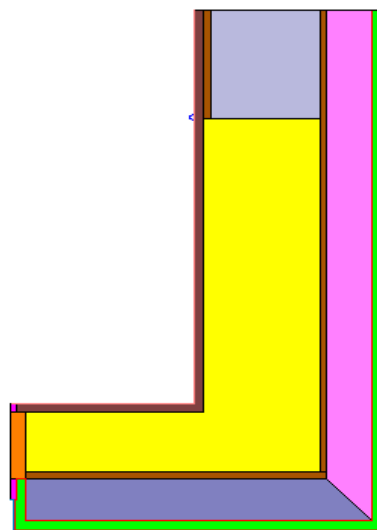


Figure. C-1 FLEXLAB X3 southeast corner wall. Steps to create the equivalent layers for the two dimensional heat flow paths.

APPENDIX D. Locations of Sensors

The figures in this appendix show the locations of the thermistors and heat flux sensors on each surface schematically. The detailed coordinates of each sensor are presented in a file name “Sensor locations.xlsx” that is contained in the datasets.

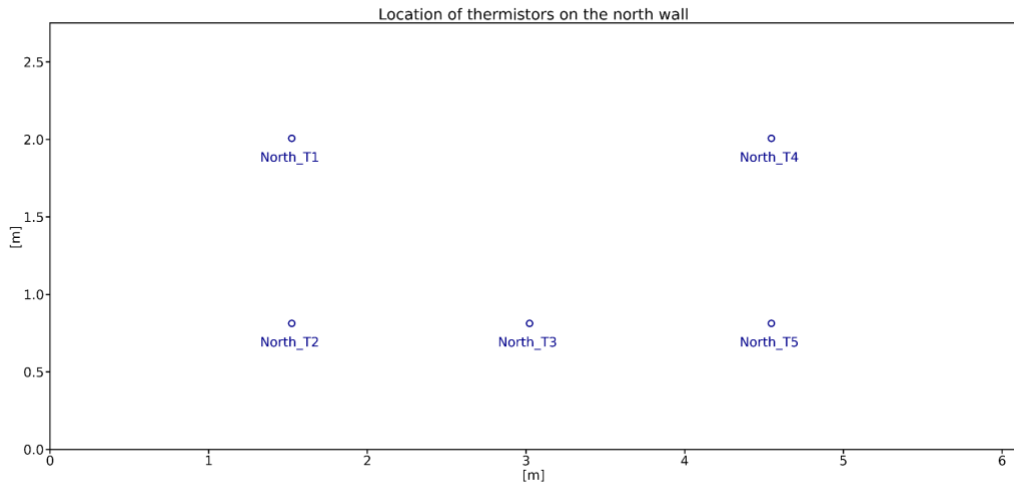


Figure D-1 Thermistor locations on the temporary north wall.

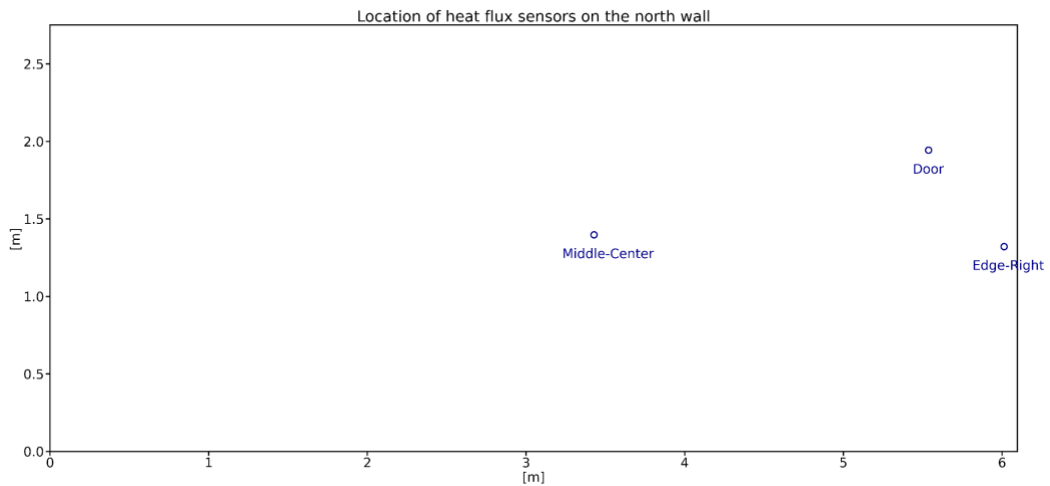


Figure D-2 Heat flux sensors on the temporary north wall.

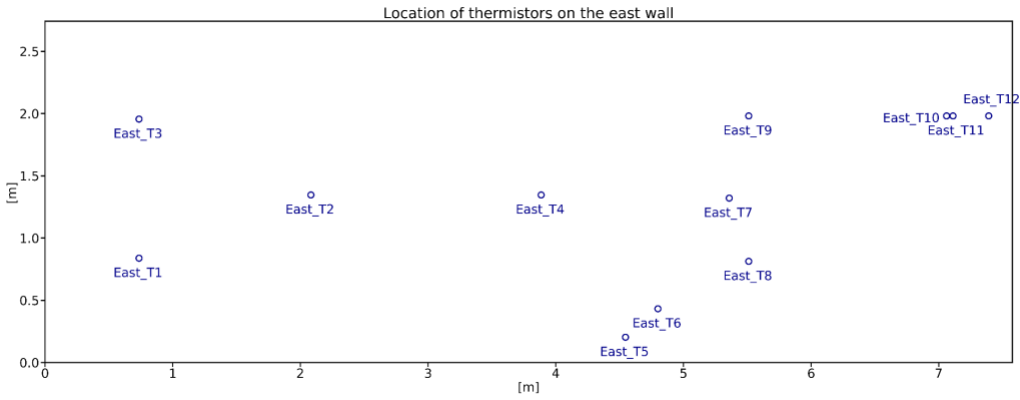


Figure D-3 Thermistors on the east wall.

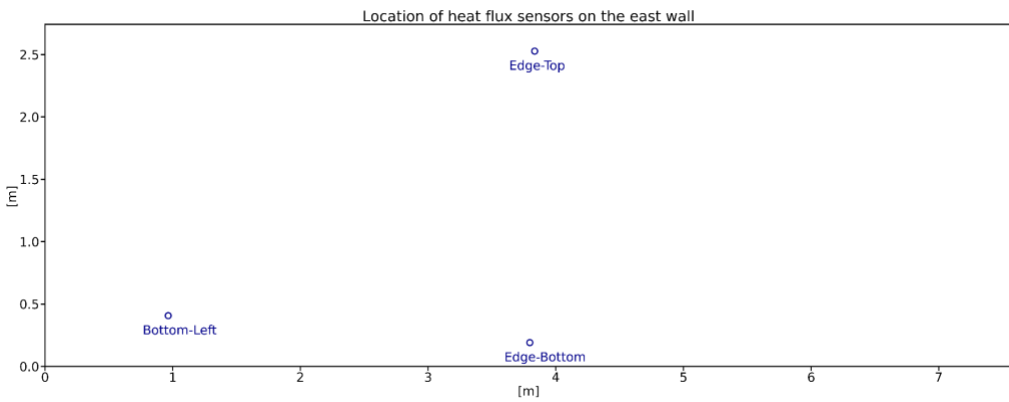


Figure D-4 Heat flux sensors on the east wall.

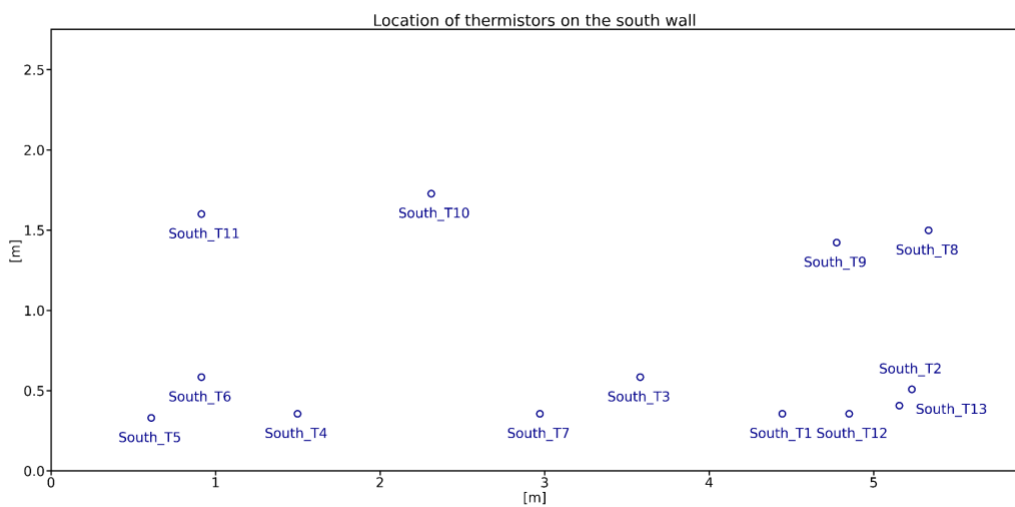


Figure D-5 Thermistors on the south wall.

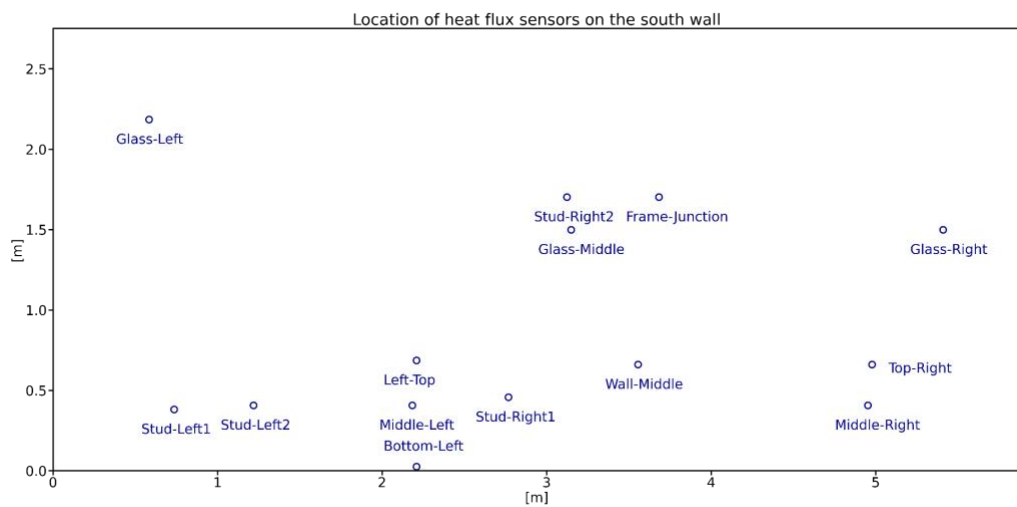


Figure D-6 Heat flux sensors on the south wall.

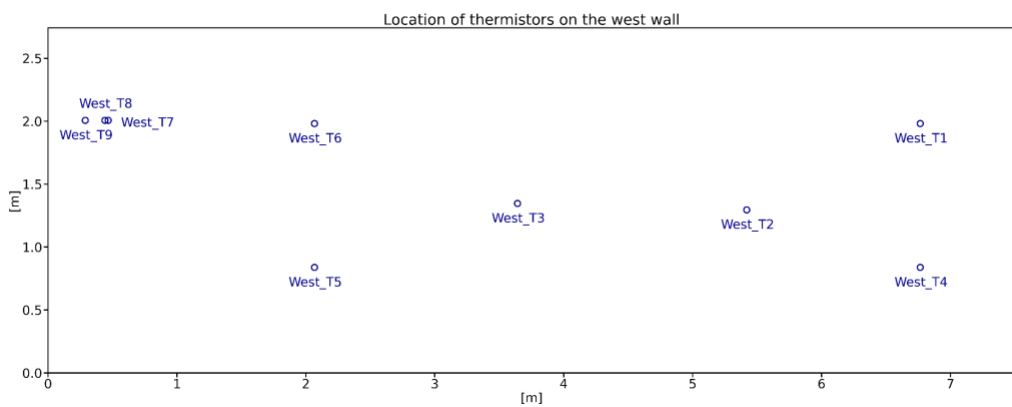


Figure D-7 Thermistors on the west wall.

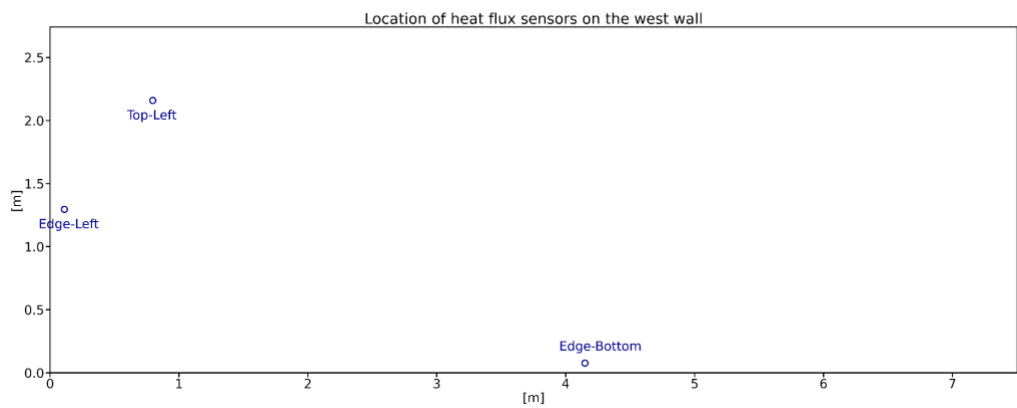


Figure D-8 Heat flux sensors on the west wall.

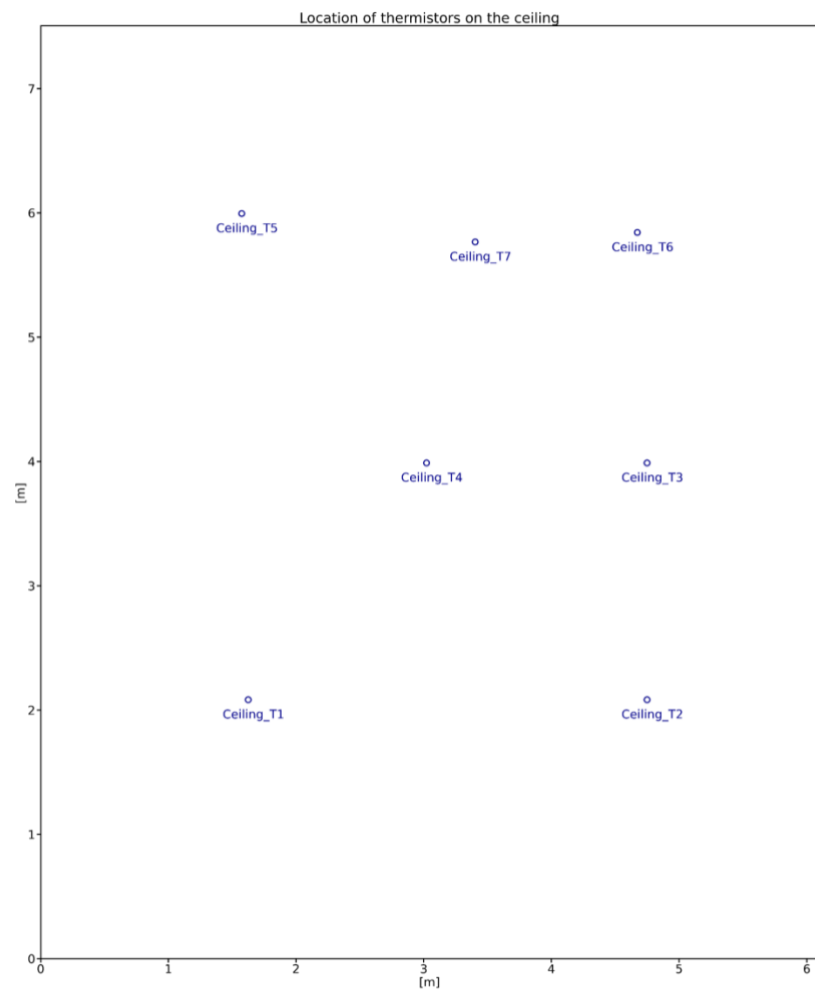


Figure D-9 Thermistors on the ceiling

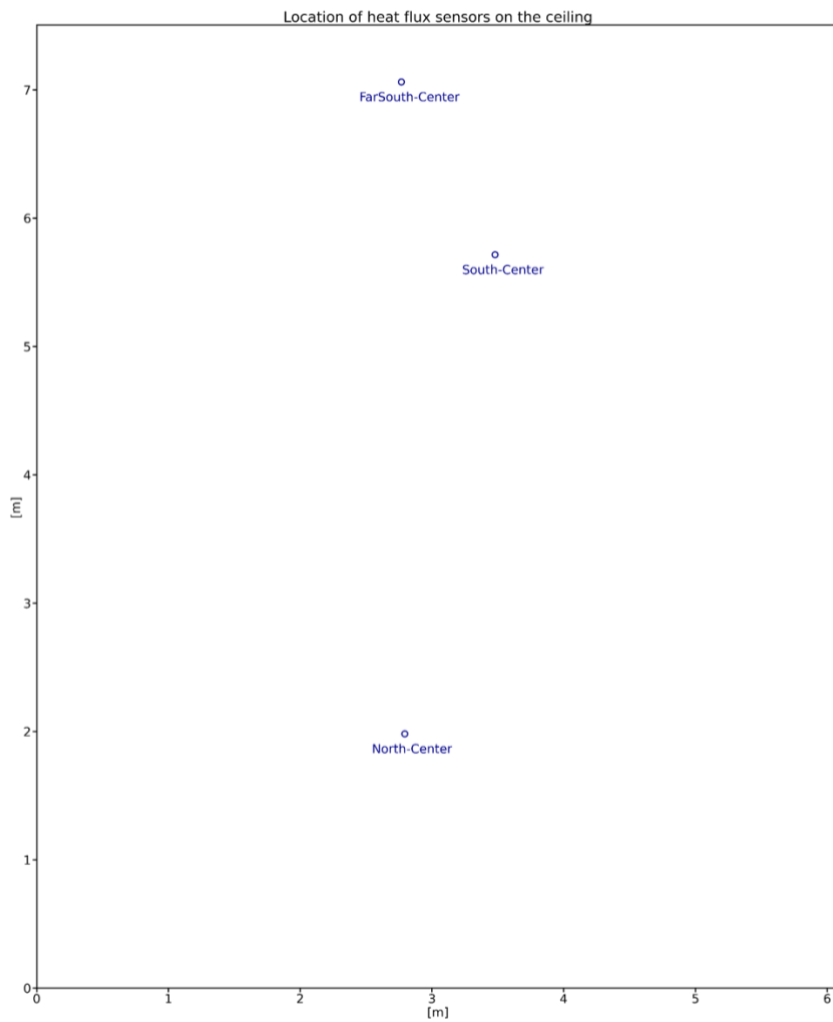


Figure D-10 Heat flux sensors on the ceiling.

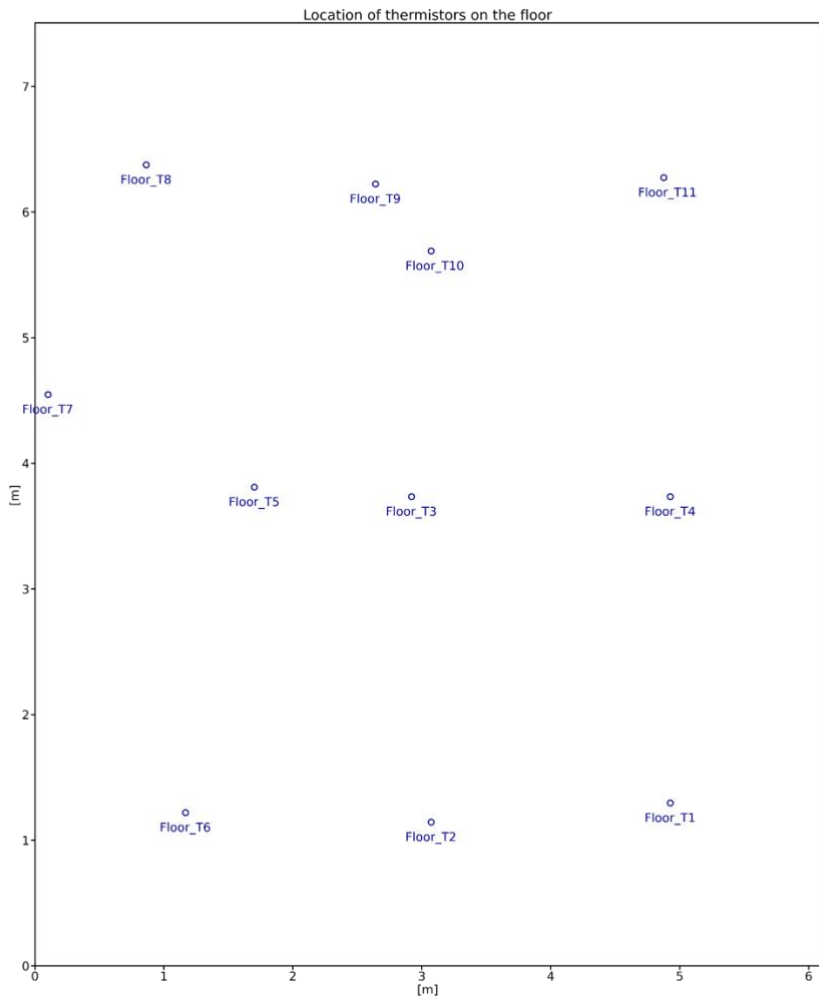


Figure D-11 Thermistors on the floor.

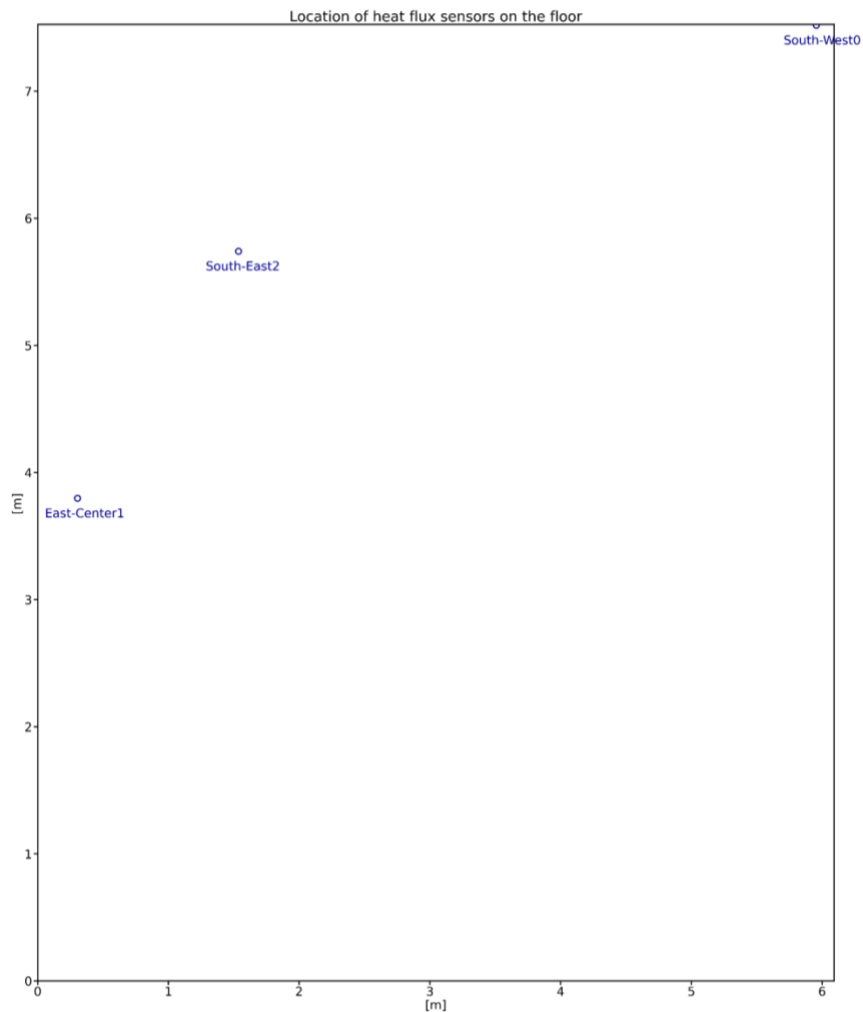


Figure D-12 Heat flux sensors on the floor.

APPENDIX E. Sun path and shading diagrams

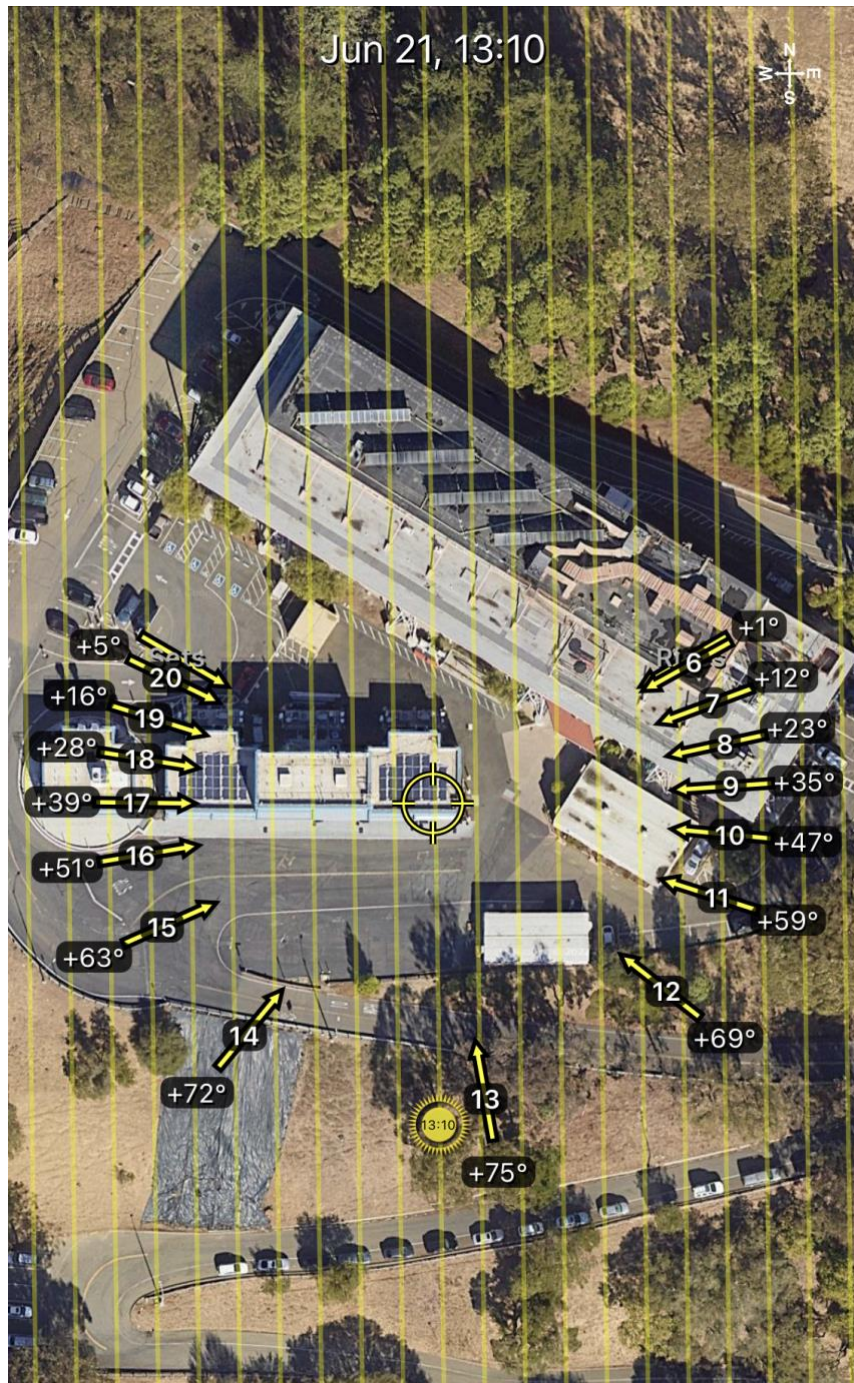


Figure E-1 Sun path diagram showing sun directions and elevations centered on FLEXLAB Cell 3B. Time of day in the image are local times (daylight savings time). All other data files and measurements ignore daylighting savings time (i.e. no time offset from March 1

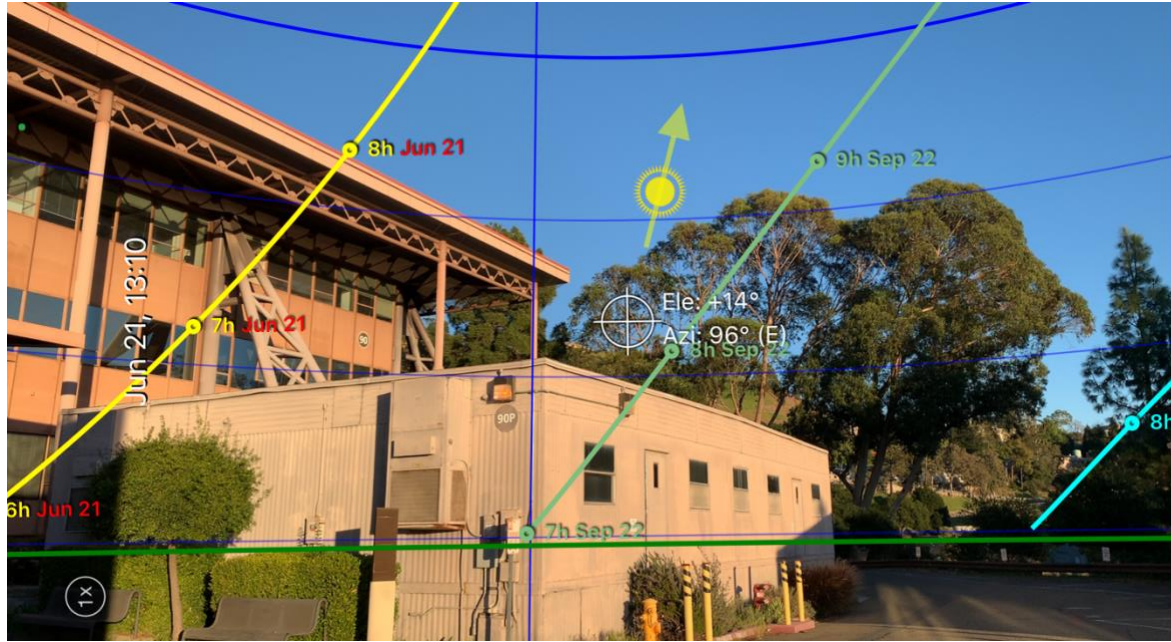


Figure E-2 Sun path diagram showing sun directions from 6-8am on June 21st (solstice) at the South-East corner of FLEXLAB Cell 3B. Time of day in the image are local times (daylight savings time).

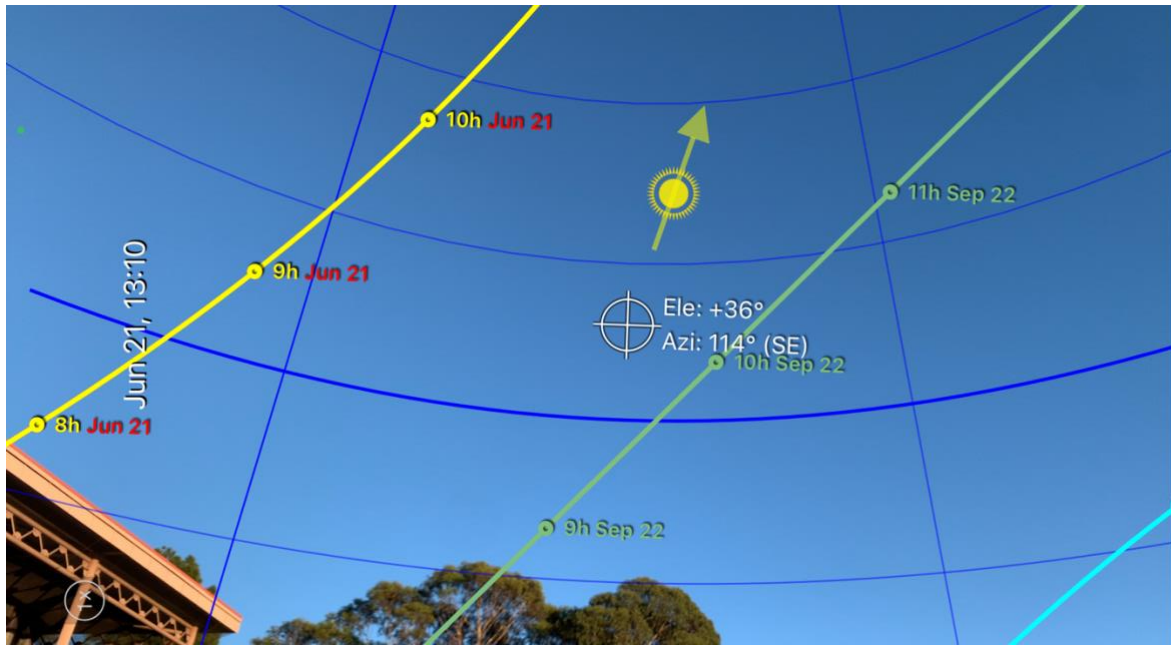
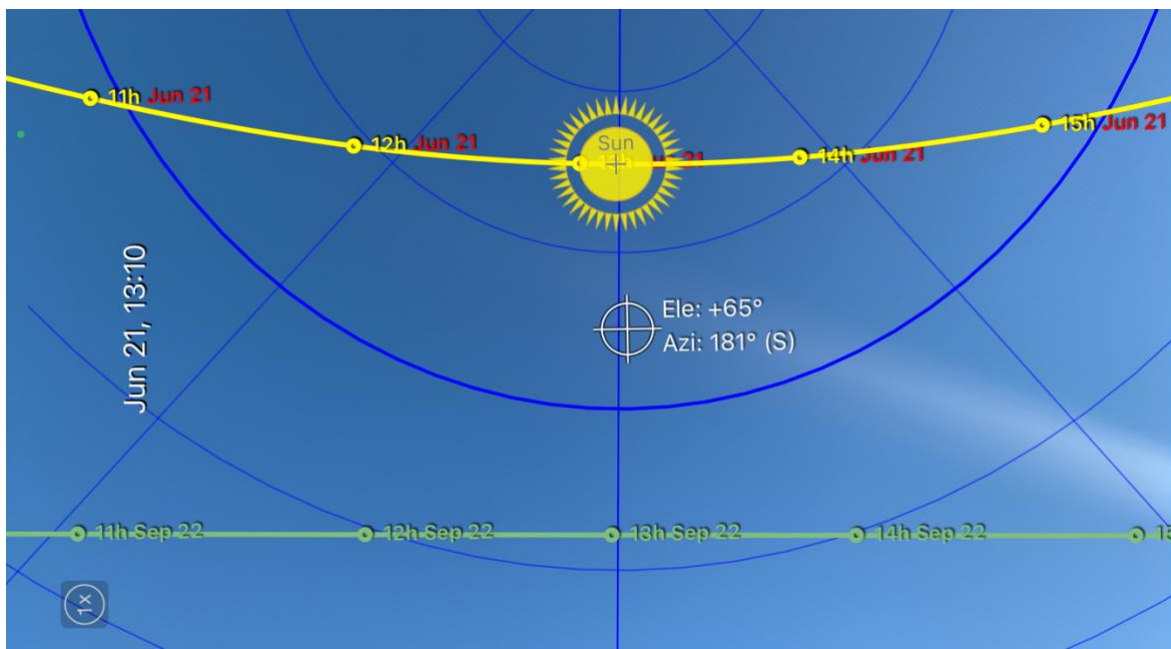
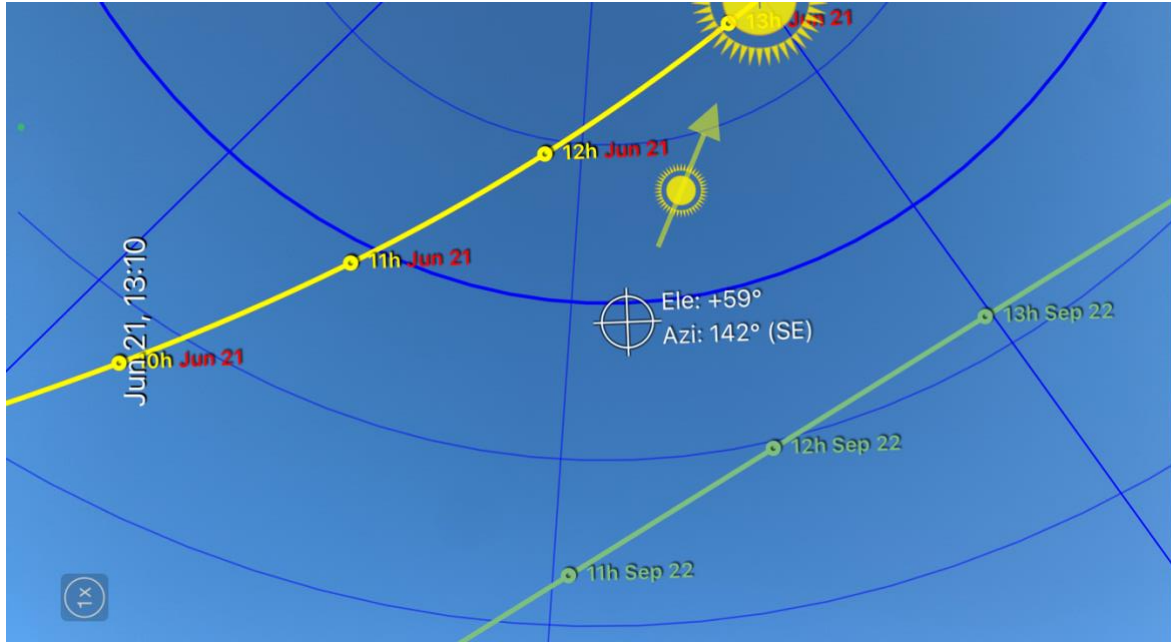


Figure E-3 Sun path diagram showing sun directions from 8-10am on June 21st (solstice) at the South-East corner of FLEXLAB Cell 3B. Time of day in the image are local times (daylight savings time).



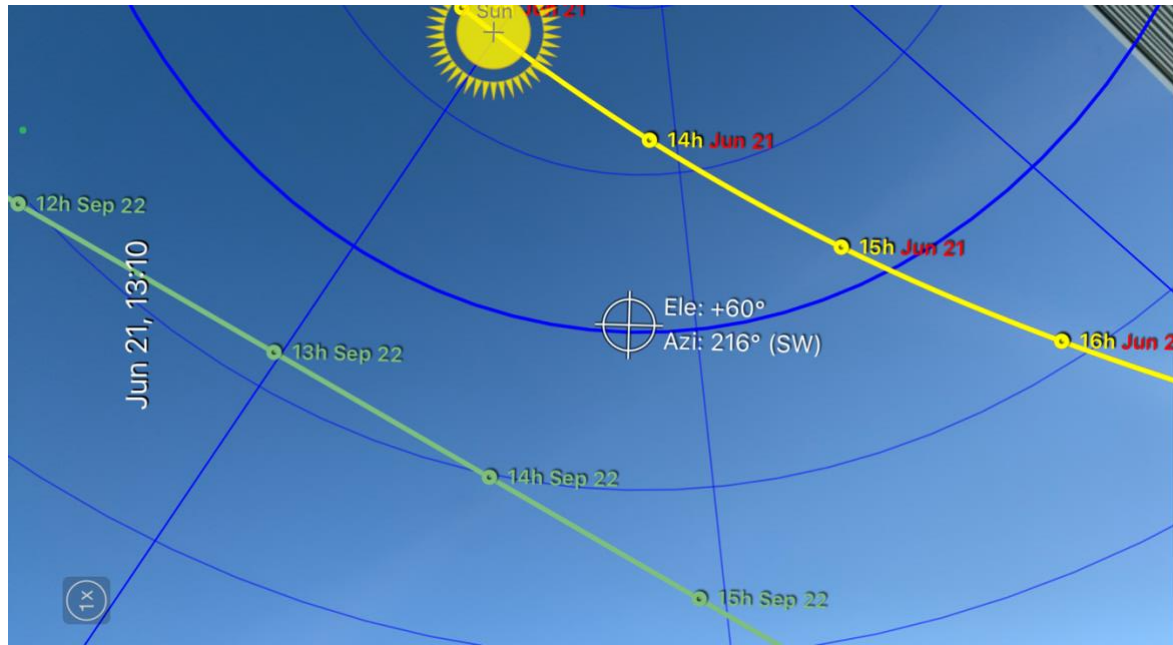


Figure E-6 . Sun path diagram showing sun directions from 1pm-4pm on June 21st (solstice) at the South-East corner of FLEXLAB Cell 3B. Time of day in the image are local times (daylight savings time).

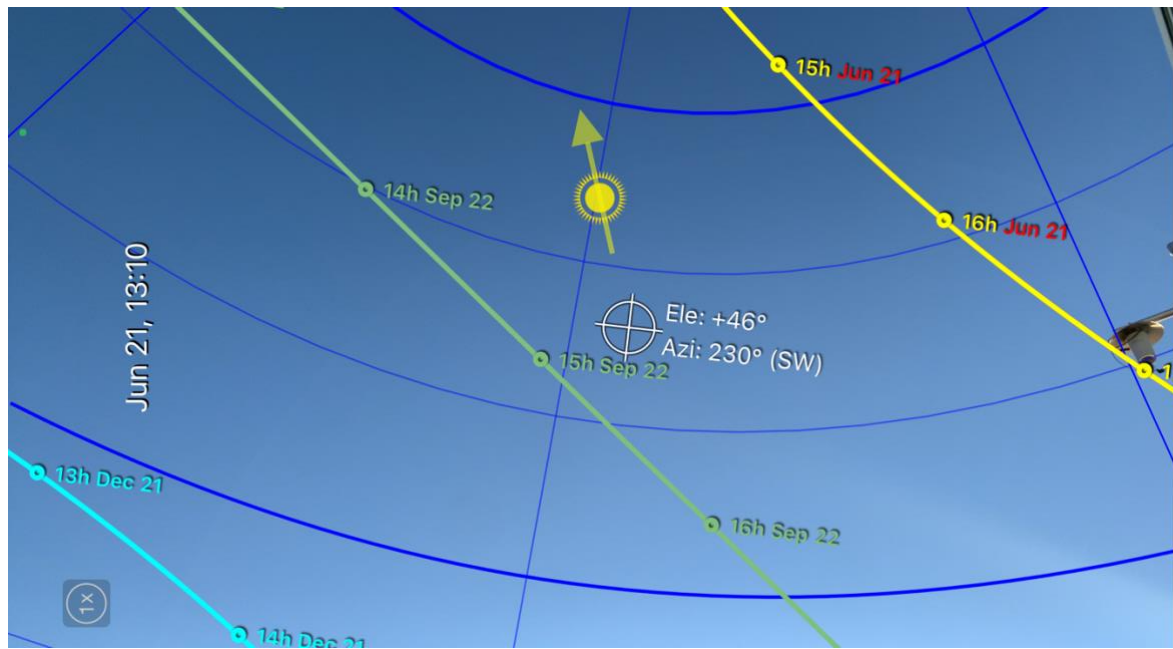


Figure E-7 Sun path diagram showing sun directions from 3pm-5pm on June 21st (solstice) at the South-East corner of FLEXLAB Cell 3B. Time of day in the image are local times (daylight savings time).

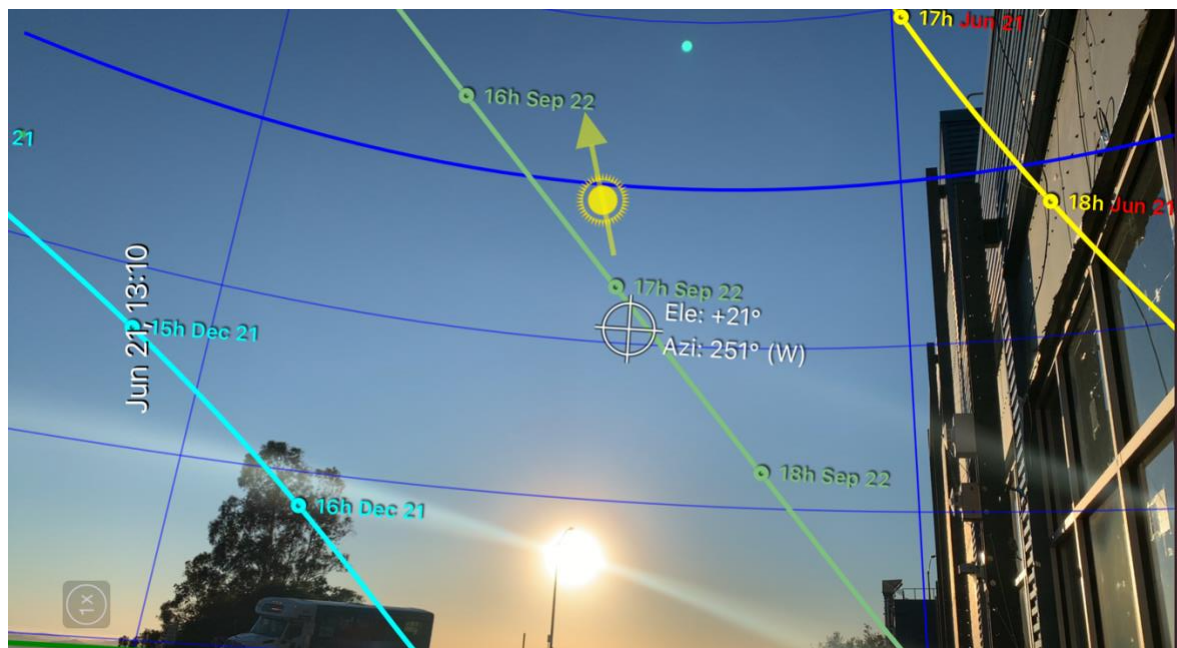


Figure E-8 Sun path diagram showing sun directions from 5pm-6pm on June 21st (solstice) at the South East corner of FLEXLAB Cell 3B. Time of day in the image are local times (daylight savings time).

APPENDIX F. Data Files

The following data files are available at <https://github.com/LBNL-ETA/FLEXLAB-ASHRAE140>

F.1 Window Files

Table F-1 Window modeling related files

Folder	File	Description
Window Models	w78-FLEXLAB-3B.mdb	WINDOW database containing the frames, glazing system and windows
Window Models	w78-FLEXLAB detailed report.txt	Detailed report from WINDOW for all 10 windows
Window Models	w78-FLEXLAB-Window_Avg.idf	Energy Plus report from WINDOW for all 10 windows
Window Models	403 HeadSill(00)-single-polyiso - A.THM	THERM file for the head and sill cross-section
Window Models	403 Jamb(00)-single-polyiso - B.THM	THERM file for the jamb cross-section
Window Models	403 Int Vertical(00)-single-polyiso-half - C.THM	THERM file for intermediate vertical cross-section
Window Models	403 Int Horz(00)-single-polyiso-half - D.THM	THERM file for intermediate horizontal cross-section

F.2 CSV Input files

Table F-2 General modeling input files

Folder	File	Description
	Meta Data.xlsx	Description of CSV file contents
Input Data	Duct blaster.csv	This file contains measured data of the duct blaster that are used to calculate the ventilation heat transfer rate
Input Data	Exterior surface temperature.csv	This file contains measured exterior surface temperatures
Input Data	Ground temperatures.csv	This file contains measured ground temperatures
Input Data	Internal heat gain rate.csv	This file contains the internal heat gain rate measured by a power meter
Input Data	Weather data.csv	This file contains measured weather data that are required by building performance simulation
Direct Validation Data	Air temperature.csv	This file contains the air temperatures of Cell 3B by thermistors on four stratification trees

Direct Validation Data	Fan coil units.csv	This file contains measured data of the two fan coil units that are used to calculate the cooling rate
Indirect Validation Data	Surface heat transfer.csv	
Indirect Validation Data/Surface Heat Flux	DropCeiling heat flux.csv	This file contains readings of heat flux sensors on the drop ceiling
Indirect Validation Data/Surface Heat Flux	EastWall heat flux.csv	This file contains readings of heat flux sensors on the east wall
Indirect Validation Data/Surface Heat Flux	Floor heat flux.csv	This file contains readings of heat flux sensors on the floor
Indirect Validation Data/Surface Heat Flux	SouthWall heat flux.csv	This file contains readings of heat flux sensors on the south wall
Indirect Validation Data/Surface Heat Flux	TemporaryNorthWall heat flux.csv	This file contains readings of heat flux sensors on the temporary north wall
Indirect Validation Data/Surface Heat Flux	WestWall heat flux.csv	This file contains readings of heat flux sensors on the west wall
Indirect Validation Data/Interior Surface Temperature	DropCeiling interior temperature.csv	This file contains readings of thermistors on the interior of the drop ceiling
Indirect Validation Data/Interior Surface Temperature	EastWall interior temperature.csv	This file contains readings of thermistors on the interior of the east wall
Indirect Validation Data/Interior Surface Temperature	Floor interior temperature.csv	This file contains readings of thermistors on the interior of the floor
Indirect Validation Data/Interior Surface Temperature	SouthWall interior temperature.csv	This file contains readings of thermistors on the interior of the south wall
Indirect Validation Data/Interior Surface Temperature	TemporaryNorthWall interior temperature.csv	This file contains readings of thermistors on the interior of the temporary north wall
Indirect Validation Data/Interior Surface Temperature	WestWall interior temperature.csv	This file contains readings of thermistors on the interior of the west wall
Auxiliary Data	Pressure.csv	This file contains measured air pressures relative to Cell 3B

Auxiliary Data	Construction.csv	This file contains the construction of different envelope sections
Auxiliary Data	Materials.csv	This file contains the properties of materials used in the construction
Auxiliary Data	No mass.csv	This file contains the properties of no-mass materials used in the construction
Auxiliary Data	Sensor locations.xlsx	This file contains the coordinates of flux sensors and thermistors on each surface

F.3 Architectural Drawings

Folder	File	Description
Drawings	FLEXLAB structural.pdf	Structural drawings for FLEXLAB
Drawings	FLEXLAB Architectural.pdf	Architectural drawings for FLEXLAB

F.4 Pictures

Folder	Sub-Folder	Description
Pictures	Overview Pictures	Pictures of each surface
Pictures	Construction	Pictures of construction details
Pictures	Sunpaths	Sunpath diagrams

F.5 Wall THERM files

Folder	File	Description
Appendix C – Walls – THERM files	Various	THERM files for various wall cross-sections